POLITECNICO DI TORINO
Dipartimento di Energia
(DENERG)

Corso di Laurea Magistrale in Ingegneria Energetica e Nucleare

Tesi di Laurea Magistrale

Theoretical and experimental analysis of atmospheric water harvesting systems for agriculture

Relatore:
Prof. Marco Simonetti
Correlatori:
Vincenzo Maria Gentile
Francesco Neirotti

Candidato:
Domenico Cristiano Mannino

Anno accademico 2020-2021

Abstract

The constant increase in World population is responsible for the huge increment in demands for essential resources as water, food and energy. These are linked together through the so-called Energy-Water-Food nexus, which is a new methodology capable of explaining how the production of one of these goods is related to the others. Energy and food sectors have already found various alternatives for the production of these goods, just think to innovative methods for renewable energy sources and modern agriculture techniques characterized by lower water intensity and soil usage. On the other hand, the problem of water scarcity is widely spread along the World and seems to be poor of solutions other than common ones. In this scenario atmospheric water harvesting "AWH" represents an innovative and recent method for freshwater production, characterized by high availability of resource and mature knowledge about the technology commonly used. The present work provides the analysis of an innovative device for AWH based on adsorption materials and developed by the SolarPenguins team of DENERG department of Polytechnic of Turin. The system makes use of Silica gel as sorption substrate, this interacts with air through mass and energy transfers and according to specific thermodynamic conditions it can adsorb, or releases water trapped in its structure. In the analysis, the device is modelled in Matlab in order to test easily its performances in different environments without the physical need to be on place. Results in term of water productivity and energy consumption are used to carry out a feasibility study regards the integration between the device and greenhouse systems, using as experimental scenario the hydroponic greenhouse built at the Energy Centre. The aim is to demonstrate the potential of this technology as water producer able to contribute on the reduction of water scarcity problem.

Ringraziamenti

Dedico questo importante traguardo a tutti coloro che mi hanno accompagnato durante il mio percorso di vita. Infatti, credo che questa laurea sia il risultato di tutte le esperienze che ho vissuto fino ad oggi, positive o negative che siano state. Ho avuto modo di imparare da ogni singola esperienza e da ogni singola persona che mi è stata vicina prima e durante (e spero anche dopo) l'avventura universitaria. Ebbene sì, la definisco proprio un'avventura perché così è stata per me. Un percorso iniziato senza alcuna consapevolezza e certezza, oltre la mia voglia di realizzarmi e di perseguire i miei ideali. Un percorso fatto di alti e bassi, gioie e delusioni, ma infinitamente bello e soddisfacente. In primis ci tengo a ringraziare me stesso per essere riuscito a spingermi oltre i limiti che credevo di avere e per non aver mai vacillato, neanche nei momenti di sconforto e dubbio che era normale si presentassero.

"Bravo Cri Cri", così direbbero alcuni tra i miei amici più cari e di vecchia data, Andrea (lo chiameremo Punzo per evitare confusione) ed Emiliano. Ci conosciamo fin da quando eravamo dei bambini e posso dire con fierezza che siamo cresciuti insieme. Grazie alla nostra amicizia sono riuscito a migliorare tante componenti del mio carattere che sembravano irrimediabili, per cui grazie dal cuore. Poi non potrei mai dimenticare la mia coppia di fatto preferita "Gig & Sulipo", con cui ho potuto legare proprio durante il percorso universitario, tra giornate di studio interminabili e arancine di tutti i gusti e le forme. Un grazie speciale va al mio amico Giulio, anche detto Jiminias. Grazie a te per essere sempre stato un amico vero, con una bontà d'animo indescrivibile. A lui dico: Believe in yourself man, you can do whatever you want when ever you want, just believe in it. Un atro ringraziamento speciale va a Marci, mio compagno di rugby (insieme ad un altro individuo che verrà poi menzionato) con cui abbiamo condiviso battaglie, con un unico imperativo: non mollare mai, lottare sempre verso la meta, qualunque essa sia. Un grazie speciale va a Casa Mannino senza la quale i Fusi di Pollo non sarebbero mai nati, che ci ha ospitato in più occasioni di quante avrei potuto mai immaginare. Grazie a tutti i Fusi di Pollo per avermi dato un valido motivo per organizzare festini e grigliate tra una sessione di esami e l'altra.

Un posto speciale è occupato da chi ha vissuto con me questi ultimi 2 anni a Torino. Per prima cosa grazie al Gruppetto composto da me, Alessia, Miriana e Roberto. Siamo stati veramente bravi e sono felice di avere intrapreso questo viaggio con voi. Ci siamo trainati a vicenda senza mai mollare, insieme con una vera squadra. Un abbraccio speciale va ad Alina, con cui ho vissuto in simbiosi per l'intero periodo della tesi e che probabilmente ha anche pensato ad uccidermi qualche volta. Grazie Ali, non ce l'avrei fatta senza di te. Poi come dimenticare Antonio, che sin dal primo giorno che ho messo piede a Torino mi ha fatto sentire subito a casa. Grazie Anto.

Manfri ed Andri (Pandolfino) abbiamo immaginato spesso come sarebbe stato vivere insieme e credo che siamo riusciti a realizzare ogni cazzata pensata a riguardo. A suon di carbonara, ragù e pezzi di carne indefiniti siamo andati avanti insieme, trainandoci l'un l'altro. Grazie di cuore, mai convivenza fu più distruttiva e divertente.

Ringrazio mio fratello Francesco per avermi sopportato come coinquilino, tra vari alti e bassi. Ti ringrazio soprattutto per avere dato modo di analizzarmi e migliorarmi grazie a nostro confronti. Credo che questa sia stata una parte veramente importante della mia crescita come persona e senza questa nostra esperienza non l'avrei mai potuto fare. Ti voglio bene Franci e ricorda che hai le capacità per raggiungere i tuoi obbiettivi, devi solo applicarle con tanta voglia ed imparare a condividerle con gli altri. Vedrai quante sorprese riceverai.

Grazie a mia sorella Carlotta, per avere sempre creduto in me fin dall'inizio e per avermi spinto quando ne avevo bisogno. Mi hai sempre portato su un piedistallo e spero di essere in grado di realizzare le tue aspettative nei miei confronti. Ti voglio bene Totta, lotta e tieni duro. La strada è in salita, ma vedrai che ci sarà una vista bellissima alla fine del percorso, proprio come i paesaggi che vedevamo in montagna.
Un pensiero speciale va agli due miei fratelli più piccoli, Lorenzo e Aurora. Grazie per volermi così bene e per dimostrarlo sempre. A voi dico questo: avete già le capacità per prendervi il Mondo, fate di tutto per diventare ciò che volete essere nella vita anche quando questo sembrerà veramente difficile. Siete svegli, intelligenti e buoni d'animo, non vi manca nulla. Spero di essere un buon fratello per tutti voi, ci provo almeno.
Grazie a Noemi per essermi sempre stata vicina e per avermi sempre sostenuto nei momenti di difficoltà. Senza la tua capacità di interlocutore molte cose non avrei potuto mai comprenderle e farle mie. Ti voglio bene.
Grazie Papà per avermi insegnato ad andare oltre tutto e tutti, a farsi forza da soli e lottare per raggiungere i proprio obbiettivi. Grazie per avermi trasmesso il senso del legame familiare e fraterno, che stanno alla base del mio essere. Grazie per essere stato un così bravo papà e per avermi fatto diventare l'uomo che sono oggi.
Grazie Mamma per non avermi mai messo limiti in nulla che volessi fare o sognare, e per avermi sostenuto sempre in tutte le scelte che ho preso. Grazie per avermi insegnato che nella vita ci si può alzare sempre, non importa cosa sia successo. La forza di volontà è l'arma più potente che esista, e questo lo so grazie a te.
Infine, un grazie speciale va alla persona che mi è stata vicina negli ultimi 4 anni, Sofia. Ci siamo conosciuti all'inizio di questo percorso, quando ero solo una matricola che si apprestava a dare le ultime materie per chiudere il primo anno di università. Grazie amore mio per avermi sostenuto sempre, per avermi fatto credere in me stesso e per aver creduto tu per prima nelle mie capacità. Questo traguardo è solo il primo passo per prenderci il Mondo, ti amo e ti ringrazio per essere stata parte necessaria di questo percorso.
A tutti vi che ho dimenticato di inserire chiedo scusa, siete veramente tanti e mi dispiace non essere riuscito a spendere una parola per ognuno di voi. Ci tengo a ringraziarvi, perché nel bene e nel male mi avete comunque trasmesso qualcosa che farà sempre parte di me.

Sommario

Figure list

Introduction

The constant rise of world population is posing new challenges to sustainable development due to the corresponding increase in demand for essential goods as water, food and energy. According to "United Nations" [1] projections, total population will reach 10 billion of individuals by 2050 providing a proportional increase for urbanization need, economic development and demands for large middle class. The fulfilment of these needs goes through the future availability of water, food and energy, necessary elements to sustain life characterized by an intrinsic mutual relationship called Water-Energy-Food Nexus.

The Water-Energy-Food nexus describes the complex and inter-related nature of our global resources system where each sphere affects the others [2]. This innovative approach arises with the purpose of analysing the interactions between these elements in order to find out alternative solutions that might ensure more efficient and sustainable results. Currently, agriculture and food sectors account for 70% of global freshwater withdrawal and for 30% of total energy consumed, making these key elements in any part of food production and supply chain [3]. At the same time, power industry is water-intensive for 90% of global generation and it makes use of 75% of all industrial-water to transport, store and transform energy, whereas the bioenergy sector is becoming attractive to produce low carbon fossil fuels from organic wastes. On the other hand, energy is fundamental to manage properly freshwater .Indeed, energy is used to extract, pump and drive treatment processes required to make water suitable to cover humans' needs.

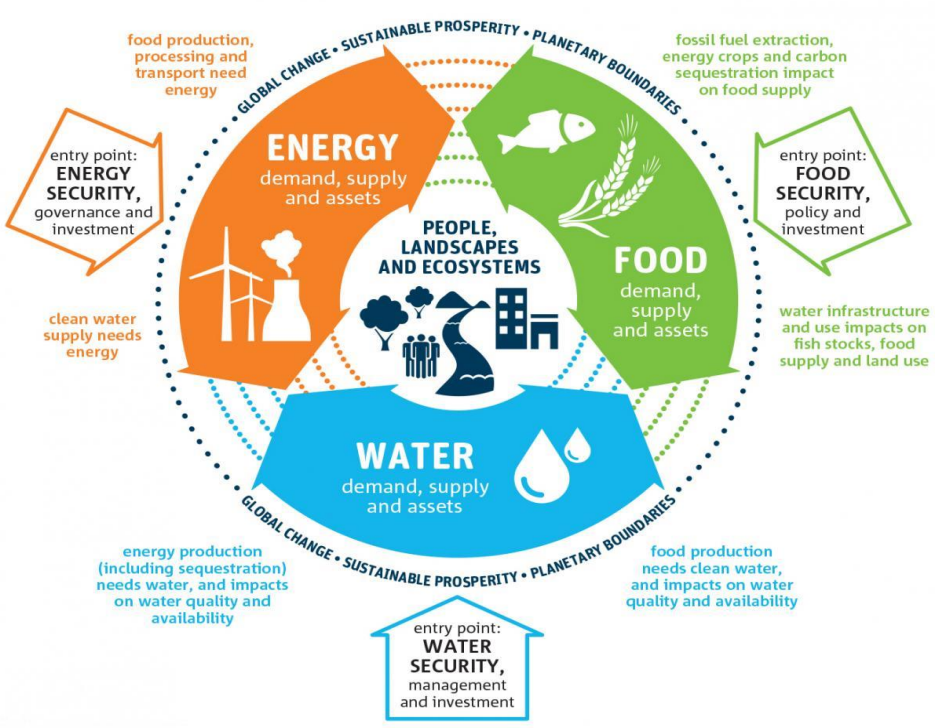

Figure 1. Water-Energy-Food Nexus [2]

According to OECD-FAO report of 2012 [4] demands for energy, water and food are expected to increase respectively of +80%, +55% and +60% by 2050. Thus a question arises: how will we be able to cover such requirements in a sustainable way?

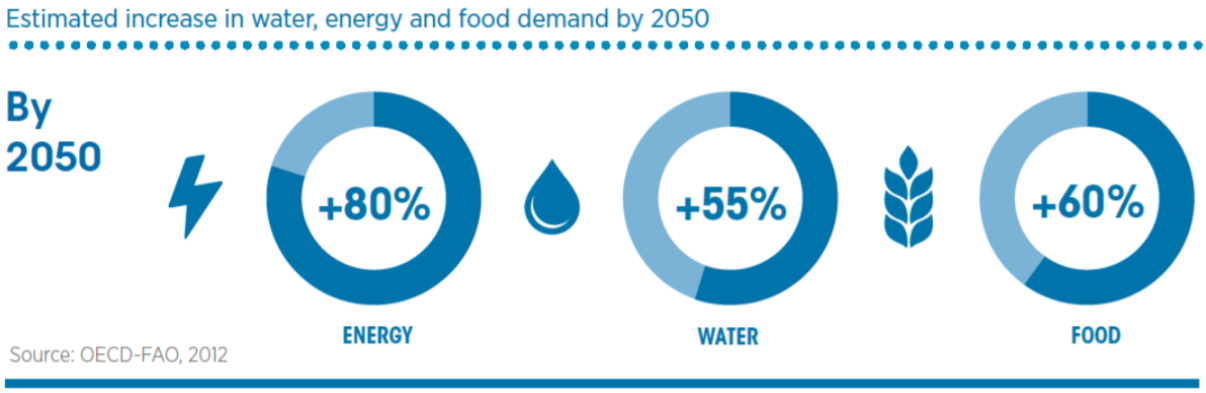

Figure 2. Estimated increase in demand for energy, water and food by 2050 [4]

Renewable Energy Sources "RES" and improvement in energy efficiency for production and consumption represent solutions for the power industry, indeed the current trend is focused onto innovative pathway based on cleaner and more sustainable forms of energy. Therefore, the decarbonization process aims in progressively reducing the use of fossil fuels in favour of alternative energy sources, without compromising the requirement of higher energy production. Hydroponic culture is a well-known technology used to cultivate plants without the soil characterized by higher quality of products, less water consumption and higher productivity per unit of land occupied. At the actual point, it seems to be the most promising method to improve the efficiency of food industry.

The production of freshwater has been empirically achieved through the developments of three main techniques: underground water extraction, desalination and Atmospheric Water Harvesting AWH. The field of AWH is dominated by lot of capturing processes, all based on water extraction from the atmosphere where water being in gaseous state in solution with air.

The purpose of this work is to investigate the feasibility of an innovative adsorption process for atmospheric water harvesting to produce freshwater suitable to cover hydroponic greenhouse requirements. In order to do so, five chapters are provided each with a precise object of study.

Chapter 1 investigates the current state of water distribution along the World, starting from the limited availability of freshwater compared to seawater and introducing the concept of water scarcity. The chapter continues with a review of main methods and technologies currently involved in freshwater collection, mainly divided in water from oceans, atmosphere and underground.

Chapter 2 describes the innovative system for atmospheric water harvesting developed at DENERG department. The device is called *Breath* and its working principle is based on physical adsorption performed by desiccant material characterized by high moisture capture capacity. The material chosen for the application is Silica gel, a widespread desiccant used in food industry with high prior knowledge.

Chapter 3 provides an overview of hydroponic greenhouse system by introducing main features and characteristics of this innovative free-soil cultivation technique. As applicative example a small scale hydroponic greenhouse developed by The SolarPenguins team of DENERG department at Energy Centre of Turin is presented. The aim is to carry out a feasibility study regards the production capacity of the device described in chapter 2. In such way the energy-water-food nexus is investigated with the aim of carrying out possible improvements.

Chapter 4 analyses the Matlab model developed to simulate the behaviour of Breath starting from a previous study about the adsorption heat exchanger within the system. In this chapter,

the modelling of components involved in water harvesting is performed. In particular, the cooling system will be described in detail and heat exchangers will be modelled according to their characteristics.
Chapter 5 presents results of experiments conducted on the integration between Breath and hydroponic greenhouse. Firstly, a series of experimental tests are used to understand parameters that drives the process. Following an application in real environments is used to develop the economic analysis of Breath. The chosen locations for simulations are Mosul, Casablanca and Bangkok. The chapter has also a paragraph dedicated to the integration of the system with renewable energy technology, with particular attention to photovoltaic systems. The idea is to develop a system energetically self-sufficient and able to minimize the impact on the environment. Eventually the chapter ends with conclusions carried out through experience, showing both weaknesses and point of strength of the model and the related technology.

1 Water analysis and production technology

Earth is covered by 71% of water classifiable in saline and fresh, where 96.5% of total amount belongs to oceans [5]. The remaining share is distributed among rivers, lakes, underground, atmosphere in vapour form, icecaps and glaciers. In particular 69.35% of freshwater is locked up in ice and permafrost, another 30% is trapped in the ground being often technically unachievable. The last 0.65% represents the quantity of freshwater allocated among lakes, rivers and atmosphere actually used to cover humans' needs. Therefore, freshwater resources are limited, and they are a rare element that has no substitutes or alternatives. Currently lakes and rivers constitute the main source of natural freshwater, followed by some underground resources technically achievable.

Moreover, freshwater is uneven distributed along the globe causing problem of scarcity in many regions often characterized by low grade of development and lower opportunities to improve their economy. During the last decades, this problem has been accentuated by the unsustainable and irrational use of water pushed by economic growth. Indeed, water can be considered the gossamer that connects the major spheres of modern economy, since it is used to produce and manufacture almost any kind of good or service. Therefore, the continuous boost of economy has led to an unsustainable increase in the environmental pressure, in particular on the water usage side. In many regions of the world, we have consistently under-priced water, wasting and overusing without care on future needs. This unregulated usage of water is the cause of the decreasing trend in water security, that means a direct increase of arid areas and decrease to water accessibility.

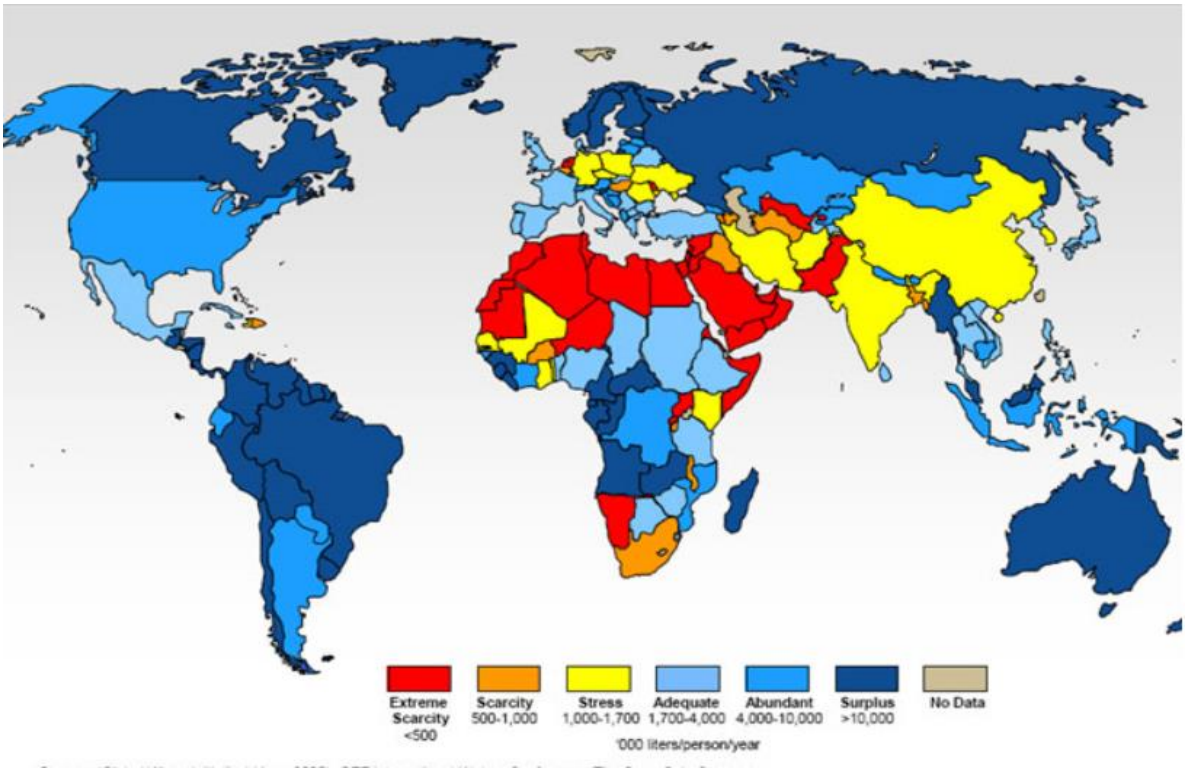

Figure 3. Yearly water availability per capita [6]

Increasing water scarcity could provide annual grain losses up to 30% of actual production, in counterflow respect targets fixed by estimated growth in population. Yet this scenario is enhanced by the raising of climate change, where a main consequence is exactly the change in water distribution. Indeed, the increase of average temperature along the globe is the main responsible for melting of glaciers, that represents the primary source of freshwater for 2 billion of people in Asia. This process risks to alter completely the equilibrium of natural ecosystems, with heavy effects on economic and political systems. Many works investigated the effects of climate change on various sphere of modern society, with particular attention to agriculture, economic growth, migration, heath and conflict. Fisher et al.(2012) [7] studied the impact of CC on US agriculture, analysing in particular effect of temperature growth. They demonstrated a reduction in profits for agriculture sector due to a lower productivity caused by adverse weather conditions. Hsiang and Jina (2014) [8] investigated the influence of CC on economic growth by analysing the trend of natural disaster in rich and poor countries. They reconstructed cyclone appearances for every country during 1950-2008 using meteorological data. Furthermore, these events were related to climate change through the analysis of temperature variation. The study proceeded with an economic evaluation of damages caused by natural disasters, using the Gross Domestic Product "GDP" as reference parameter. The results carried out negative effects of cyclones on long-run economic developed. Indeed, a country struck by a natural disaster orients internal policies and resource to recover damages, as consequence any other planned economic investment is slowed down.
In this prospective, climate change achieves a new consideration assuming the aspect of a socio-economic crisis affecting any major sphere of our society, including the natural water cycle.

1.1 Desalination

Desalination is a widespread process characterized by huge energy requirement and used to remove dissolved salts and other minerals from seawater in order to get water suitable for human consumption, agricultural purposes and industrial processes [9]. Indeed, the cost of water desalination is ten times higher than any other water treatment method, therefore it is important to underline that desalination is a good choice if no other option is available. The development of this process has the aim of carrying out a valid solution in those regions characterized by limited freshwater reserves and high availability of saline or brackish water. The main problem is the high energy consumption that characterizes the process, this is the highest among all methods used to get freshwater. Concerning this aspect, many works have investigated successfully the integration between desalination and renewable energy sources in order to make the process more sustainable.
Thanks to improvements achieved in these studies, desalination has been implemented on a large scale throughout World and has reached the target of 15906 plants installed [10]. Moreover, the cumulative desalination capacity is approximately 95.37 million of cubic meters per day of freshwater, which represents about 5% of domestic use [10]. This process had an exploit in Middle East and North Africa that hold almost half of global capacity installed (47.5%), followed by East Asia and Pacific (18.4%), North America (11.9%) and Western Europe (9.2 %).
Basically, seawater is collected and pre-treated before entering the desalination process. Pre-treatment stage is performed to get a physical separation of any substance different from the

saline solution such as algae, sand and waste. Following, solution constituents (brine and water) are physically separated via desalination process, that differs according to the technology chosen to drive the process. Finally, pure water undergoes a post-treatment process to get the right level of salinity depending on requirements for the final use.

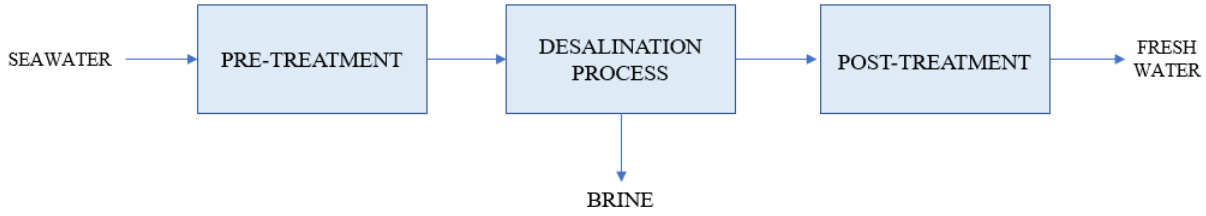

Figure 4. Basic scheme of desalination process [9]

Desalination technologies are divided in two main groups according to the different physical approaches used to treat saline or brackish water. These are:

- Thermal distillation
- Membrane desalination

Thermal distillation makes use of thermal energy to heat the treated solution up to reaching the vaporization point for water. Therefore, water in gaseous state separated from brine is condensed through cooling process; the primary challenge is to recover heat from condensation with the lowest temperature difference in order to maximize the efficiency of the process. The process can be integrated with solar-thermal or geothermal system used as heat source.
Membrane desalination is based upon the usage of filtration systems to physically separate water and brine. Reverse Osmosis "RO" is the representative of this category whose working principle can be explained as follows: electric pumps provide a pressure gradient that forces the solution to pass through a selective membrane, which allows the water flow and blocks solid salt particles. The process is electricity-driven, so it is usually coupled with solar photovoltaic system that works as energy source.
Next paragraphs provide an overview of main technologies currently used to perform desalination.

1.1.1 Thermal desalination process

In this subparagraph will be described the main processes actually used to drive thermal desalination. These are:

- Multi Effect Distillation
- Multi Stage Flash
- Vapour Compression Desalination
- Solar evaporation

Following a brief introduction to each process is presented.

1.1.1.1 Multiple Effect Distillation "MED"

Multiple Effect Distillation "MED" is a multiple stages process where feedwater is heated by steam in tubes [11] [12] The process is made of three or more evaporator called effects, characterized by a decreasing working temperature from the first step to the last. Considering a single effect, the heating process provides the evaporation of a share of feedwater which is separated from the brine, that is collected by gravity and extracted by centrifugal pumps. The produced steam enters the following stage and it is used as heat source to vaporize the remaining stream of feedwater. The process continues until the temperature of the obtained stream is high enough to drive an other stage, so the number of stages is limited by the minimum temperature difference between one effect and the next one. MED system also makes use of ambient pressure reduction in each step to enhance the spray effect on water and improve vaporization, without supplying additional heat after the first effect. The produced water is partially recycled to the external steam generator to cover water demand.

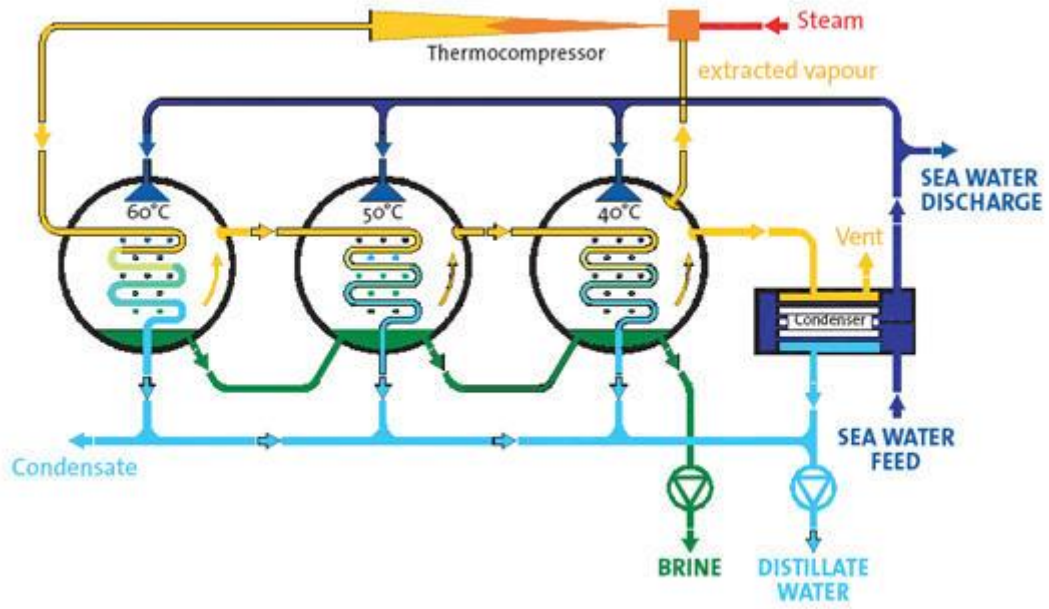

Figure 5. Multi Effect Distillation process [12]

MED unit account for 8% of global desalination capacity [13] with typical scale of 2000-10000 [m^3/day] and first effect working temperature of 70°C, so it can be supplied with low exergy heat either from industrial and renewables thermal systems.

1.1.1.2 Multi Stage Flash "MSF"

The multi-stage flash "MSF" distillation process is based on the principle of flash evaporation, where feedwater evaporates by reducing the pressure as opposed to raising the temperature [14] [12] The system is made of an heat source, a heat recovery unit and heat rejection sections, used to control the temperature of entering seawater and reject the excess heat provided by the brine heater. The MSF system usually works in a range of temperature of 90-120 °C, which increases at each stage without overcoming the related saturation temperature of heated seawater, that would minimize vapour production. At the same time, the consecutive pressure reduction allows the flashing of feedwater that starts to boil rapidly and separates from brine, used as heating medium. The evaporator is equipped with demisters to minimize carryover of

brine droplets, decarbonator to manage the formation of acid compound as those derived from CO_2, and vacuum deaerator to remove no condensable gases as O_2, N_2 and CO_2.
The water vapour is cooled by the cold seawater entering the flash chamber to get distillate, which is collected at each stage at the bottom of the chamber. Then, the latent heat released during condensation is used as heat source for the incoming stream, that goes from one stage to the next in order to make water vapour without the need of additional heat. Produced freshwater is characterized by low degree of salinity (2-10 ppm of dissolved salts), so it requires a post-treatments process to achieve potability.

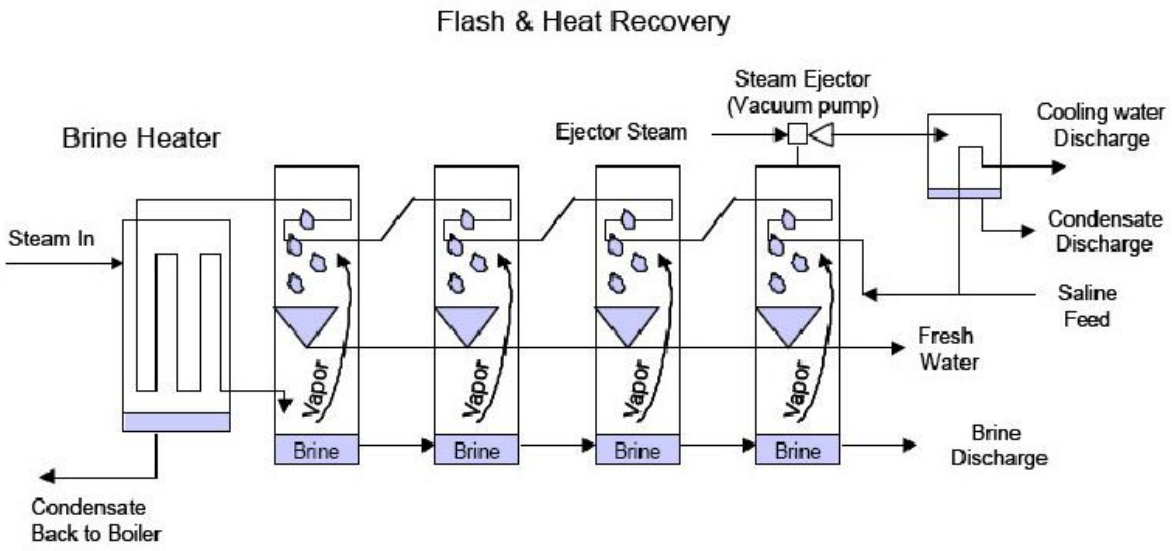

Figure 6. MSF schematic representation [12]

MSF technology accounts for 26.8% of total desalination capacity being the second most used process to distillate brackish and seawater. The common plant scale is 2500-75000 m^3/day [15] with an average energy consumption of 80.6 kWh of thermal energy plus 2.5-3.5 kWh of electricity per cubic meter of water produced.

1.1.1.3 Vapour Compression Desalination "VCD"

Desalination process based on the reduction of boiling point temperature of the solution by reducing the pressure in the evaporator [16] [12]. The main feature of VCD system is the heat source which is directly provided by the compression of vapour realized in two different ways:

- Mechanical compressor
- Steam jet compressor

The mechanical compressor electrically driven creates a vacuum within the evaporator and compresses the produced vapour. The pure water in gaseous state has high temperature and pressure, so it is circulated through the initial heat exchanger to heat incoming seawater that partially evaporates, increasing the share of vapour available. At the same time vapour is cooled by feedwater and freshwater is produced.
The steam jet compressor, also called thermo-compressor, uses a venturi orifice at the steam jet to produce vapour and takes it out the evaporator by generating a negative pressure gradient respect the ambient pressure. Freshwater in gaseous state is compressed by the steam jet, so it

become suitable for condensation. Therefore, the mixture releases thermal energy to the incoming feed through tube walls in the evaporator. In both cases the working temperature is below 70 °C, which an advantage in order to reduce risk of corrosion.

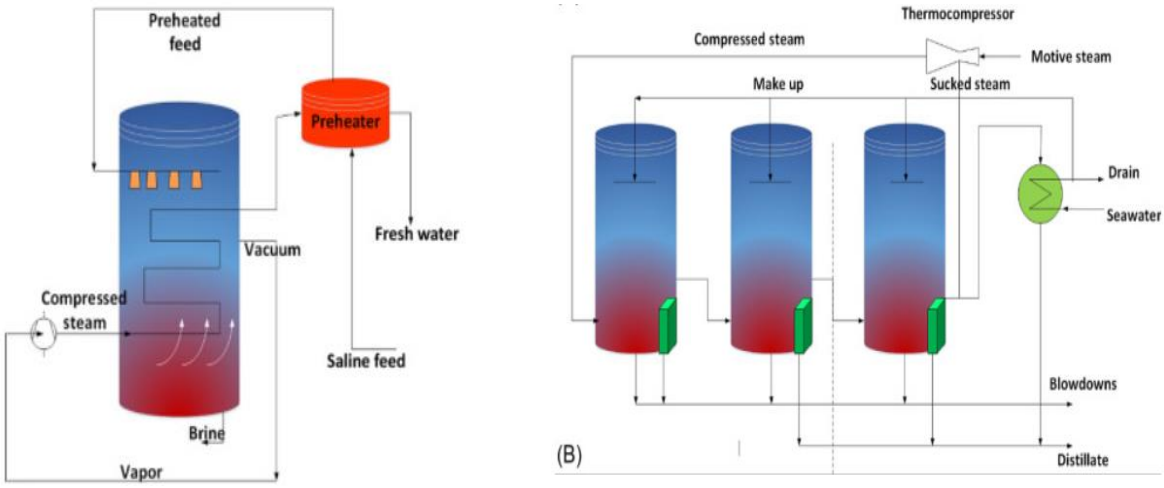

Figure 7. Schemes of mechanical (Sx) and thermal (Dx) VCD [12]

The production of mechanical VCD is constrained between 100-3000 m^3/day, whereas the capacity of steam jet system is much higher 10000-30000 m^3/day. Typically, these systems are installed for small-scale desalination units such as resorts, industries and drilling sites. VCD systems are quite simple to build and run, reliable and very efficient, indeed power consumption is about 8 kWh per cubic meter of freshwater produced.

1.1.1.4 Solar evaporation

The direct use of solar radiation for desalination purposes is the oldest method ever adopted and takes example from the hydrologic-cycle [12]. Indeed, energy from the Sun is used to realize the separation between water and brine in a fixed volume. Then water vapour is put in contact with a cool surface to perform condensation, so pure water is collected in droplets.
Greenhouse solar still is a practical example of technology based on this physical approach [17]. These are made of an airtight insulated basin covered with a tilted glass sheet that acts as cold surface. The inclination of glass sheet is required to guide pure water droplets toward the storage, avoiding the flow back to seawater solution. Solar stills are characterized by a simple architecture, that makes the technology interesting especially in rural and poor regions of developing countries. For this reason, many innovative schemes have been developed in order to increase efficiency and productivity. Unfortunately, results still show poor improvements and thresholds related to high investment costs, vulnerability to weather variations and requirement of large collector area to maximize productivity, that currently is 2-7 l/m^2/day depending on design of the system.

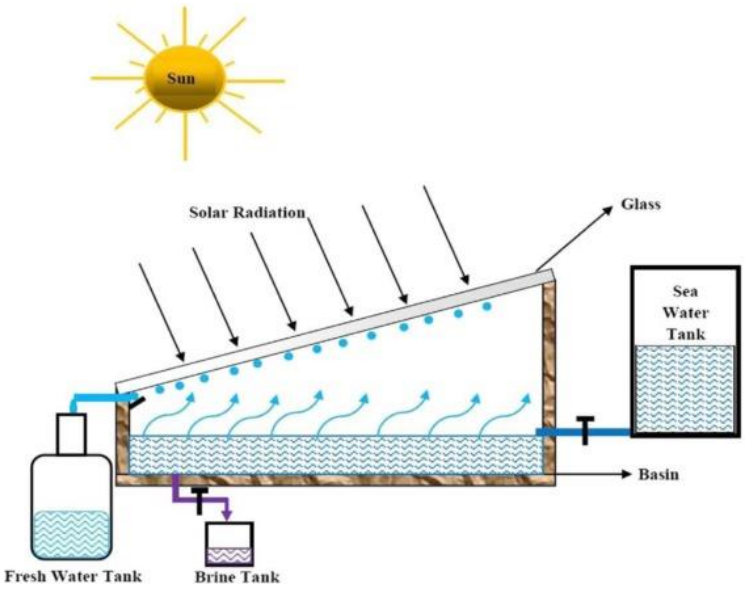

Figure 8. Representation of Solar still [17]

1.1.2 Membrane desalination process

The paragraph wants to describe methods used in membrane desalination processes. These are listed below:

- Membrane Distillation
- Reverse Osmosis
- Electrodialysis

Following a brief introduction to each process is presented.

1.1.2.1 Membrane Distillation "MD"

Membrane distillation process relies on the use of selective membranes to separate different physical phases as liquid and vapour. The process can be schematized as shown in the next figure.

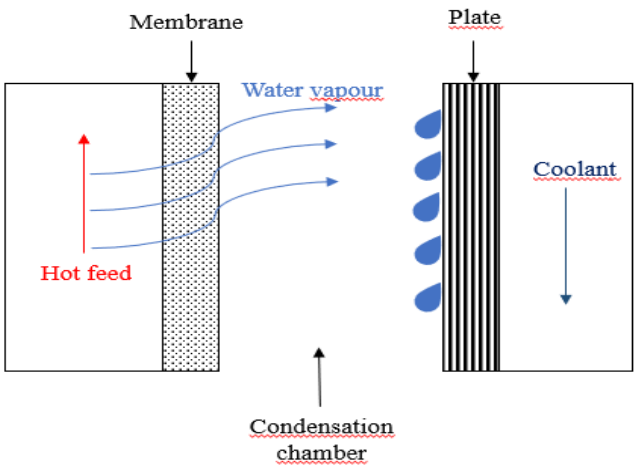

Figure 9. Scheme of membrane distillation

The hot feedwater releases vapour that passes through the membrane before reaching the cooling plate where condensation occurs. The membrane allows the passage of vapour phase only, while the entire process is driven by the partial vapour pressure difference between the two boundary surfaces, in turn derived from temperature gradient.
The membrane is made of hydrophobic synthetic material with pores diameter of 0.1-0.5 µm, characterized by non-polar molecules. Considering the polar nature of water molecules, no interaction between membrane and water is possible, therefore the material is not wetted by the liquid [18]. Moreover, even if pores size is much higher than the molecules, the strong water surface tension avoids liquid water enters the material. This mechanism takes the name of capillary action that has been widely investigated by Lee,Jongho Karnik, Rohit in [18]. In this process the membrane acts only as a barrier between two phases, without being directly involved in the separation. The main advantages of MD are the small operating pressure difference (hundreds kPa) and the low working temperature in the range 60-90 °C, that allows integration with low exergy energy sources.

1.1.2.2 Reverse Osmosis "RO"

Reverse osmosis [12] is the most widespread desalination process accounting for 60% of overall water treatment capacity. The process derives from the osmosis phenomena describable as follows: considering two solutions of the same solvents at different concentrations, putting these in contact through a semipermeable membrane that allows solvent flow only, we can observe the passage of solvent from the solution at lower concentration to that at higher level. This process happens naturally at ambient pressure in order to compensate the concentration gradient across boundaries of the membrane. RO desalination is based on the inverse reaction, therefore energy is required to force solvent of high concentration solution going through the membrane, so diluting low concentration solution and increasing the concentration difference. Considering desalination purpose, high concentrated solution is brackish or sea water whereas pure water is used in the other side of the membrane. The pressure gradient across the membrane is provided by pumps fed with electricity, whose duty is to increase feedwater pressure above osmotic value. The working pressure varies depending on the treated solution. Seawater usually requires 41-69 bar whereas brackish water 2-17 bar, but the effective value is direct proportional to total dissolved solids.

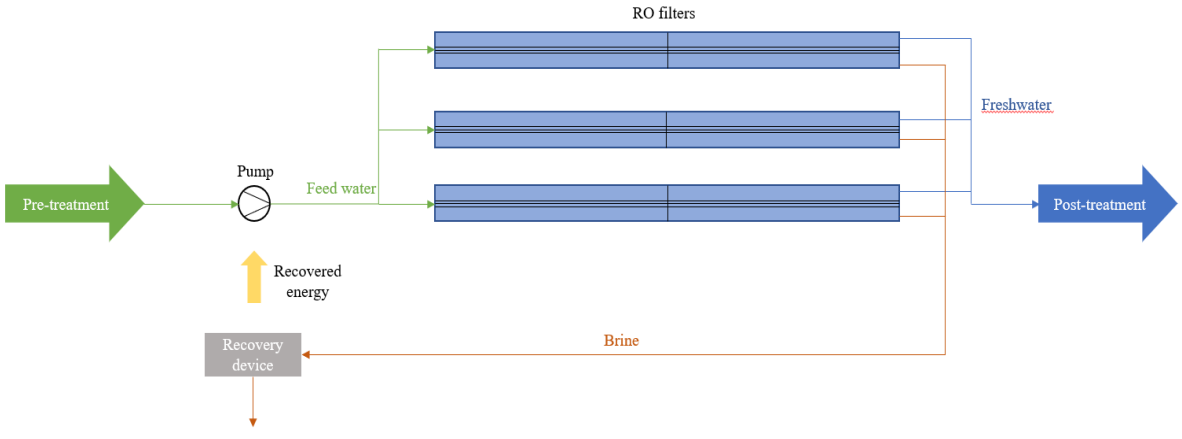

Figure 10. Schematic representation of RO system

The high penetration of this technology in the market has been pushed forward thanks to improvements in membrane resistance to compression, lifetime and separation capacity. Furthermore, the integration with an energy recovery device has sensibly reduced costs for water, decreasing energy consumption from 6-8 [kWh/m^3_{water}] to 2-5 [kWh/m^3_{water}]. These devices are able to recover the energy embedded in the brine exiting the process, which is converted to get back mechanical work. Nowadays the average production cost is 0.5 [$\$/m^3_{water}$] with a production capacity of 55-65 litres of freshwater every one hundred litres of feedwater.

1.1.2.3 Electrodialysis "ED"

Electrodialysis desalination "ED" is a water treatment process based on electrochemical reactions to perform salts separation [19]. The single stack is a multilayer structure composed by electrolyte membranes, electrodes, salt solution and water feed systems. Cathode and anode are used to generate a voltage difference across the stack that drives chemical reactions within each layer. Electrolyte is a polymeric compound able to transport ions with a fixed charge according to its chemical composition. Indeed these materials are characterized by high concentration of a specific ion which confers the skill of conducting that species only, avoiding the passage of any other molecule, ion or electron. These layers are called Ionic Exchanged Membranes "IEMs". Therefore, salt solution and pure water are respectively supplied to the inner and side chambers of the stack, separated by IEMs, and voltage gradient is applied to drive redox reactions in order to get chemical separation of species involved. Basically, the purpose of the process is to perform split of ions in solution with the aim of recombing them in different molecules easily removable. Pure water provides ions OH^- and H^+ while seawater generates K^+, Na^+,Mg^{2+} ,Ca^{2+}, SO_4^{2-} , Cl^-, derived from salts in seawater solution as NaCl, $MgCl_2$, $CaCl_2$, $CaSO_4$ and $MgSO_4$. IEMs work as barrier to nutrients migration, which prevents or allows ions from passing, in agreement with their electric charge. This varies ions distribution within stack chambers, that naturally interact each other producing solid or liquid compounds according to following reactions:

$$Na^+ + OH^- \rightarrow NaOH_s \quad (2.1)$$

$$K^+ + OH^- \rightarrow KOH_s \quad (2.2)$$

$$H^+ + Cl^- \rightarrow HCl_l \quad (2.3)$$

$$2H^+ + SO_4^{2-} \rightarrow H_2SO_{4_l} \quad (2.4)$$

$$Ca^{2+} + 2OH^- \rightarrow Ca(OH)_{2_s} \quad (2.5)$$

$$Mg^{2+} + 2OH^- \rightarrow Mg(OH)_{2_s} \quad (2.6)$$

ED is characterized by lower energy consumption than other distillation technology (1.5-4.0 [kWh/m^3_{water}]), modest desalination cost 0.7 [$\$/m^3_{water}$] and typical plant maximum capacity of 45000 [m^3_{water}/day].

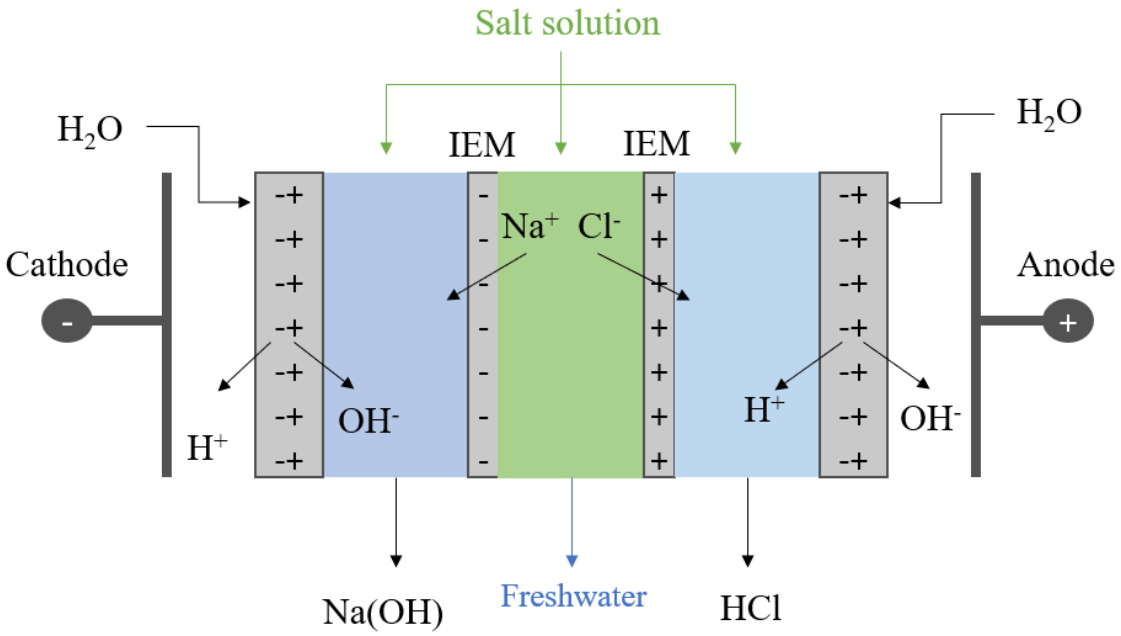

Figure 11. Electrodialysis process

1.2 Atmospheric Water Harvesting "AWH"

Atmospheric water harvesting "AWH" is a widespread process suitable to produce freshwater from ambient air. The development of this field has been pushed by the increase in air conditioning and dehumidification demands, strictly connected to rise in world population and climate change. In addition, it seems to be an alternative solution to water scarcity especially in arid and hot regions. Nowadays, technologies used to AWH can be classified in two categories: condensation and sorption. These differ according to the physical or chemical approach that drives the process. In such applications, physical parameters used to quantify comfort standards are temperature and relative humidity "RH", whose managing can be done through heat exchanges. Condensation technology is generally integrated in air conditioning system of any scale, and it is required in order to control humidity level in air used for space heating or cooling. RH can be easily reduced by cooling ambient air below the dew point in order to get an oversaturated mixture that produces liquid water.

Sorption process makes use of sorption materials in liquid or solid state to extract water vapour from air. The process can be either physical or chemical according to the type of bound formed between involved molecules [20]. Moreover, sorption processes can be classified in two categories: absorption and adsorption. In absorption process the interaction between absorbent and absorbed takes place inside the control volume without the occurrence of any chemical bounds. Instead, adsorption is a surface phenomenon where the adhesion of adsorbed material occurs only onto the surface of the sorbent. This is an example of chemisorption, indeed sorbent and adsorbed interact through Van der Wall's forces or covalent bonds. In addition, absorption process is endothermic whereas adsorption is exothermic, and the heat released is the sum of two contributes: latent heat of evaporation of the adsorbed liquid and the heat of wetting. In any case, sorption processes are suitable to manage RH level in environments since they directly

extract water vapour from air, while space conditioning can be partially performed using this method.
Performance of condensing technologies is often evaluated as harvested water per hour "WHR" and power consumption per unit mass of water harvested "UPC" , defined as follows:

$$WHR = \frac{m_{water}}{h_r} \quad \left(\frac{kg_{water}}{h}\right) \quad (2.7)$$

$$UPC = \frac{P}{m_{water}} \quad \left(\frac{kWh}{kg_{water}}\right) \quad (2.8)$$

Next paragraphs intend to provide an overview about procedures mainly involved in AWH.

1.2.1 Vapour Compression Cycle "VCC"

Vapour compression cycle "VCC" has been the first invented and commercialized cooling system, actually characterized by low expense, high efficiency and technological maturity at any scale. The working cycle is the inverse of thermal Rankine cycle, ideally describable as the occurrence of an isentropic transformation followed by isobaric cooling process, an irreversible expansion and an isothermal evaporation of the working fluid, that represents the useful effect provided by the machine. In practise the system is composed by a mechanical compressor either fed with electrical or mechanical energy, a condenser, a throttling valve and an evaporator. The pump initializes the process by increasing the pressure and the temperature of the working fluid up to feasible state to enter the condenser, where it is cooled following an isobaric curve. The refrigerant in liquid state goes through the throttling valve, which expands producing a liquid-vapour mixture ready to reach the evaporator. Eventually the working fluid absorbs heat subtracted to the external environment, vaporizes and closes the cycle. In this application, water production can be obtained at the evaporator level, where air is usually cooled below the dew point in order to manage both temperature and humidity.

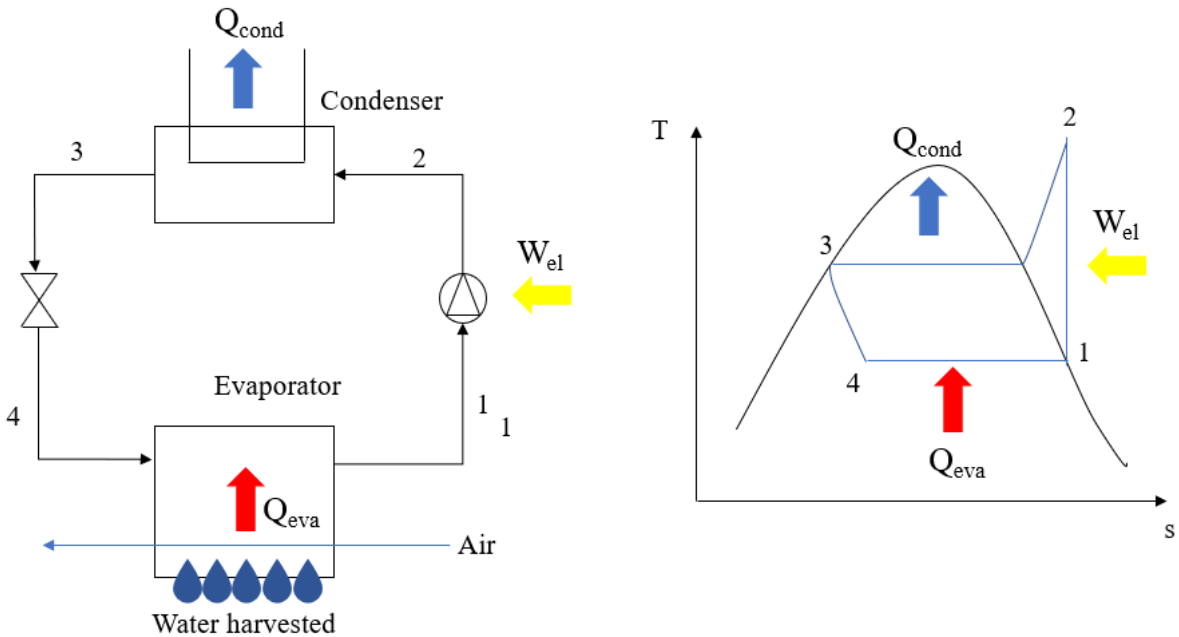

Figure 12. VCC system and working cycle

The evaporation step must ensure vapour phase only exiting the process in order to avoid failure of the compressor. Indeed, presence of liquid provides additional pressure load on the engines of the compressor causing the possible rupture of the system. The expansion process performed by the regulating valve is necessary to reduce the pressure in order to decrease the boiling point of the refrigerant below ambient air temperature.
Looking at water harvesting performance we discover that WHR varies in the range 1.5-425 [kg h^{-1}] while UPC is around 0.69-4.2 [kWh kg^{-1}], both functions of air inlet conditions, cooling capacity of the machine and working mode as air cooler or/and dehumidifier.

1.2.2 Thermoelectric Cooler "TEC"

Thermoelectric cooler "TEC" [21] [22] is an heat pump based on the Peltier's effect, that can transfer heat from one side of the device to the other using electrical energy as input. The system is made of boundary plates where cooling and heating process take place, and an inner layer made of two semiconductors opposite doped and alternated each other. The p-n type distribution generates a charge gradient that support the thermoelectric effect. Moreover, semiconductors pillars are connected thermally in parallel and electrically in series and finally embedded using a thermally conducting plate made of ceramic, that also avoid the need of an additional electrical insulator.
The Peltier's effect is the heat transport generated by a voltage difference across a thermoelectric device as the one described [23]. In particular, when voltage is applied and current flows through the device, this causes a charge transport in the p-n layer that drives the heat transfer between boundary layers. Therefore, electric work produces a temperature difference on the external surfaces able to provide either heating or cooling. In addition, cooling is performed without the usage of any refrigerant, avoiding problems of toxicity and refilling due to working fluid losses or fatigue failure.

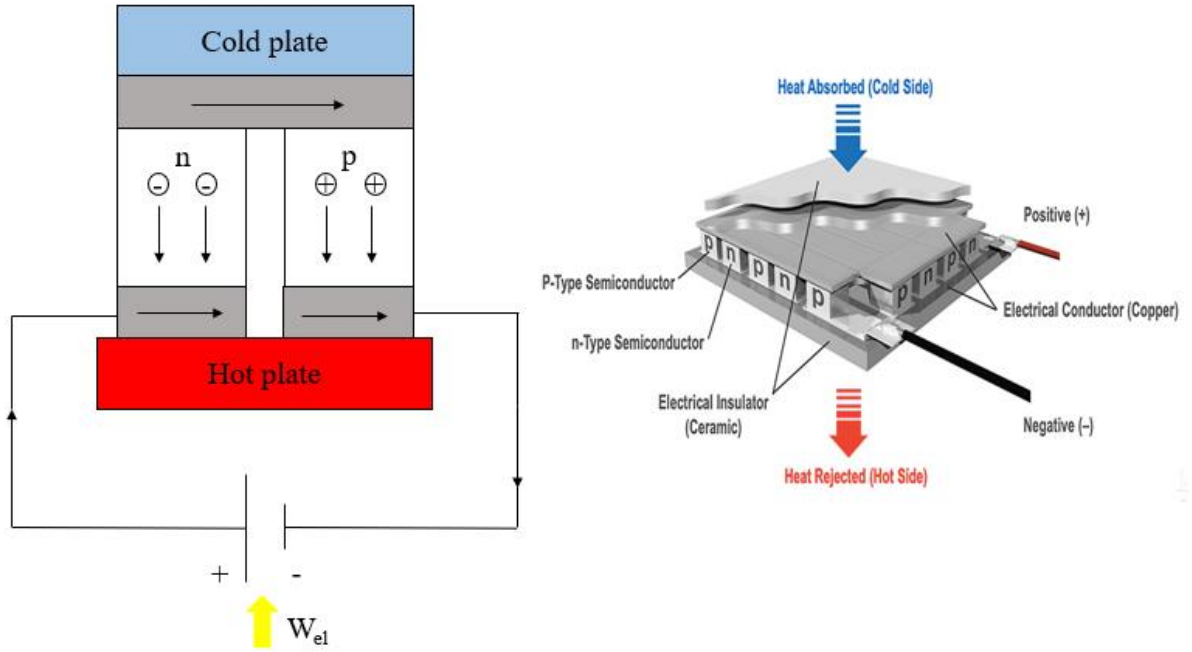

Figure 13. Scheme and 3D representation of TEC device [22]

The main feature of TEC device is the absence of moving parts, which limits the failure rate of the component, reduces vibration and increases the lifetime. As result, the system appearances very reliable. TECs are involved in many fields other than space conditioning, such as satellite and spacecraft applications, or informatic scopes. In the first example, TECs are used to avoid overheating of the craft side exposed to direct sunlight. Indeed, the device transfers heat to the cold and shaded side of the craft, that releases the energy in space as thermal radiation. In alternative, TECs provide cooling effect to hardware components since they can be made in a very compact volume. On the performance point of view TEC systems appear very limited. Actually energy efficiency is lower than other cooling technologies such as VCC and the heat flux generated per unit of area is constrained to small values, limiting the application.

1.2.3 Absorption Chiller

Absorption chiller is a well-known technology that realizes the compression of the refrigerant using thermal energy instead of electricity, therefore the mechanical compressor is substituted with a thermal compressor that works with proper liquid refrigerant/sorbent solutions [24]. The working fluid is usually an aqueous solution where water can act either as refrigerant or absorbent according to the chosen mixture. Ammonia water NH_3-H_2O and lithium bromide LiBr-H_2O are typical solutions used in absorption applications. The refrigerant is the most volatile chemical species among the two, so in the previous examples these are ammonia and water respectively. In any case, absorption chiller can be schematized as a closed system made of four heat exchangers, two throttling valves and an internal recirculation pump. The system can be divided in two sections, one that manipulate the solution made of generator and absorber, and the other used to achieve the useful effect constituted of condenser and evaporator. Basically, solution at high concentration (strong solution) is heated up to get the evaporation of the refrigerant. The vapour of pure solvent is cooled in the condenser and forced through a regulating valve, that further reduces temperature and pressure. The liquid refrigerant enters the evaporator and absorbs heat extracted from the internal environment, achieving the gaseous state. Finally, the refrigerant reaches the absorber together with the weak solution from the generator, that has been forced to pass through a second throttling valve in order to meet physical requirements of the other stream. Therefore, the strong solution is restored and pumped to the generator to start another cycle. The useful effect can be obtained either at the condenser or the evaporator according to heating or cooling need, indeed the machine works as common heat pump . Therefore, the coefficient of performance “COP” can be defined as heating device or chiller.

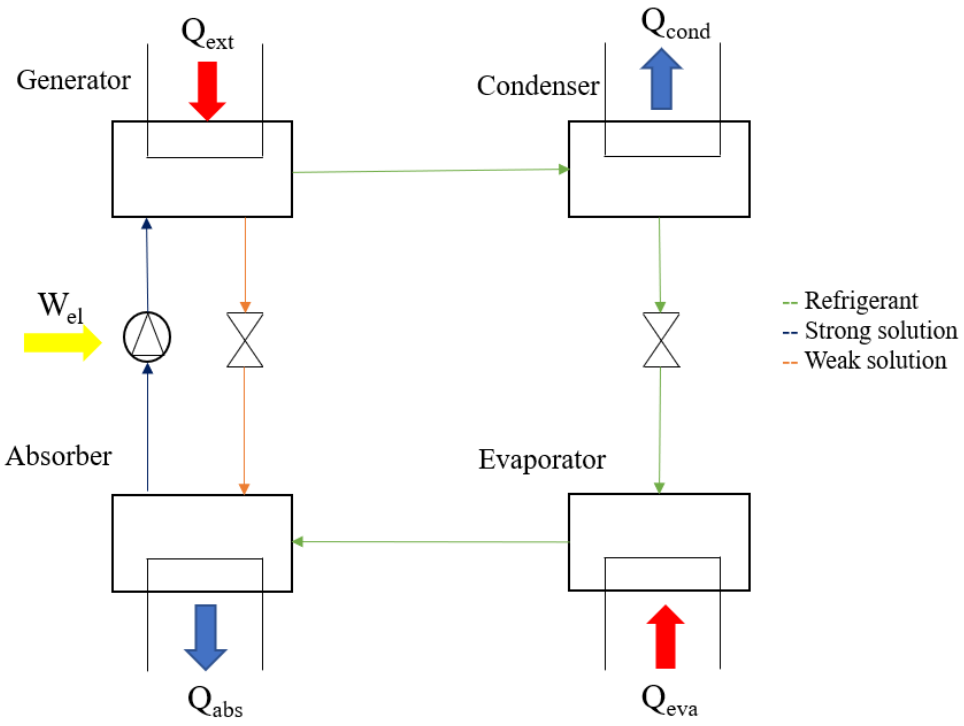

Figure 14. Working principle of absorption chiller

An internal heat recovery is performed between the solution exiting the absorber and the weak mixture leaving the generator. Water harvesting can be performed at the evaporator level by cooling air below the dew point. In this way both temperature and humidity can be controlled. Water harvesting efficiency has been carried out from literature looking at the paper of Ibrahim et al. regarding absorption chiller driven by solar thermal energy [24]. WHR typical values are 5.1-6.6 [kg h^{-1}], whereas no references for UPC have been found .

1.2.4 Adsorption Chiller

Adsorption chiller is a new and eco-friendly technology suitable for air cooling and dehumidification, belonging to the sorption categories for AWH. The process uses solid or liquid sorption substances as water adsorbent, coupled with a liquid refrigerant to provide the conditioning effect. Solid sorption systems make use of silica gel as adsorbent and water as refrigerant. The adsorption property of silica gel comes out from its high porosity, indeed 1 m^3 gel has pores surface of about $2.8x10^7$ m^2 [25].The system is made of adsorption chambers and salt solution storages, in addition to other common components such as fans and pumps. The usage of different adsorption chambers is required since the solid material cannot be circulated. The entire process is driven by a thermal compressor instead of a mechanical one. Moreover, the use of fixed adsorbent requires no moving parts other than regulating valves. Therefore, these systems are usually characterized by low vibration, high reliability and long lifetime.
Thermal energy is supplied to the dilute solution that releases water in gaseous state. Vapour reaches the condensation chamber where cooling source performs condensation before the expansion step. The substance passes through a throttling valve that deceases pressure and temperature of the mixture up to requirements of the evaporator, where the cooling effect is achieved. Indeed, evaporator takes heat from the external environment, decreasing the

temperature of the outlet working fluid. As consequence, water evaporates and it is adsorbed. Considering the exothermic nature of adsorption, a cooling tower is used to manage the temperature and the pressure of the sealed system. As explained for the previous technologies, water harvesting can be done in the evaporator, where the heat exchange can lower the temperature of the feed air below the dew of the feed air.

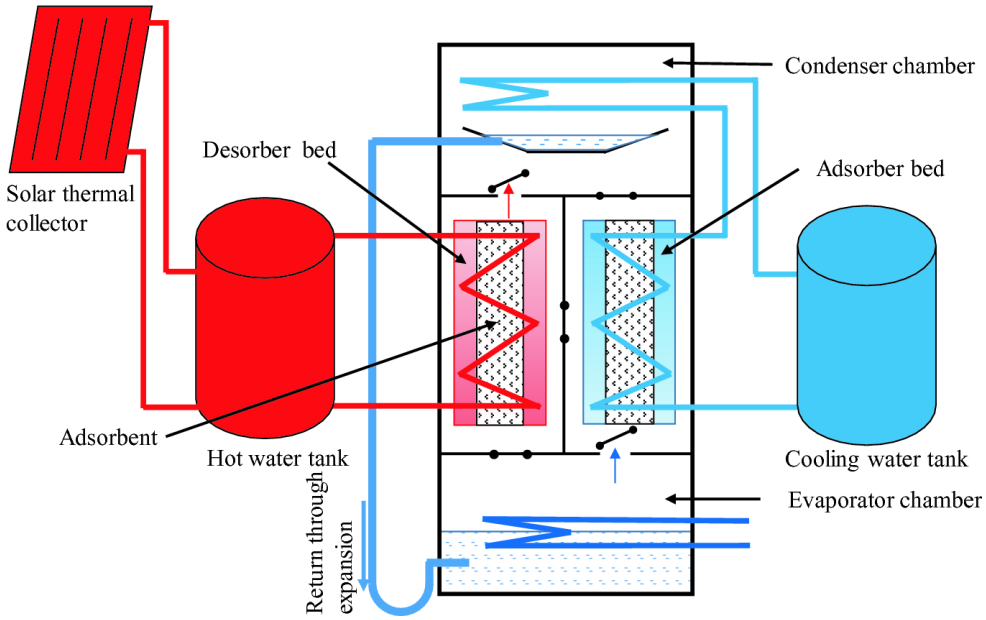

Figure 15. Adsorption chiller system [26]

The main advantage of adsorption chiller is the low-grade heat required to drive the process. Usually, regeneration phase needs thermal energy supply below 100°C, but applications with silica gel as adsorbent require heat fed in a range of 50-70 °C .

1.2.5 Fuel Cell

The alternative solution to produce freshwater is represented by the fuel cell, an electrochemical device able to drive spontaneous redox reactions in order to deliver electric power and water as by-product. Fuel cells are an example of open electrochemical system where reactants and products are respectively supplied and delivered from/to the external environment. The working principle makes use of free electrons released during the oxidation step to generate current flow and voltage across electrodes of the system. Water synthesis is a widespread reaction used in fuel cell applications; therefore it will be taken as example to describe the system in details, considering also the purpose of this chapter.

An isolated cell is formed by three layers and an external circuit required to deliver power. In boundary layers redox reactions take place, while the last one works as selective membrane for ions. This layer is called electrolyte and has the ability of transferring ions blocking the passage of electrons. The others are called anode and cathode. At the interface between electrolyte and boundary layers an additional material is used as bridge for ions transport. This portion is occupied by the catalyst, substance in solid state able to reduce the energy required to obtain an activated complex in the site of reaction. Practically, the catalyst participates to the reaction without modifying the chemistry, but it only improves the kinetic acting only as substrate where the charge separation happens. Moreover, catalytic reaction is a type of adsorption process

between a fluid and the solid surface of the catalyst, driven by thermodynamic parameters as temperature, pressure and moles adsorbed.
The process begins by suppling separately hydrogen and oxygen to boundaries, then the external circuit is closed and the electrochemical reaction starts. The material used for the electrolyte influences the half reactions at anode and cathode since it defines the direction of ions within the cell. Currently the most used electrolyte are Nafion and Yttria-stabilized zirconia ("YSZ"), respectively involved in the two representative FC technologies: proton exchanger fuel cell ("PEMFC") and solid oxide fuel cell ("SOFC"). In PEM fuel cell, the electrolyte transfers hydrated protons H^+ requiring a minimum degree of humidity for the membrane. Indeed, ions transfer in Nafion is performed by water clusters, whose ionic conductivity is proportional to water content within the membrane. Therefore the need of membrane humidification forces the system to work at temperature lower than 100°C , usually constrained in the range 50-80 °C, and at ambient pressure. Considering the kinetic of the process, this is not improved by temperature since its low value, so platinum is used as catalyst in order to improve the rate of reaction. Platinum is a high-quality catalyst that suffers poisoning from carbon-containing molecules, forcing the system of being supplied with high ultra-pure reactants. SOFC instead has opposite properties, indeed YZS ionic resistivity is inverse related to temperature and it offers best performance for temperature above 700°C. The high working temperature per se enhances the kinetic of the reaction, without the need of high-quality catalyst conferring very good fuel flexibility. On the other side, the machine is not dynamic and is affected by slow start, due to the transient needed to reach the working temperature. In addition, investment costs are badly affected by high quality materials for auxiliaries that must faces high thermal loads. Next figures show the scheme of both types of FC, outlining differences in half reactions imposed by the electrolyte.

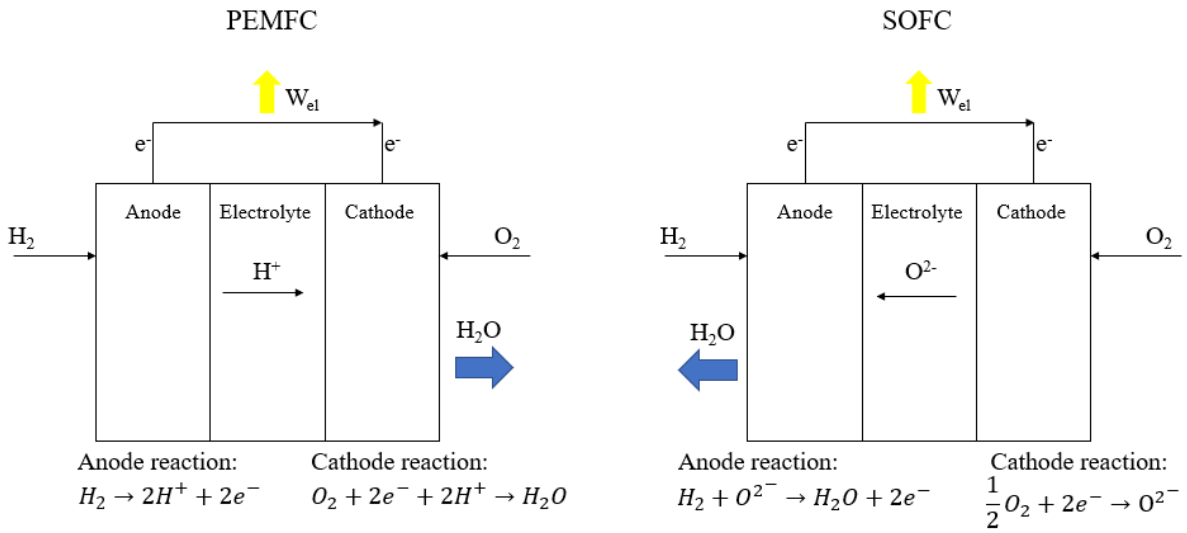

Figure 16. Working scheme of fuel cell technologies

The schemes provide an overview of how fuel cells work, but these represent only a single functional unit of the entire system. Indeed, a stack is made of many cells' series connected and embedded between two end-plates, which represent anode and cathode of the stack. The electrical connection is performed in order to increase the voltage, whose typical value is 0.5-0.6 V per single unit. Water productivity depends on the size of the device and it can be

calculated using the Faraday's law, that carries out the relationship between species reacting in an electrode and the current "I" that flows in the external circuit.

$$n_i = \frac{I}{z_i * F} \left(\frac{mol}{s}\right) \quad (2.9)$$

where:

- "F" is the Faraday's number equal to 96487 [C/mol]
- "z_i" is the number of electrons delivered or recombined in the complete redox reaction, for water z_i is 2.

Water is partially used inside the stack in order to increase the efficiency of the process. In PEMFC, water is required to keep humid the electrolyte membrane constantly dried by the internal heat produced during adsorption. In SOFC water is partially recirculated at the anode in order to avoid problem of carbon deposition and to increase the kinetics of the process. The usage of water as oxygen carrier, produces the steam reforming of methane entering the anode, delivering hydrogen and carbon monoxide which becomes the new fuel, characterized by higher rate of reaction. The remaining water extracted from the system requires post treatment process to ensure potability. Moreover, FCs deliver electric power and thermal energy perfectly suitable to drive auxiliaries or integrated processes. These systems are not already commercialized on big scale because of high investment costs which causes no payback time before the end of the lifetime, due to huge expense for construction materials. Anyway, FCs have huge potential if compared to common technology. Indeed the average conversion efficiency is higher 60%, so future developments are focused on capital cost reduction to ensure production on large scale.

1.3 Groundwater Extraction

The last alternative for water collection is represented by groundwater extraction. Basically, the process makes use of underground reservoirs of freshwater derived from the natural hydro-cycle. Indeed, freshwater from rainfalls can be collected in rivers and lakes or it can fall on the ground and absorbed by the soil starting a natural process of diffusion led by gravity [27]. According to different geological soil structure, water permeates different layers up to achieve a natural underground cave made of hydrophobic material. The cave acts as natural basin to store freshwater suitable to cover local water demand. These natural storages are currently used as freshwater resources in many regions of the word thanks to the development of extraction techniques.

Groundwater extraction requires a well to reach the natural storage and a pump to extract freshwater. According to the size of the storage and to the rate of extraction, feasibility studies must be performed in order to ensure mechanical stability to the soil. Indeed, the lack of underground water layer provides an empty space that causes the slipping of ground with direct consequences on structural integrity of above layers. Preliminary analysis is performed by taking soil samples in order to understand the lay of the land and the underground distribution of water. The aim is to find out a map of groundwater reservoirs, underlining eventual connections and estimating the size to carry out the techno-economic analysis, that should provide positive results in order to realize the opera.

Soil draining can be done in several ways, but one of the most widespread is the Wellpoint system [28], suitable for land characterized by high porosity. Once having identified the natural storage, a series of mini wells are installed in that area realising an interconnected network through the use of manifolds. Vacuum pumps extract water by depressurizing each single channel, indeed the pressure gradient pushes water to leave the storage and reach the ambient surface. Once the pumping process takes place, the depressurization affects also ground layers around the well generating a cone called “cone of influence”, whose amplitude is affected by soil characteristics.
Wellpoints are equipped with filtration devices to avoid the extraction of debris with water. These are meshed with different diameters, usually made in steel. The usage of mesh introduces pressure drops proportional to the length and filtering capacity, which has to be taken into account during the project phase, in order to size the pump properly. The number of weelpoints is function of the hydraulic mass flow taken out the ground, strictly dependent on soil permeability. Indeed, high permeable soils usually characterized by the presence of sand and gravel, require high pumping power since the mass flow involved is high. On the contrary, in grounds with low permeability (silt and clay) hydraulic mass flow is much lower, so it is the power needed to drive the draining process. Summing up, the power for extraction is function of the hydraulic mass flow taken out from the ground. As consequence the number of extraction sites is function of soil permeability, therefore the same number of wellpoints can be used to drain underground reservoirs of different size considering the same drawdown.

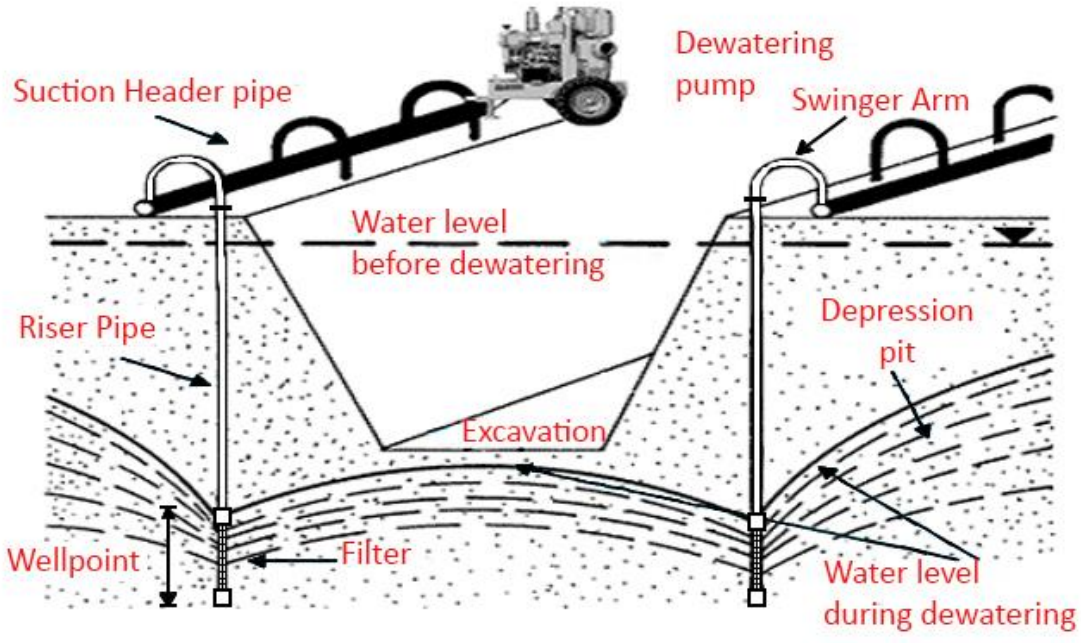

Figure 17 Wellpoint system design [28]

Wellpoint systems are used also in building structure field as tool to temporary reduce groundwater level during the excavation phase. In particular these system are suitable for several applications involving water extraction. These are :

- Water supply from underground reservoir
- Management of groundwater levels
- Water extraction for agricultural purpose
- Seawater extraction for desalination plants
- Groundwater extraction in landfill sites to avoid reservoir contamination

Wellpoint system represents the cheapest and easiest solution for groundwater extraction, but it still faces several limits related to soil stratigraphy and composition.

2 Breath System

In the present chapter Breath system for atmospheric water harvesting will be described in all its components and working principle. The system has been developed by the energy department "DENERG" of Polytechnic of Turin in two different configurations based on the same working principle. The first type is the lab prototype designed to test the capability of the device, whereas the other configuration has been constructed with an improved design that could be suitable for commercialization. In both cases, this device is a water producer that makes use of adsorption material to harvest water vapour from atmospheric humidity. The material chosen for the application is Silica gel, a polymer derived from silica dioxide with proved adsorption property. Indeed, Silica gel is a porous medium characterized by high specific surface area that allows water vapour capture under specific thermodynamic condition [29]. This material has been widely used in industry either as desiccant and chemical reactant for chromatography thanks to the high knowledge matured. Anyway, the object of the chapter is the device designed for commercial purpose, whole embedded in a cubic structure of 1 meter side. Basically, the system makes use of two heat exchangers to perform adsorption and desorption alternately, in order to maximize the performance by reducing timeframe between these stages. Indeed, common applications use a single heat exchanger that drives separately adsorption and desorption, avoiding any chance of performing them at the same time, so limiting the efficiency of the entire system.

Breath is integrated with thermal solar collectors that supplies the heat required to drive regeneration of silica bed inside the heat exchanger. In this prospective, this device aims in being environmentally friendly as much as possible according to decarbonization guidelines.

Looking at the physics behind the phenomenon, it is important to underline different requirements of process steps in terms of thermodynamic inlet conditions of working fluids. Figure 18 provides a simplified scheme of system operation.

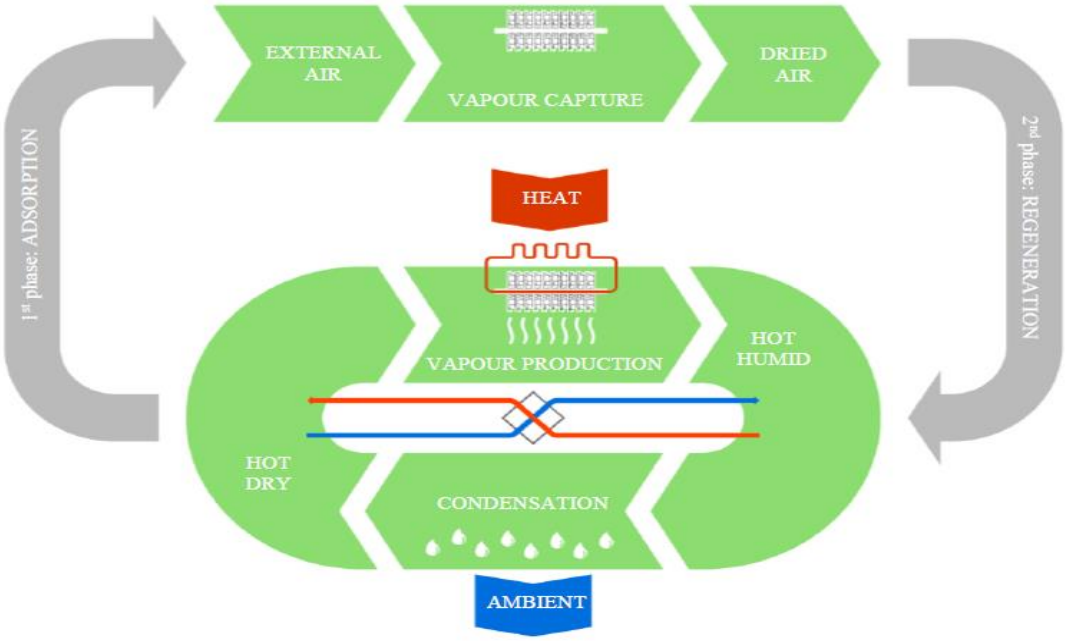

Figure 18. Schematic description of Breath working principle

The process begins with adsorption. Therefore, ambient air is forced through the heat exchanger where interacts with silica bed that adsorbs water vapour. The exothermic nature of adsorption provides an outlet air stream characterized by low moisture content and higher temperature than the inlet one. This step is performed in a closed loop in order to adsorb as much water as possible, therefore air is recirculated continuously during the process and eventually it is rejected in the external environment. Once sorption bed reached the saturation point, the following step regards water collection. Therefore, desorption is driven by regenerating the silica bed. Indeed, a peculiar feature of silica gel is its variation of water affinity with temperature. In particular, the gel presents hydroscopic property for temperature below 50°C whereas it is hydrophobic above this threshold. Moreover, desorption process is endothermic, so it requires heat to be performed. For these reasons, regeneration is realized using water flow at 50-80°C supplied by the solar thermal circuit. This hot water stream has two useful effects: firstly the heating of the sorption bed that initializes the oozing process, secondly it enhances the moisture gradient between inlet and outlet because air stream for desorption is heated isothermally. Indeed, common sorption processes follow an isenthalpic transformation, so during regeneration air stream increases moisture content and decreases the temperature, passing from point 1 to point $2_{iso\text{-}H}$ in Figure 19. Then air charged of vapour goes inside the condenser to harvest water. Unfortunately this process has limitation, indeed the moisture difference between inlet and outlet of the condenser is almost 4-5 [g_{water}/kg_{air}] , therefore water production is very limited and also related to sensible heat exchange. In this context the isothermal heating of incoming air is a perfect trick to improves water harvesting. According to the transformation, air stream for regeneration is heated through latent heat to reach the saturation curve of psychrometric diagram, in point $2_{iso\text{-}T}$. The improvements are clearly visible, in fact the moisture content of this point is much higher than that of $2_{iso\text{-}H}$, which is translated in a proportional increase in water harvested during condensation. This improvement is graphically shown by the higher distance between point 3 (air state after condenser) and point $2_{iso\text{-}T}$ along the saturation curve. The same result could be achieved by increasing the temperature of air in state 1 above 70°C, but it would require a substantial amount of thermal energy.

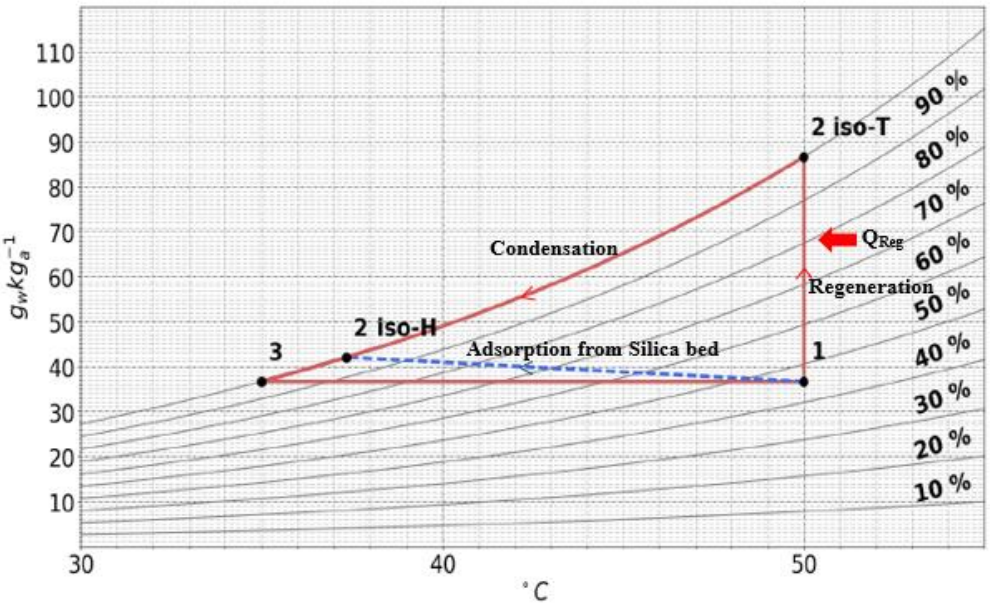

Figure 19. Psychrometric transformation of working air for regeneration

2.1 Components description

The paragraph offers a detailed overview of components and sensors within the hardware of the prototype. The system is characterized by three loops, one works with ambient air while the others respectively manage harvested water and water for regeneration. These two are:

- The condenser circuit: closed loop that collects water by condensing vapour extracted from silica bed and delivers heat to external environment.
- The solar circuit : closed loop acting as heat source of the system, indeed it delivers the heat needed during regeneration using thermal solar collectors and water as working fluid.

Instead, air loop has the duty of taking in and out the system ambient air, whose pathway is regulated by a 4-way valves able to alternatively address air to regeneration and adsorption loops. A brief description of components will be given following.

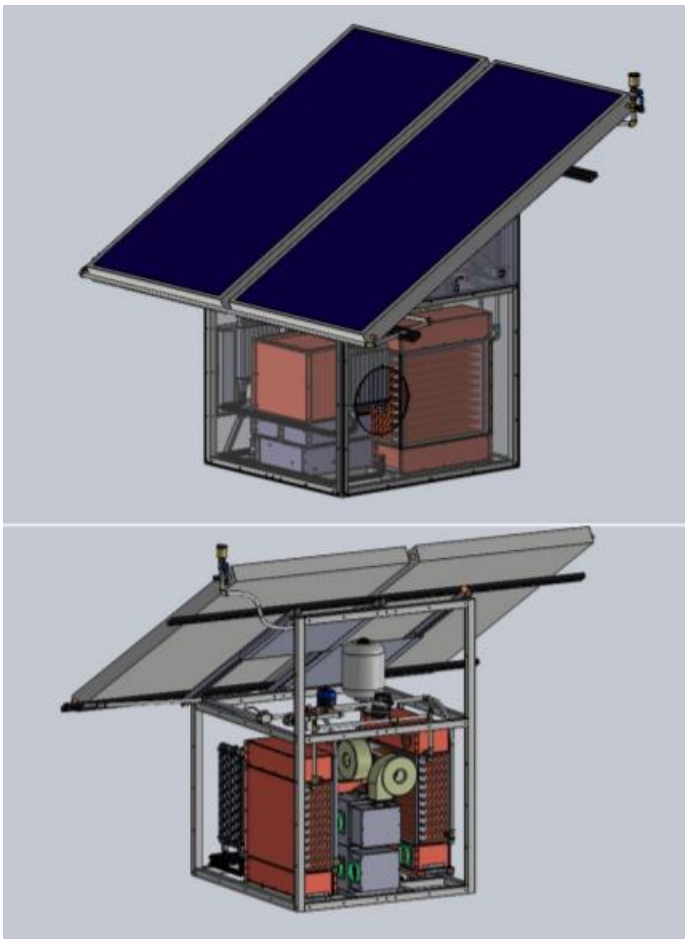

Figure 20. 3-D representation of Breath

Solar collectors. A pair of flat plate solar collectors is installed on the top of the machine with a tilt angle of 30°and 2 [m^2] of gross area each. In addition, the design allows both parallel and series connections according to project specifications.

Batteries. The two batteries within the system are conventional heat exchanger filled with silica gel spheres of 3 [mm] of diameter. The geometry of each battery is 630x485x190 [mm] and these are installed symmetrically on left and right sides of Breath considering the frontal view. The total mass of silica embedded in a single battery is 18.77 kg.

Figure 21. Adsorption battery

Condenser. The condenser is in charge of cooling air stream below the dew point and pre-heating the air exiting the system directed toward the adsorption battery. The entire process is realized separately in the upper and lower sections of the condenser. In particular, the upper part is equipped with a heat exchanger used to cool down the stream before reaching the bottom of the condenser. The heat extracted goes to the battery involved in regeneration, in this way an internal heat recovery is performed. In the lower part condensation takes place using a radiator interconnected with the condenser circuit, that customs water as working fluid. After air cooling, freshwater is collected at the bottom and water flow of condenser circuit is regenerated. This process is performed by two radiators that treats half of the total mass flow involved and exchange heat with ambient air, used as cold shaft.

Double four-way valve. The double four-way valve is the component responsible to switch working function of heat exchangers, from adsorption to regeneration and vice versa. It makes use of an actuator placed on top to change the position of the inner shaft, that alternately closes 2 out of 4 ways available.

Figure 22. Four-ways valve

Fans. The system presents a total number of four fans, two used to move air in the regeneration/adsorption circuits (F2 and F1 respectively) and the others (F3 and F4) embedded in the condenser circuit to cool down water flow. The firsts are centrifugal blowers with nominal rated power of 65W, where only F2 can be regulated to test the system at different flow rates. Fans in the condenser are axial type characterized by maximum rated power of 170W with the possibility of being regulated.

Figure 23. Centrigugal (Sx) and axial (Dx) blowers

Sensors. The system is equipped with several sensors that constantly control temperature and relative humidity of the process.
In particular, temperature sensors are LM35 type thar supplies an output voltage linear function of the temperature measured in input. The accuracy of the instruments varies according to ambient temperature from a minimum of +-1/4°C at T_{amb}=25°C to a maximum of +-3/4°C over the full range [-55,150]°C.
Instead relative humidity is constantly controlled by the HIH-4000 Series Humidity Sensors, which realizes the analogical-analogical conversion suppling linear voltage in output. Moreover, the accuracy of the sensor is +-3.5%.

In both cases sensors provides analogical outputs, then converted by controllers which acts as the brain of the entire process. The next table summarises all sensors involved, location and fluid checked.

NAME	FLUID	TYPE	LOCATION
TBD1	Air	Temperature	Inlet Bed Dx
TBD2	Air	Temperature	Outlet Bed Dx
TBS1	Air	Temperature	Inlet Bed Sx
TBS2	Air	Temperature	Outlet Bed Sx
TBD3	Water	Temperature	Inlet Bed Dx
TBD4	Water	Temperature	Outlet Bed Dx
TBS3	Water	Temperature	Inlet Bed Sx
TBS4	Water	Temperature	Outlet Bed Sx
TC1	Air	Temperature	Inlet Condenser
TC2	Air	Temperature	Outlet Condenser
TPD	Water	Temperature	Outlet Solar Collector Dx
TPS	Water	Temperature	Outlet Solar Collector Sx
RHBD1	Air	Relative Humidity	Inlet Bed Dx
RHBD2	Air	Relative Humidity	Outlet Bed Dx
TAMB	Air	Temperature	Ambient

Table 1. Sensors inventory

Arduino. Arduino is a Programming Logic Controller “PLC” used to collect and read signals coming out from sensors. It is used as intermediate component between sensors and Controllino, whose function is explained below.

Controllino. Controllino is a PLC usually involved in industrial application, suitable for receiving analogical signals and converting these in analogical or digital output to components of the system. In practise, this device implements a control logic program in order to enhance the performance of the system.

Loadcell. The loadcell acts as scale to measure the weight variations of the battery. Indeed, the heat exchanger varies its mass according to adsorption and desorption phase performed, therefore the total amount of water collected from air can be easily evaluated having knowledge of mass of empty battery.

3 Hydroponic Greenhouse Culture

In the following chapter, the greenhouse developed by DENERG at Energy Centre will be described in detail. The greenhouse has been developed with the purpose of being a useful tool for different experimental studies involving the energy-water-food nexus.
The innovative feature of the system is the development of hydroponic technique for plant grow, as substitute of common agriculture. Therefore, the chapter begins with a brief introduction regards hydroponic culture, then continues with the description of the greenhouse and components. In this work the greenhouse has been integrated with Breath system, in order to carry out the capability of this device in sustaining user requirements.

3.1 Experimental greenhouse

The hydroponic culture is a substitutive technique to common agriculture based on soil-free cultivation, where the ground is substituted with an inert substrate and the plant is fed with nutrient solution at high minerals content [30]. This technique can be considered as the upgrade of traditional method since it improves the productivity and quality of products, reduces both water consumption and land use, and eliminates the presence of parasites. The absence of soil provides several advantages to cultures. The entire system achieves a reduction in control variables needed because less factors contribute to plant development. Indeed, monitoring in agriculture is quite complex and not always achievable due to the unpredictable behaviour of ground in terms of water losses, nutrients adsorption and distribution, Ph, and mechanical stability, which is influenced by atmospheric conditions [31]. Ultimately, the ground plays three roles in common agriculture: it works as anchoring substrate for the plant ensuring mechanical stability, it supplies all nutrients required by the culture and it promotes interactions both positive and negative with other organisms.
In hydroponic cultures the anchoring function of soil is successfully substitute by wires where required. Indeed, many cultures do not need external mechanical support other than the intrinsic one. The usage of inert substrate is adopted to improve diffusion and adsorption of nutrients embedded in the fed solution; therefore, the substrate should be characterized by porous and aseptic materials to ensure the best growth of the culture. Thanks to substrate properties, roots do not develop as in traditional agriculture, indeed the plant finds every nutrient in the thick inert layer and the root has no anchoring duty. Moreover, the absence of soil avoids any possible interaction with other organisms, deleting any chance of contamination. The nutrients solution is usually supplied by a fertigation system, which manages the fed according to the type and the actual condition of the culture. Culture state is evaluated through the monitoring of the following parameters: Ph, electric conductivity, mass flow rate and chemical composition of nutrients solution. This monitoring process is performed in closed loop, the fed is used to optimize Ph and electric conductivity, which represents the drivers of the entire system.
The greenhouse developed at Energy centre is characterized by the Nutrient Film Technique NTF, a configuration with no inert substrate and stepwise function of fed solution. A water pump is responsible for the fed, that is delivered to growth tray and collected at the bottom. Special attention must be payed to the nutrient flow, indeed undesired stop will provide a dried environment, very stressful for plant growing.
Once the fed reaches the growth tray, plants naturally orients roots toward the flow, developing their structure deep into the tube. The tray is slightly tilted to set the direction of solution flow,. This configuration avoids waste of solution, indeed the excess is collected and reinserted in the

reservoir. The absence of inert substrate ensures lower capital cost and still high performance. In particular, NFT systems are suitable for short term cultures, with a growth-time around 30-50 days.

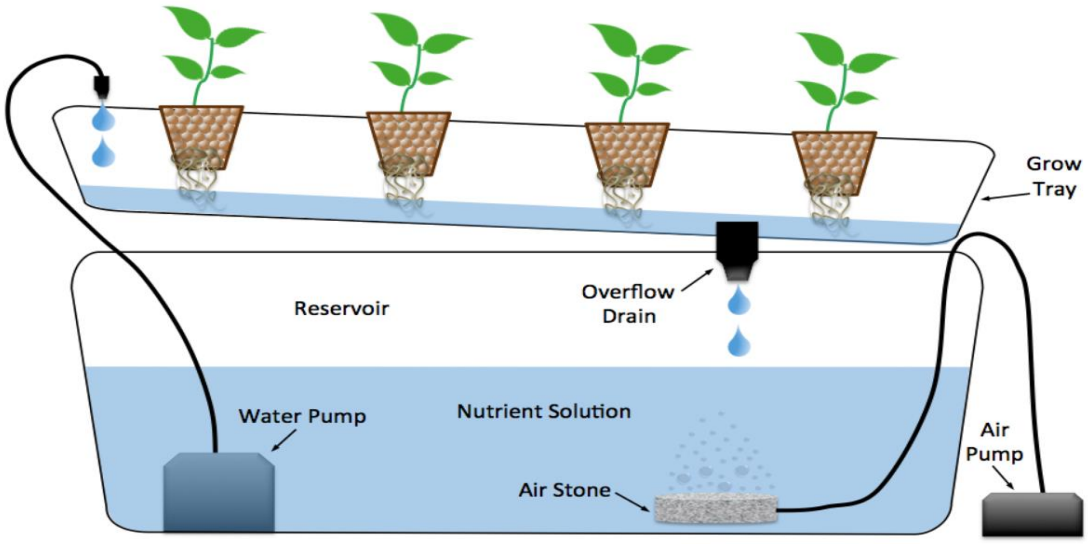

Figure 24. NFT general configuration [30]

The experimental system is composed by an external structure in aluminium with a plastic cover used to create an insulated environment and by a warehouse to host components that regulate the process. In the warehouse we find two vessels respectively used to store freshwater and nutrient solution, a fertigation device, a hot water storage and an electric panel.
The greenhouse hosts two cases where the culture is placed. The cases are isolated from the external environment using plexiglass sheets all along sides of the parallelepiped structure, in this way it is possible to control the amount of air available to cultures. Plexiglass sheets have been installed on aluminium profiles properly designed according to the existing structure. Aluminium supports are used because of better mechanical and thermal resistance respect silicon, which may provide mould formation in humid environments.
Each case is equipped with three grow trays where plants are hosted and fed solution flows inside, and inlet and outlet collectors respectively used for distribution and collection of feeding flow. Moreover both cases have been opportunely tilted in order to ensure the inclination required to drive water flow, otherwise the water loop could not be closed and the fed solution would stagnate within the grow tray.

Figure 25. Hydroponic greenhouse at Energy Centre

The pathway of nutrient solution begins and ends in a plastic case used as storage (Vessel 1), where a water pump provides continuity of operation. Cleary the back flow from greenhouse is less compared to the input since plants adsorbs a share to cover their needs. For this reason, a self-regulation is implemented in place by using communicating vessels. Indeed the fresh nutrient solution is hosted in a second bigger storage(Vessel 2) in communication with the previous one, so whenever the level of first vessel goes below a prefixed threshold the other supplies a certain amount of liquid in order to recover the lack.

The system is also equipped with the fertigation device whose duty is to mix fresh water and nutrients to form the fed solution according to the type of growing culture. Freshwater incoming flow is managed by a regulating valve, in turn regulated by the control unit. The valve is a three ways kind characterized by two inlet ports and one outlet connected to Vessel 2. Concerning the inlet, the valve is connected to aqueduct and to Breath. Inputs are regulated by the control unit. As general rule of thumb, Breath gets the priority as water feeder and water from aqueduct is taken only when the first one is unable to cover greenhouse requirements.

The purpose behind greenhouse development is to create an eco-friendly test-habitat, able to minimize the impact on the environment as much as possible. According to this, the system has been equipped with solar collectors in loco that should provide the thermal energy needed for the correct operation of the entire plant. Indeed, thermal energy can be used both in the greenhouse for air conditioning reasons and in Breath during regeneration as heat source.

The total hosting capacity of the greenhouse is 180 plants, considering that each grow tray is equipped with thirty empty spaces designed for culture.

4 Numerical Model of Breath

The development of an interactive model of Breath has been performed using Matlab software. Starting from the previous model of adsorption heat exchanger still developed in Matlab, the aim is to design a code able to represent the cycle in figure 21. The model wants to simulate the behaviour of system both in adsorption and regeneration for different inlet conditions. In particular regeneration is the most complex phase to simulate. Indeed, air dehumidification performed in the condenser has to be modelled together with desorption process in the adsorption heat exchanger ADS-HE.

The condensation unit is made of a heat recovery unit "HRU" that preheats the air flow exiting the condenser using the air stream from ADS-HE, and the condenser which drives dehumidification using water as cooling fluid. In turn the condenser consists of two cooling units, one in contact with working air of Breath and the other used to cool down water flow exiting the dehumidification process. The functional scheme of the system is shown in figure :

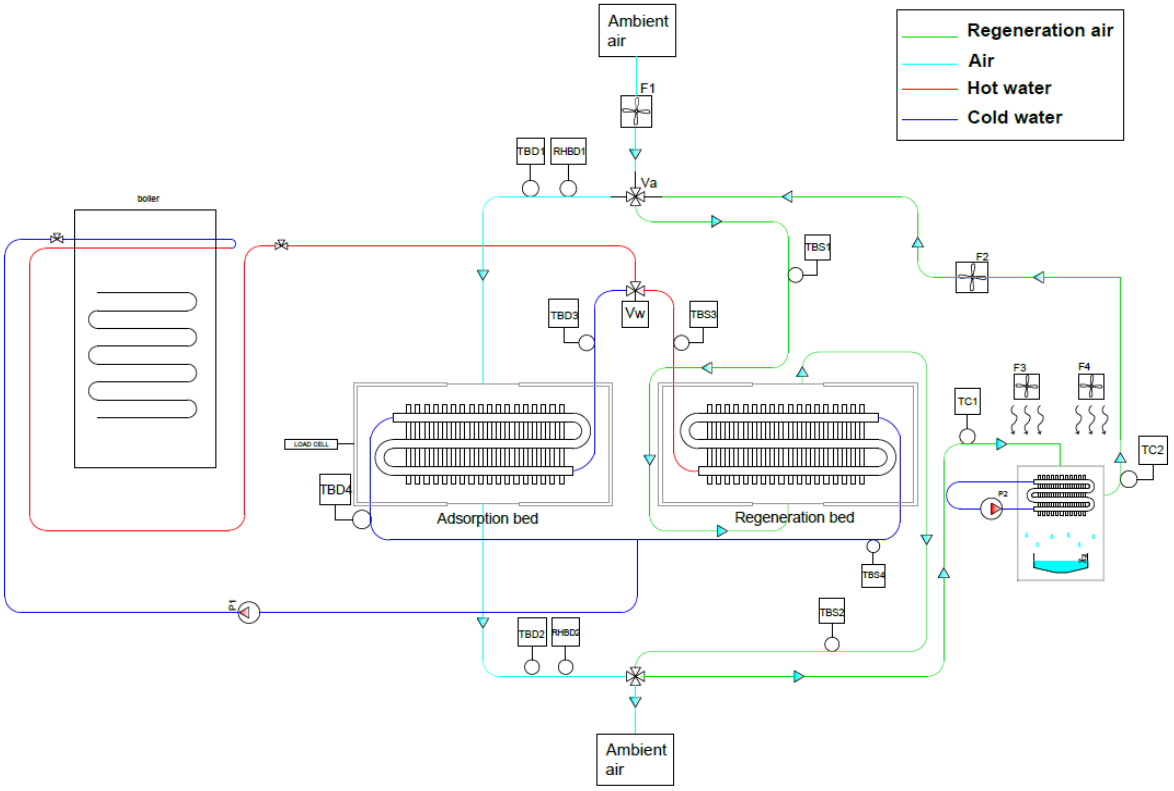

Figure 26. Functional scheme of Breath

Air transformations during regeneration can be represented in the psychrometric diagram as shown below:

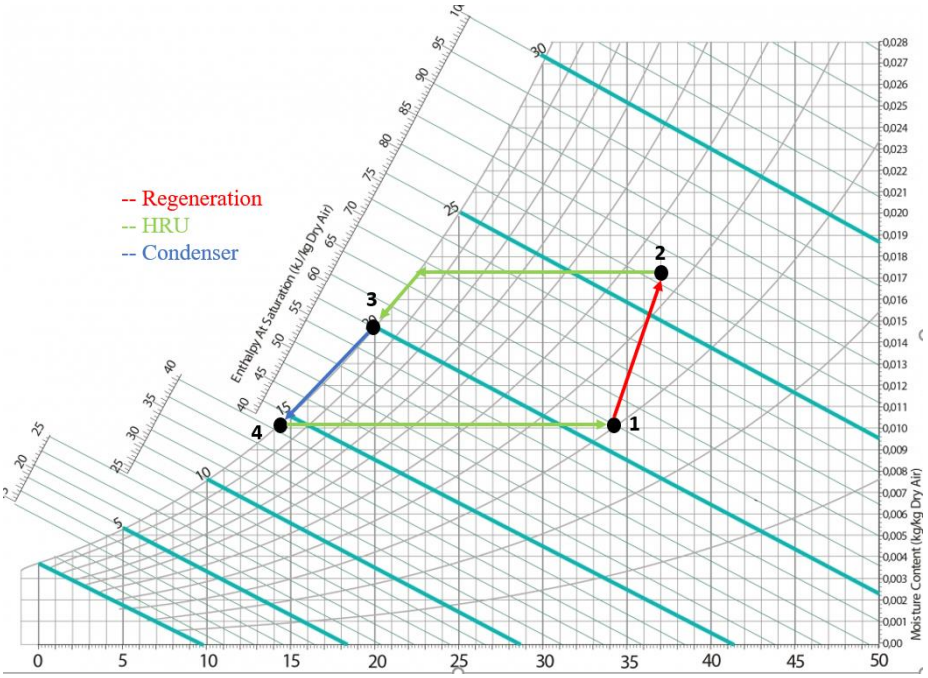

Figure 27. Physical transformation of air during regeneration

Looking at the psychrometric chart is possible to analyse air transformations in any component of the system for the regeneration phase. Air taken from the environment enters the machine at condition 1and it is used to regenerate the sorption bed of the ADS-HE. At the end of the process air reaches state 2 where it results hotter and more humid due to adsorption of water. Then air is forced through the HRU where it releases heat to the counter air flow, whose inlet physical condition is represented by point 4. Point 3 represents the outlet of HRU and the inlet of the condenser, where air follows the transformation 3-4 along the saturation curve. Therefore, air is brought below the dew point in order to drive water harvesting process. Eventually air returns to HRU where it is preheated before entering the ADS-HE to continue regeneration.
The chapter illustrates the physical model, describing the operation of each component and the corresponding Matlab code designed to represent the system.

4.1 Packed Adsorption Heat Exchanger

The physical model of packed adsorption heat exchanger results in a set of mass and energy balances that describes adsorption/desorption process of water vapour in silica gel packed structure. Starting from six hypothesis, the model is a set of mass and energy balances regarding the interaction between air, vapour, silica gel and the heat source. The hypothesis are listed below:

- Adsorption/Desorption processes involve only water vapour and sorbent, so the presence of any other non-condensable gases is neglected.
- Adsorption heat is generated within the pores of the sorbent and it is function of water uptake of the material.
- Adsorption/Desorption processes are much faster than other phenomena. Therefore , near the sorbent surface the local equilibrium between water and silica gel can be approximated using adsorption equilibrium curves. In this way, vapour mass transfer is function of equilibrium conditions. Moreover, vapour diffusion within particles has a

significant role on global mass transfer resistance, due to the long duration of experiments.

- Phenomenon are considered mono-dimensional and developed along the air flow direction
- Conduction and radiative heat exchanges can be neglected since convection between air and solid surface of silica particles is the dominant heat transfer mechanism.
- Thermal losses toward external environment are neglected thanks to the abundant insulation use to isolate the system.

Starting from these assumptions, the equations describing mass and energy balances can be analysed in detail.

$$\varepsilon_b \rho_a \frac{\vartheta x_a}{\vartheta t} dv = -\dot{m}_a \frac{\vartheta x_a}{\vartheta z} dz - \dot{G} dv \quad \left[\frac{kg}{s}\right] \quad (5.1)$$

$$\rho_b \frac{\vartheta W}{\vartheta t} = \rho_a K_G a_s (x_a - x^*) = \dot{G} \quad \left[\frac{kg}{m^3 s}\right] \quad (5.2)$$

$$\varepsilon_b \rho_a c_{p_a} \frac{\vartheta T_a}{\vartheta t} dv = -\dot{m}_a c_{p_a} \frac{\vartheta T_a}{\vartheta z} dz + h_t (T_s - T_a) dv - U_L a_L (T_a - T_{amb}) dv +$$

$$+ U a_F (T_a - T_w) dv \quad [W] \quad (5.3)$$

$$c_{p_b} \rho_s (1 - \varepsilon_b) \frac{\vartheta T_s}{\vartheta t} dv = H_a \dot{G} - h_t (T_s - T_a) \quad [W] \quad (5.4)$$

$$\rho_w c_{p_w} \frac{\vartheta T_w}{\vartheta t} dv = -\dot{m}_w c_{p_w} \frac{\vartheta T_w}{\vartheta z} dz - U a_F (T_w - T_a) dv \quad [W] \quad (5.5)$$

where:

-ρ_b is the bulk density of silica gel in [kg/m^3]
-ρ_a is the air density in [kg/m^3]
-ρ_w is the water density in [kg/m^3]
-W is the silica moisture content, dimensionless
-K_G is the global water mass transfer coefficient
-a_s is the surface area of silica sphere per unit of volume [1/m]
-x_a is the moisture content of air [kg/kg]
-x^* is the equilibrium value between the air and solid sorbent [kg/kg]
-ε_b is the silica bed porosity equal to 0.427
-$\dot{m}_a$ is the air mass flow rate [kg/s]
-$\dot{m}_w$ is the water mass flow rate [kg/s]
-c_{p_a} is the specific heat of air [J/kg/K]
-c_{p_b} is the specific heat of silica bed [J/kg/K]
-T_a is the air temperature [°C]
-T_s is the silica bed temperature [°C]
-T_w is the water temperature [°C]
-h_t is the convective heat transfer coefficient between air and silica bed [W/m^2/K]

-U_L is the transmittance coefficient for heat exchange with ambient air [W/m^2]
- U is the transmittance coefficient for heat exchange between air and water [W/m^2]
-a_i is the reference contact surface of heat exchange [m^2]

Equation (5.1) accounts for the mass balance between air and the water vapour, (5.2) explains the time dependency of water uptake to the mass transfer rate Ġ; (5.3) is the air thermal balance derived from the interaction between air, silica bed and water/heat source; (5.4) is the thermal balance of the sorption bed, whereas (5.5) is the thermal balance of heat source using water as working fluid. The model requires additional auxiliary equations to evaluate all parameters involved in energy and mass balances.
Considering the diffusion phenomena , it describes the mass transfer of water vapour molecules inside the structure of Silica gel bed and it is represented through the mass transfer coefficient "K_G", that accounts for all interactions along the diffusion path. Its evaluation requires the knowledge of global resistance, which consists of two contributes: the convective mass transfer resistance between the bulk of the air stream and the boundary layer of sorbent surface, and the interparticle vapour diffusion. The equation to estimate K_G takes advantage from electric circuit theory. Therefore, the resistance analogy is applied as follows [32]:

$$\frac{1}{K_G a_s} = \frac{1}{\frac{h_m}{\rho_a} a_s} + \frac{1}{(1-\varepsilon_b) K_p K_0} \quad (5.6)$$

When the transition from convection to diffusion occurs, water molecule starts to diffuse through particles of sorption bed until a site of reaction is reached. This phase is called interparticle diffusion and it is represented by the coefficient "k_F" which is function of temperature and water uptake. This coefficient multiplied by air density returns the convective mass transfer coefficient "h_m , in turn function of molecular diffusivity of water vapour in air "$D_{m\_H2O\text{-}air}$", Reynolds and Schmidt numbers as explained in the formula showed below [33]:

$$h_m = k_f \rho_a = \frac{D_{m_{H_2O-air}}}{2 * R_p} (2 + 0.6 R_e^{0.5} Sc^{0.33}) \rho_a \quad (5.7)$$

$$D_{m_{H_2O-air}} = 1.735\ x\ 10^{-9} \frac{(T_a + 273.15)^{1.685}}{P_{atm}} \quad \left(\frac{m^2}{s}\right) \quad (5.8)$$

where :

-R_p is Silica sphere radius equal to 1.5 mm

Afterward water molecule is ready to interact directly with sorbent particle, therefore diffusion continues along surface and inside pores of Silica particle. According to electrical resistance analogy, these phenomena contribute in parallel since water cannot diffuse on the surface and in the pore at the same time. The first mechanism is represented by D_S, a coefficient affected by heat generated during adsorption H_{ads}. The second mechanism is designed as the series interaction between molecular diffusivity "D_m" and the Knudsen diffusivity D_{Kn}, which is function of bed temperature and mean particle radius r_p. The result of these three mechanisms is expressed through the global effective diffusion coefficient D_{eff}, computable as follows [33]:

$$D_{eff} = \frac{1}{R_{surface}} + \frac{1}{R_{pore}} = \frac{1-\varepsilon_p}{\varepsilon_p}\frac{K_0 D_s}{\tau_p} + \frac{1}{\frac{\tau_p}{Dm}+\frac{\tau_p}{D_{Kn}}} \left(\frac{m^2}{s}\right) \quad (5.9)$$

$$D_{Kn} = r_p 22.86(T + 273.15)^{0.5} \left(\frac{m^2}{s}\right) \quad (5.10)$$

$$D_s = \frac{D_0}{\tau_s} e^{-0.947\frac{H_{ads}}{T+273.15}} \left(\frac{m^2}{s}\right) \quad (5.11)$$

$$K_0 = \frac{\rho_s w}{\rho_a x_a} \left(\frac{m}{s}\right) \quad (5.12)$$

where:

-K_0 is the equilibrium constant during diffusion
-ε_p is the mean particle porosity equal to 0.35
-τ_p is the tortuosity factor equal to 1

Having knowledge of D_{eff}, the mass transfer coefficient due to porous internal resistance K_p can be evaluated and used to compute "K_G":

$$K_p = 60\frac{\varepsilon_p D_{eff}}{D_p^2 K_0} \left(\frac{m}{s}\right) \quad (5.13)$$

Eventually the model requires additional auxiliary equations to evaluate all parameters involved in the previous set of equations.
Air physical conditions needed in the model are the moisture content x_a, the specific heat $c_{p,a}$, the saturation pressure of water vapour at given temperature P_{sat}, the density ρ_a and the dynamic viscosity μ_a. These are evaluated using formula listed below [34] :

$$\mu_a = \frac{T_a+300}{50} 23.6\, x\, 10^{-7} + 184.6\, x\, 10^{-7} \ (Pa\ s) \quad (5.14)$$

$$c_{p_a} = 1884\, x_a + 1004(1 - x_a) \left(\frac{J}{kg\ K}\right) \quad (5.15)$$

$$\rho_a = \frac{352.98}{T_a+273.15} \left(\frac{kg}{m^3}\right) \quad (5.16)$$

$$P_{sat} = 0.0004677\, T^4 + 0.02444\, T^3 + 1.359\, T^2 + 45.98\ T + 604.6 \ (Pa) \quad (5.17)$$

$$x_a = \frac{0.622\, RH_a\, P_{sat}}{101325 - RH_a\, P_{sat}} \left(\frac{kg_w}{kg_a}\right) \quad (5.18)$$

Silica gel properties used for the simulation are the specific heat c_{ps} and the heat of adsorption H_{ADS}, both function of sorption bed temperature and water uptake as shown by equations (5.19), (5.20) and (5.21):

$$c_{p_s} = 4186\, W + 921 \left(\frac{J}{kg\ K}\right) \quad (5.19)$$

$$H_{ADS|\,W\leq 0.05} = 3500 - 13400\,W \quad \left(\frac{J}{kg}\right) \text{(5.20)}$$

$$H_{ADS|\,W>0.05} = 2950 - 1400\,W \quad \left(\frac{J}{kg}\right) \text{(5.21)}$$

In addition to physical properties listed above, the set of equations requires also the estimation of the global heat transfer coefficient *U* to solve the thermal balance between silica gel, air and the heat source. Considering the geometry of the heat exchanger, the coefficient *U* is calculated with the formula (5.22) [34] [35]:

$$\frac{1}{UA} = \frac{1}{\eta_0 h_t\, A} + \frac{\ln\left(\frac{D_o}{D_i}\right)}{2\pi L\, k_{cu}} + R_i \quad \left(\frac{K}{W}\right) \text{(5.22)}$$

where:
- A is the surface involved in the heat exchange made of fins and tubes
-k_{cu} is the thermal conductivity of copper

The internal thermal resistance R_i is evaluated differently according to the phase performed by the device. Indeed during adsorption, the process is not driven by the external heat source, therefore water flow inside tubes is null and the thermal resistance R_i is estimated as the conductive resistance of a pipe made of water. Instead regeneration requires thermal energy, so the heat source is activated and hot water flows within tubes. In this case R_i is purely convective term and it is evaluated through the convective coefficient "h_i" function of Reynolds Prandtl and Nusselt numbers. Equations to estimate R_i in the two cases are shown below:

$$R_i = \frac{\ln\left(\frac{D_i}{D_c}\right)}{2\pi L\, k_w} \quad \left(\frac{K}{W}\right) \quad \text{(5.23)}$$

$$R_i = \frac{1}{h_i\, A_i} \quad \left(\frac{K}{W}\right) \quad \text{(5.24)}$$

$$R_e = \frac{\rho w L}{\mu} \text{(5.25)}$$

$$N_u = 0.023\, P_r^{0.4}\, R_e^{0.8} \text{(5.26)}$$

where :

-k_w is water thermal conductivity [W/m/K]
-ρ is the density of considered fluid [kg/m^3]
-w is the velocity of considered fluid [m/s]
- μ is dynamic viscosity of considered fluid [Pa s^{-1}]

The convective heat transfer coefficient "h_t" used in (5.21) and (5.3) has been estimated as function of those numbers previous mentioned, whose relationships can be summarized as follows:

$$h_t = \frac{k_a}{2\,R_p}(2 + 0.6\,R_e^{0.5}P_r^{0.33}) \quad \left(\frac{W}{m^2\,K}\right) \text{(5.27)}$$

where :

-k_a is air thermal conductivity [W/m/K]

Water physical properties involved in the model are the specific heat $c_{p,w}$, the thermal conductivity k_w, the dynamic viscosity μ_w, the density ρ_w and the Prandtl number $P_{r,w}$. The equations to estimate these quantities have been taken from [36]. These are shown following:

$$c_{p_w} = 4.2174356 - 0.0056181625\,T_w + 0.0012992528\,T_w^{1.5} - 0.00011535353\,T_w^2 + 4.14964 * 10^{-6}\,T_w^{2.5} \quad \left(\frac{J}{kg\,K}\right) \text{(5.28)}$$

$$k_w = 0.5650285 + 0.0026363895\,T_w - 0.00012516934\,T_w^{1.5} - 1.5154918 * 10^{-6}\,T_w^2 - 0.0009412945\,T_w^{0.5} \quad \left(\frac{W}{m\,K}\right) \text{(5.29)}$$

$$\mu_w = \frac{1}{557.82468 + 19.408782\,T_w + 0.1360459\,T_w^2 - 3.1160832 * 10^{-4}\,T_w^4} \quad (Pa\,s) \text{(5.30)}$$

$$\rho_w = 999.79684 + 0.068317355\,T_w - 0.010740248\,T_w^2 + 0.00082140905\,T_w^{2.5} - 2.3030988 * 10^{-5}\,T_w^3 \quad \left(\frac{kg}{m^3}\right) \text{(5.31)}$$

$$P_{r_w} = 1/(0.074763403 + 0.0029020983\,T_w + 2.8606181 * 10^{-5}\,T_w^2 - 8.1395537 * 10^{-8}\,T_w^3 \text{(5.32)}$$

Eventually mass and energy balances have been solved by developing the theory of partial derivative equation. All equations have been discretized in space dividing the z direction in finite elements of discrete dz of 3mm, and in time with a finite timestep of 1 second.
Backward finite difference method has been used to approximate numerically space derivatives, whereas time derivatives have been modelled using backward Euler, so avoiding problems of solution instability.

- Backward finite difference method : $\frac{\vartheta x}{\vartheta z} = \frac{x_i - x_{i-1}}{\Delta z}$ (5.33)

- Backward Euler method : $\frac{\vartheta x}{\vartheta t} = \frac{x_i^{t+\Delta t} - x_i^t}{\Delta t}$ (5.34)

4.2 Heat Recovery Unit HRU

The heat recovery unit ("HRU") is an air-air counterflow heat exchanger that drives an internal heat recovery between air going toward the condenser ant the air stream directed to ADS-HE. The purpose of this component is to avoid any energy waste and at the same time to satisfy thermal requirements of each component. The first air stream undergoes the transformation 2→3 during which air releases heat that could be either latent or sensible, therefore partial condensation can be achieved in this first step. The other air stream follows the line 4→1.
The HRU can be described as a hexagonal prism with four apertures needed for air inlet and outlet and characterized by hundreds of channels where heat exchange takes place. Channels are realized using plastic fins that works as contact surface between working fluids. An illustration of the system is shown in Figure 28 :

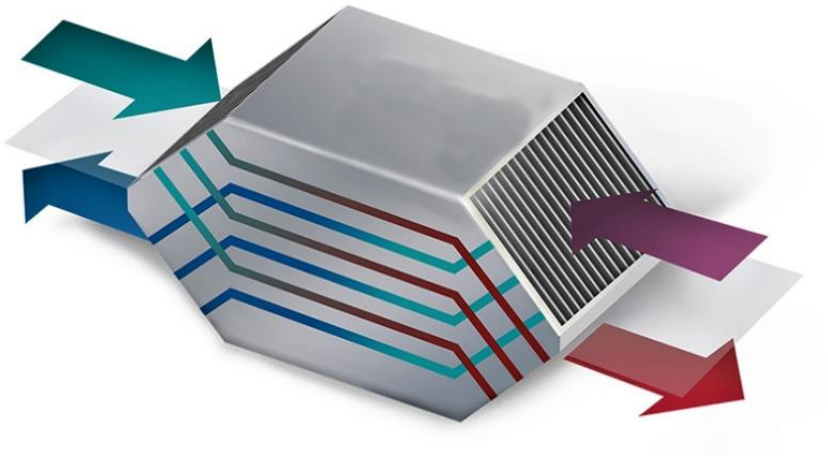

Figure 28. HRU illustration

The predominant heat transfer mechanism is convection between air streams, whose temperature is function of the characteristic length of the exchanger. Indeed, the temperature profile cannot be constant since an air stream is cooled while the other is warmed, therefore outlet temperatures are unknown and depend on the heat transfer capacity of the heat exchanger. In order to evaluate the heat transferred and exiting temperatures the ε-NTU method has been applied inside the stricture of the code [37] [38]. The method is based on the evaluation of heat exchange efficiency "ε" as function of the geometry and type of fluids involved. Basically the efficiency is defined as the ratio between the real power exchanged "$\dot{Q}$" and the maximum thermal power exchangeable "$\dot{Q}_{max}$":

$$\varepsilon = \frac{\dot{Q}}{\dot{Q}_{max}} = f(NTU, \omega) \quad (0 < \varepsilon < 1) \quad (5.35)$$

By definition the power "$\dot{Q}_{max}$" is given by the minimum thermal capacity rate "C_{min}" times the difference between the inlet temperatures of the hot and cold fluids. In turn the thermal capacity rate is defined as the product between the specific heat and the mass flow rate of the considered

fluid. Considering the definition of cold and hot fluids, equations below illustrates the procedure:

$$\dot{Q}_{max} = C_{min}\left(T_{hot,IN} - T_{cold,IN}\right)(W) \quad (5.36)$$

$$C_{min} = \min\left(c_{p_{hot,IN}} * m_{hot}\,, c_{p_{cold,IN}} * m_{cold}\right)\left(\frac{W}{K}\right) (5.37)$$

According to the ε-NTU theory, the efficiency can be calculated using empirical equations that describes "ε" as function of two parameters : *NTU* and ω. The *NTU* is the number of transfer units defined as the ratio between the overall transmittance "*U*" times the contact area of heat transfer "*A*", and the minimum thermal capacity rate. Instead "ω" is the heat capacity ratio, given by minimum thermal capacity rate "C_{min}" divided the maximum of the same quantity "C_{max}".

$$NTU = \frac{UA}{C_{min}} \quad (5.38)$$

$$\omega = \frac{C_{min}}{C_{\max}} \quad (5.39)$$

Concerning our application, the first step has been the evaluation of the product between the heat transfer coefficient "*U*" and the heat transfer area "*A*" as the inverse of the overall thermal resistance "*R*" of the heat exchange . This quantity is function of internal and external convective resistances, and of the conductive resistance. Modelling the phenomena as the convective heat transfer between two fluids at different temperature separated by the fin, resistance can be evaluated as follows:

$$R = \frac{1}{UA} = \frac{1}{h_i A} + \frac{s}{(\lambda\, A)} + \frac{1}{h_e A} \quad \left(\frac{K}{W}\right) \quad (5.40)$$

where :

- λ is the thermal conductivity of the material of the fin, equal to 0.05 W/(m K)
- s is the thickness o the fins, equal to 0.5 mm
-h_i and h_e are internal and external convective coefficients

The evaluation of "*R*" requires several auxiliary equations to estimate internal ed external convective coefficients. These can be obtained from the relationships with Reynolds, Prandtl and Nusselt numbers shown in (5.25) and (5.26). In addition, the Nusselt number is related to the convective coefficient that way:

$$N_u = \frac{h\, d}{\lambda} \quad (5.41)$$

where:

- d is the characteristic length of the heat exchange expressed in [m]

Air velocity of both streams is needed to estimate Reynolds numbers, and it is derived from the mass flow rate entering the HRU and the inlet surface "A_{in}", which is the total aperture area of the HRU channel depurated by the surface covered by fins. Instead the contact area of heat exchange "A" is the area of a single fin times the number of fins also multiplied by a factor "2", because a fin provides two contact surfaces, one for each side. Finally, the effectiveness is calculated using the relationship for counter-current heat exchanger where the working fluids remain unmixed:

$$A_{in} = A_{tot} - n_{fin} * L * s \quad [m^2] \quad (5.42)$$

$$A = 2 * n_{fin} * L * P \quad [m^2] \quad (5.43)$$

$$\varepsilon = \frac{1-e^{-NTU\,(1-\omega)}}{1-\omega\, e^{-NTU(1-\omega)}} \quad (5.44)$$

where :

- L is the length of a fin [m]
- P is the height of a fin [m]
-n_{fin} is the number of fins

Once the effectiveness is obtained, the real power exchanged "Q̇" can be easily calculated through the inverse formula of (5.35) and an energy balance can be carried out. Indeed applying the first law to each side of the system we discover that the power "Q̇" is lost by the hot fluid and acquired by the cold fluid, therefore outlet temperature can be evaluated for both streams.
Concerning the hot fluid it is necessary to evaluate if dehumidification arises within the HRU. Indeed may happen that, the heat "Q̇" causes condensation of moisture if it overcomes the sensible enthalpy jump available at point 2. In this case the remaining share of "Q̇" is consumed in the form of latent heat, since the hot fluid reached the saturation curve. For this reason, the code is equipped with a check loop that compares "Q̇" to the enthalpy gradient of dew point "ΔH_{dew}", which depends on inlet conditions of air in point 2. The enthalpy gradient of dew point is the specific heat of air in condition 2 times the difference between air temperature and the corresponding temperature of dew point "$T_{2,dew}$", calculated according to its definition. In practise if the heat exchanged is higher than "ΔH_{dew}" air releases moisture (condition 1), otherwise the streams undergoes a cooling process at constant moisture (condition 2).
If condition 1 occurs, the code evaluate physical conditions of state 3 by solving a set of equations made of the energy balance between sensible and latent heat (5.44), air moisture (5.18) and saturation pressure (5.17) functions. The system has unique acceptable solution since we have number of unknows equal to number of equations.
On the other hand, the heating process 4→1 is assumed at constant moisture and the outlet temperature of cold fluid can be evaluated by applying the energy balance. The procedure is described through formula listed below:

$$T_{2,dew} = f^{-1}(Psat)|_{x_2,RH=100\,\%} \ (°C) \quad (5.42)$$

$$\Delta H_{dew} = c_{p_2} * \left(T_2 - T_{2,dew}\right) \left(\frac{J}{kg}\right) \quad (5.43)$$

$$\dot{Q} = \dot{m} \left(c_{p_2}(T_2 - T_3) + r_w(x_2 - x_3)\right) (W) \quad (5.44)$$

$$\dot{Q} = \dot{m}\, c_{p_4}(T_1 - T_4)\, (W) \quad (5.45)$$

where :

-$\dot{m}$ is the air mass flow rate, constant along the cooling system according to mass balance [kg/s]

The solution of the system provides a fifth-grade equation where temperature of state 3 is the unknown, so in theory five different values of "T_3" are achieved but only one is acceptable. The code automatically rejects solutions not belonging to real numbers and retains the smallest value between the two alternatives available. Indeed, the other real solution provides a results that is out of bonds of the analysis, with a temperature value too high to be considered.
The model of HRU has been developed in Matlab as a function which takes in input physical conditions of states 2 and 4 , and returns moisture and temperature of points 3 and 1. Initial conditions of state 4 are assumed equal to ambient air conditions, then these are updated using results provided by the model of the condenser.

4.3 Condenser

The condenser is the unit in charge for air dehumidification and water harvesting. It can be described as cross-flow heat exchanger with hundreds of fins, that realises air transformation from state 3 to state 4 in Figure 27. The cooling fluid is water, whose duty is to reduce the average temperature of the battery below air dew point by absorbing heat released from air. As result water in outlet has higher temperature that needs to be reduced to ensure continuity of operation. The water regeneration process is performed through the external cooling unit made of fans F3 and F4, and of two fins batteries, with the same geometry of the one used inside the condenser. Each fan treats half of the total water flow rate and they work exactly in the same way with the same cooling effectiveness. Therefore the model has been developed considering only one external battery and assuming that water temperature after regeneration is equal for both circuits. The hypothesis behind the model are listed below:

- The bypass factor "B_f" of the battery of the condenser is set 0.1, therefore air outlet conditions are obtained assuming the adiabatic mix between the mass flow involved in the process and the share that escapes dehumidification. Naturally the air of bypass keeps physical properties of state 3. The subscript used to represent treated air is "4,sat", whereas "4" describes final conditions of air after mixing.
- The temperature "$T_{4,sat}$" of air post condenser is equal to the battery temperature "T_{batt}", because during the energy transfer air flow reaches thermal equilibrium with the heat exchanger.
- The moisture "$x_{4,sat}$" is evaluated as the moisture content of air along saturation curve and for the given temperature "$T_{4,sat}$".

- The storage function of water mass is negligible since the water flow rate is much higher than corresponding water mass embedded inside the water circuit.
- At the beginning of the process all species involved are in thermodynamic equilibrium with the external environment.

Considering the first hypothesis, energy and mass balances for state 4 can be written as follows:

$$\dot{m}\, h_4 = \dot{m}\left(1 - B_f\right) h_{4_{sat}} + \dot{m}\, B_f\, h_3 \ \ [W] \quad (5.46)$$

$$\dot{m}\, x_4 = \dot{m}\left(1 - B_f\right) x_{4_{sat}} + \dot{m}\, B_f\, x_3 \ \ \left[\frac{kg}{s}\right] \quad (5.47)$$

Instead, air temperature at the end of the process "T_4" is calculated using the relationship between enthalpy, temperature and moisture of humid air. The equation is shown below:

$$T_4 = \frac{h_4 - 2501.2\, x_4}{1.005 + 1.82\, x_4} \ \ [°C] \quad (5.48)$$

The model of the condenser is developed as a function that takes in input physical conditions of air in state 3 and ambient, of fins battery and water inlet temperatures. In output the code provides new values of temperature for the battery and water after the interaction with the external cooling system, and conditions of air in state 4. In addition, the simulation is developed considering that water pump "P_2" and fans "F_3" and "F_4" works at full regime, avoiding any kind of regulation.
The total water mass flow rate is derived from the power of the pump (42 W) and assuming a maximum prevalence "H_t" equal to 6 m. Water properties are evaluated using water-related equations described in the first paragraph of this chapter.
On the other side, the mass flow rate of external cooling system is evaluated considering that the entire electric power is used to increase the kinetic energy of ambient air. The equation used to estimate air speed due to either fan F_3 or F_4 arises from the Bernoulli's theorem assuming negligible variations of geotedical height gain and piezometric height.

$$v_{a_{amb}} = \left(\frac{2\, P_{vent}}{A_{vent}\, \rho_a}\right)^{\frac{1}{3}} \ \ \left(\frac{m}{s}\right) \quad (5.49)$$

where :

-P_{vent} is the electric power of fan F_3 or F_4 , equal to 170 [W]
-A_{vent} is the passage surface of air flow
-ρ_a is the density of ambient air

Concerning dehumidification phase, the thermal power absorbed by the battery "$\dot{Q}_{3\rightarrow4}$" can be calculated as sum between sensible and latent enthalpy variations along the transformation 3→4. This quantity is the result of two phenomena that involves treated air and the heat exchanger: the temperature difference between inlet air and the fins battery, and the moisture gradient across inlet and outlet of the system.

$$\dot{Q}_{3\to4} = \dot{m}\left(1 - B_f\right)\left[c_{p_{a_3}} * (T_3 - T_{batt}) + r_w\left(x_3 - x_{4_{sat}}\right)\right] \ (W) \ (5.50)$$

Applying the First law to both sides of the heat exchanger we know that "$\dot{Q}_{3\to4}$" is also the thermal power supplied to water, so water outlet temperature can be estimated as follows:

$$T_{w_2} = T_{w_1} + \frac{\dot{Q}_{3\to4}}{c_{p_w}\dot{m}_w} \ (°C) \ (5.51)$$

The regeneration of condenser cooling fluid led by the external circuit is the next physical phenomena to be modelled. The problem looks like the one already examined in the HRU, indeed inlet temperature of working fluids are known, while outlet values are undetermined. Still in this case the ε-NTU method is applied, considering water as the hot fluid and ambient air as the cold one. In the application we are assuming that temperature does not change during the pathway between the outlet of the condenser and the inlet of external cooling circuits, and vice versa. Indeed, the system is well insulated, and the extension of the circuit is small enough to neglect thermal losses.

Anyway, may happen that the battery inside the condenser is not able to perform dehumidification because the external cooling circuit cannot further reduce water temperature. Cleary this situation depends on the external environment that acts as cold well, and in particular on ambient air temperature. Indeed, the power extracted from cooling water cannot be enough for reducing the temperature of the battery below the dew point and dehumidification process is replaced by a cooling process at constant moisture. For this reason, the model is equipped with a check-loop that evaluates if there is the condition to get water condensation. The condition assumed is that the temperature of the battery has to be lower than dew point at least of a factor 2, which is a minimum ΔT_{min} pre-fixed.

At the end of the process, the algorithm evaluates the power subtracted from water and the new inlet temperature at the condenser "$T_{w,1}$". Eventually the new temperature of the battery is evaluated as follows:

$$T_{batt} = \frac{T_{w_1} + T_{w_2}}{2} + 1 \ (°C) \ (5.52)$$

5 Results of experimental procedure

The chapter presents results of the experimental procedure developed to test performances of Breath. In order to do so, thirteen tests out of forty-five have been selected as representative of the entire experimental procedure. The aim is to understand how environment conditions influence the operation of the system. Tests are divided in two categories according to the simulated working phase. Even tests represent adsorption while regeneration is simulated through odd type. The analysis continues with the model validation of those components responsible for water harvesting in regeneration: HRU and condenser.

The chapter goes on with the development of a case study, considering climate conditions of three different locations: Mosul, Casablanca and Bangkok. Performances of Breath in this environment are used to build a techno-economic study about the integration between the device and the hydroponic greenhouse described in chapter 4. In the analysis it is studied an added scenario regarding the use on photovoltaic system to cover electrical need of Breath during operation, and results are provided in terms of discounted cash flow analysis.

Eventually the chapter ends showing points of strength and weaknesses of the technology and the related model.

5.1 Experimental test of Matlab model of Breath

As previously mentioned, thirteen experimental tests are used to study the performance of the system. These are taken in couple in order to simulate a complete adsorption-regeneration cycle, except for Test n° 1 which represents the first regeneration phase ever driven by Breath. These tests have been chosen among forty-five experiments, where external ambient conditions are used as reference parameters for the selection. The idea is to uses those tests that better describes the behaviour of our system according to different external air properties.

In order to be able of comparing all tests on the same basis, it is assumed that a complete working cycle lasts for 24 h, where adsorption phase takes 15 h while regeneration the remaining 9 h. This choice is done in agreement with experimental results already analysed in previous works on ADS-HE [39]. These demonstrated that regeneration is quite faster that adsorption, because it is driven by an external heat source that improves the kinetic of the process.

The first part of the analysis involves the identification of those parameters that mostly influences the performance of the model. Project parameters identified by simulations are : air flow rate "$\dot{m}_a$" , initial wate uptake "W_i" and the temperature of the battery of the condenser "T_{batt}". This last variable is considered in regeneration tests only since it does not influence the performance of the ADS-HE during adsorption.

Test characteristics and properties are summarized in the table below:

TEST	TYPE	T_amb	x_amb
-	-	[°C]	[g/kg]
1	Rig	37.4	36.3
2	Ads	30.4	22.3
3	Rig	30.7	9.8
8	Ads	29	11.6
9	Rig	22.2	16.3
22	Ads	22	6.45
23	Rig	25	20.7
28	Ads	20	8.6
29	Rig	24	17.4
32	Ads	22	8.2
33	Rig	26	22.1
36	Ads	22	6.1
37	Rig	29	25.9

Table 2

Next paragraphs provide results of testing process divided according to the simulated working phase.

5.1.1 Results of adsorption test

Results are provided in graphical form and these are classified according to project parameters analysed. The idea is to realize a sensitive analysis for those parameters already mentioned.

5.1.1.1 Influence of air flow rate

Adsorption tests have been simulated using four different values of air flow rate by acting on the percentage of fan regulation. The values used in the simulation are 25%, 50%, 75% and 100%. Variables used to identify the behaviour of the model are air conditions after adsorption process (temperature and moisture), and the water uptake of sorption bed. For all simulations the initial value of water uptake is fixed equal to 0.005.
Results are shown in the following figures:

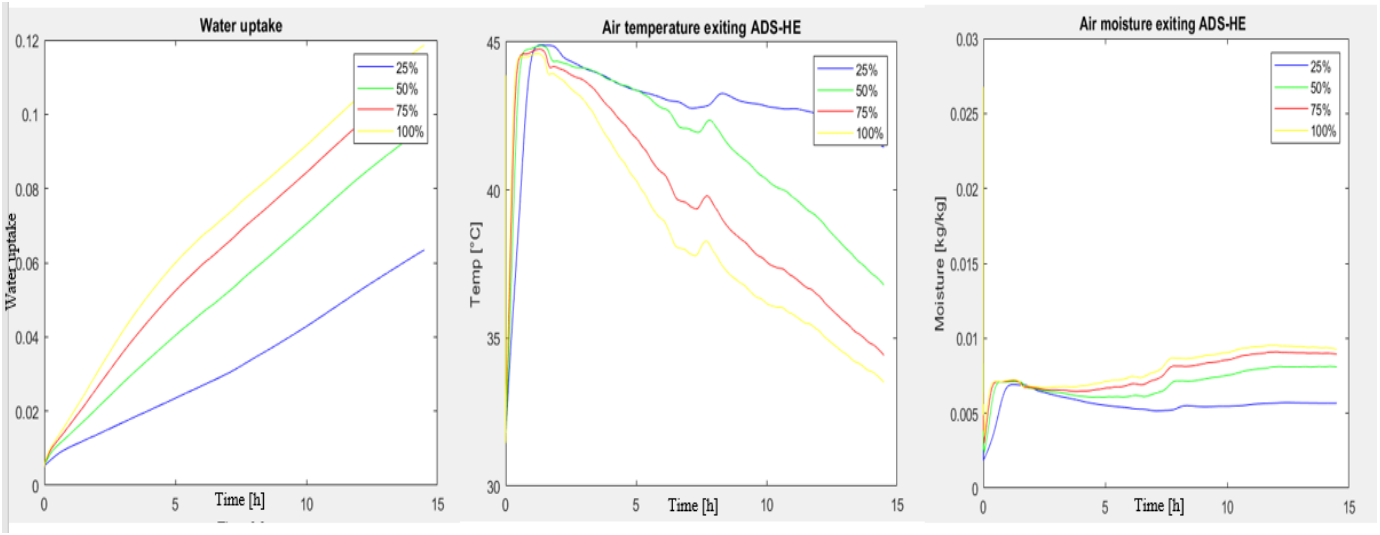

Figure 29. Test n° 2 – Air flow rate influence

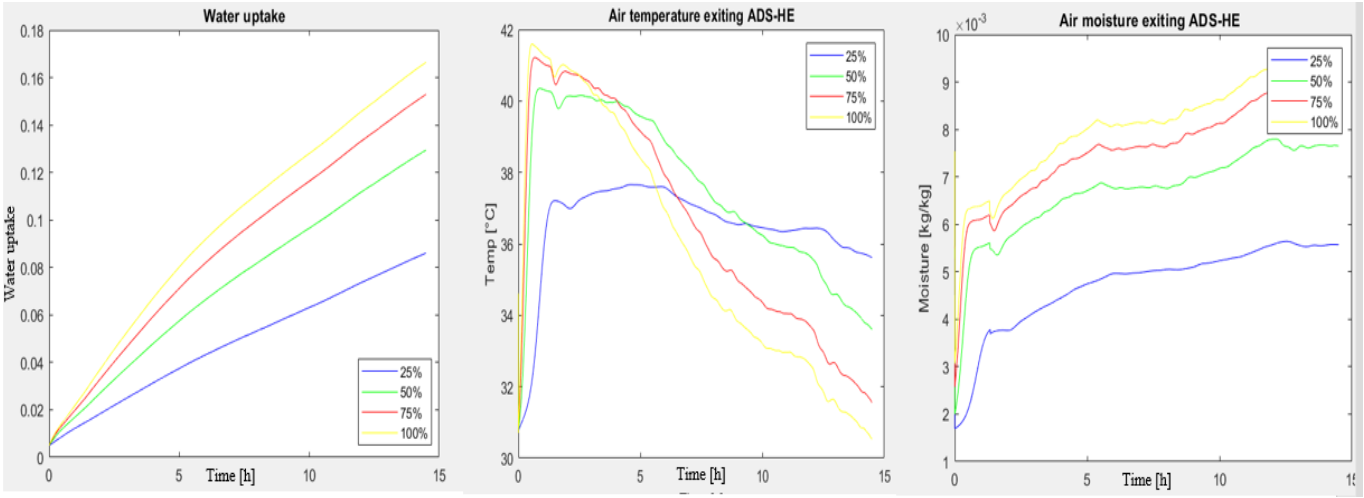

Figure 30. Test n° 8 – Air flow rate influence

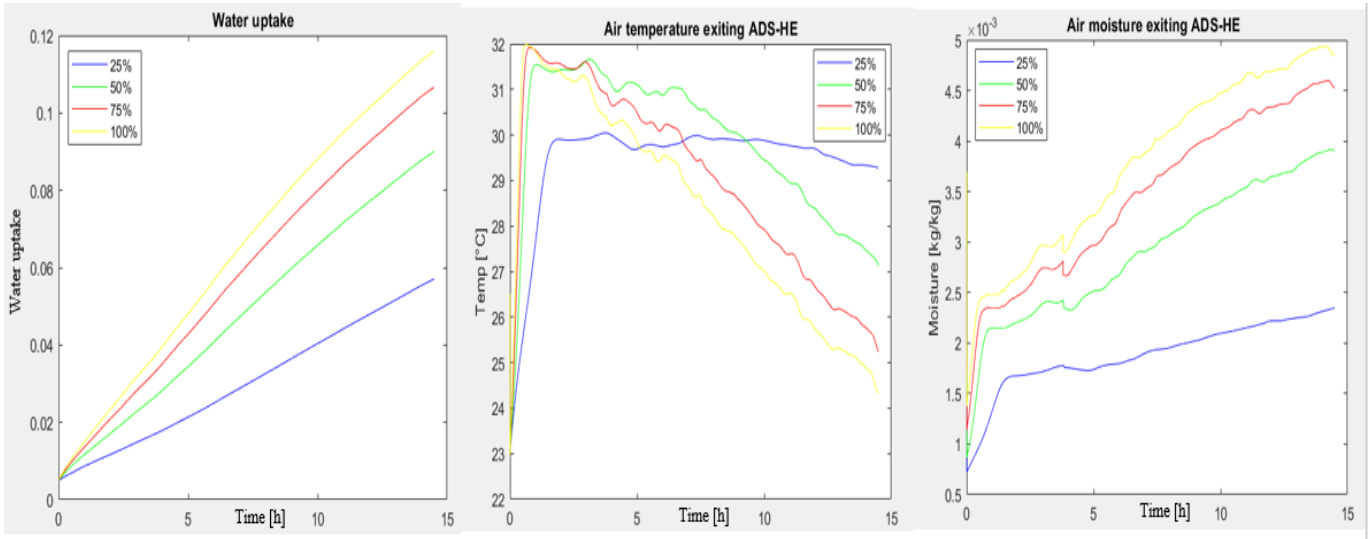

Figure 31. Test n° 22 – Air flow rate influence

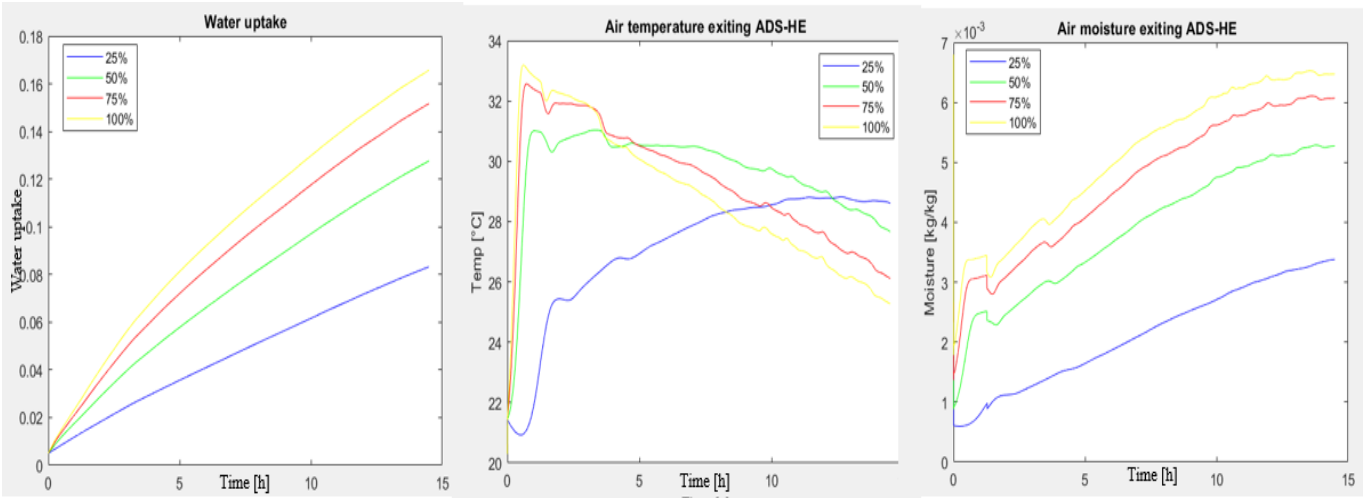

Figure 32. Test n° 28 – Air flow rate influence

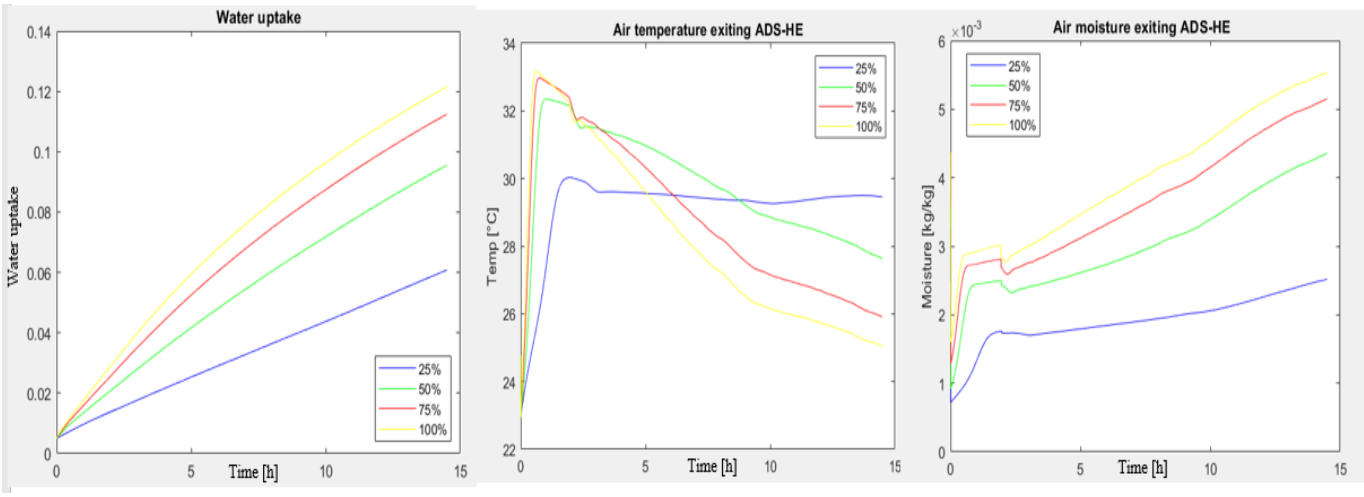

Figure 33. Test n° 32 – Air flow rate influence

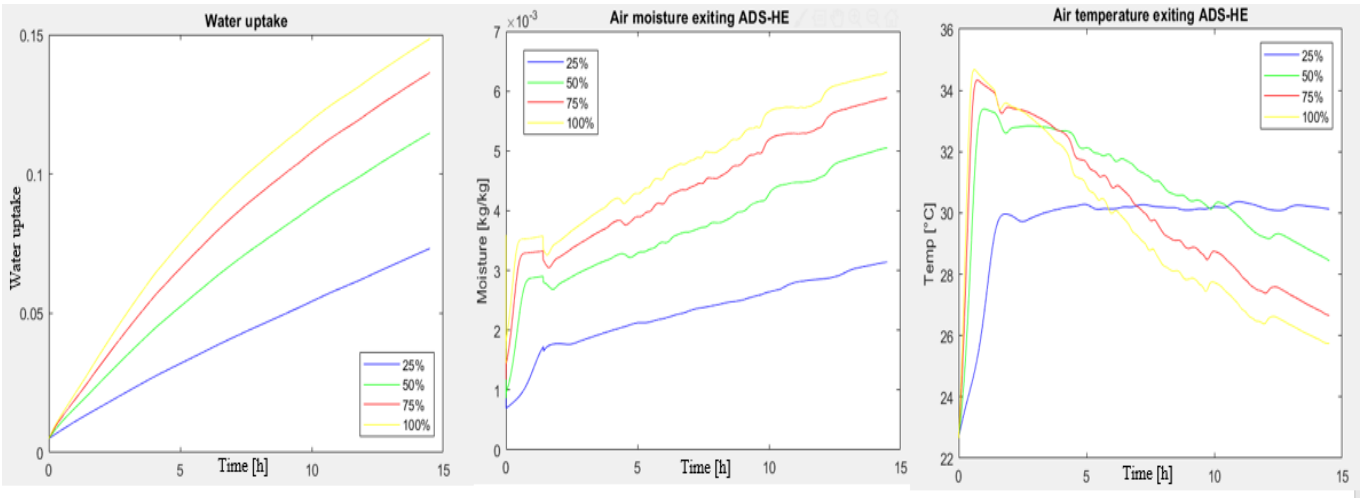

Figure 34. Test n° 36 – Air flow rate influence

Analysing these figures is possible to outline the influence of air flow rate on adsorption process. In particular, water uptake and moisture content in outlet seem to be direct proportional to the air flow rate. This means that the increase in air flow rate produces a proportional grow in vapour partial pressure, which can be considered the driver of adsorption process [33], indeed water uptake increases. On the other hand, the increase of air flow rate decreases the contact time between air and the sorption bed. As consequence air tends to release less water resulting wetter at the outlet of ADS-HE. In addition, temperature of outlet stream is inverse related to "$\dot{m}_a$" always caused by the reduced contact time. Indeed, adsorption process is exothermic and the heat produced is proportional to moisture adsorbed. Moreover, lower the interaction time is, lower the energy exchanged in the control volume. These two factors combined explain the trend of temperature. Concerning our application, we can assume that 90% of fan regulation is a proper value to run adsorption process, indeed no significant changes are recorded in the range of regulation 75-100 %.

5.1.2 Influence of the initial water uptake

The water uptake is a parameter that accounts for the amount of water embedded in sorption bed structure and it is an dimensionless number. The aim of this paragraph is to demonstrate the influence of its initial value over the simulation. In order to do so, simulations have been made using the following initial values: 0.005, 0.01, 0.015, 0.02. In all simulations, blowers have been regulated at 90% of their nominal power.
Still in this case results are taken directly from graphical evaluations.

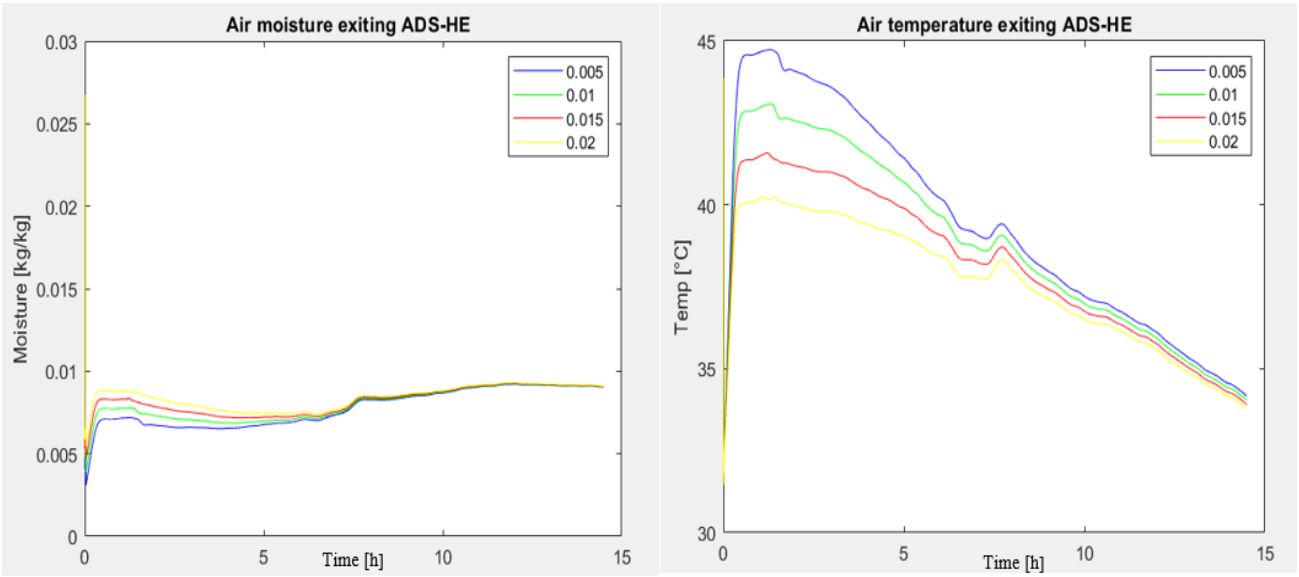

Figure 35. Test n° 2 –Initial water uptake influence

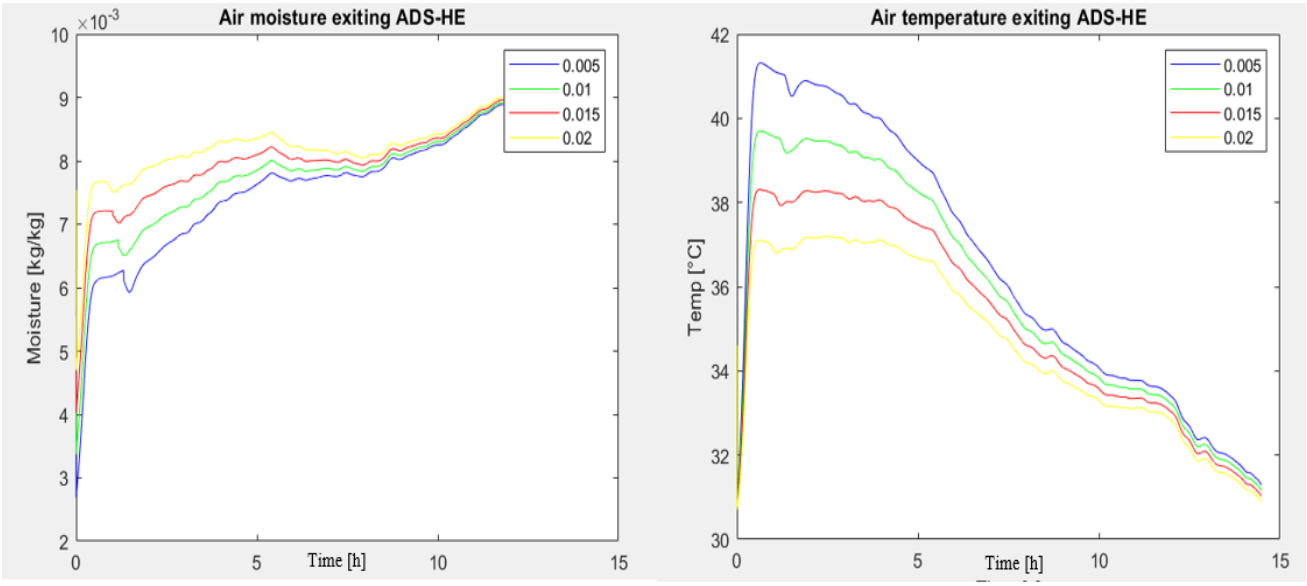

Figure 36. Test n° 8 –Initial water uptake influence

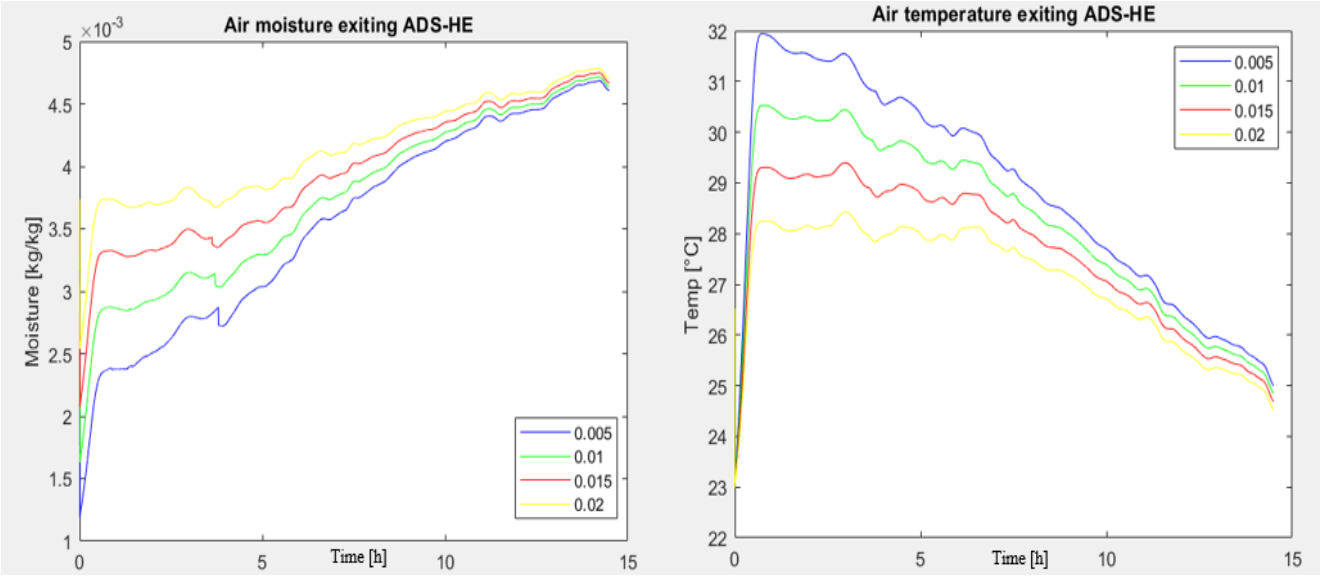

Figure 37. Test n° 22 –Initial water uptake influence

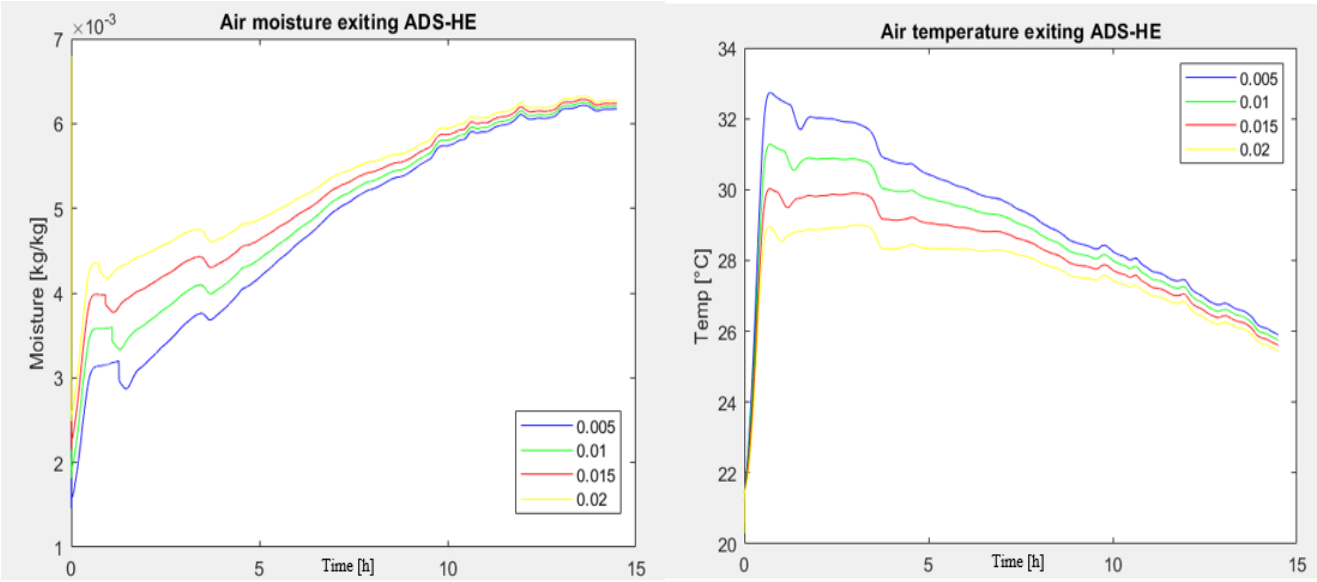

Figure 38 Test n° 28 –Initial water uptake influence

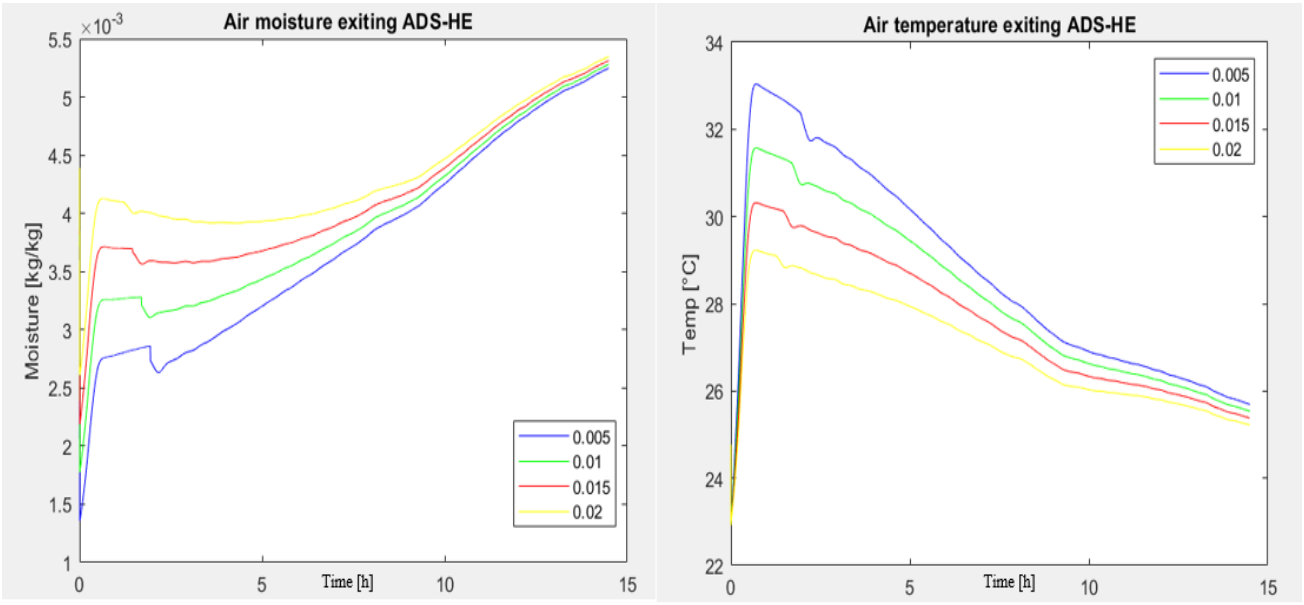

Figure 39. Test n° 32 –Initial water uptake influence

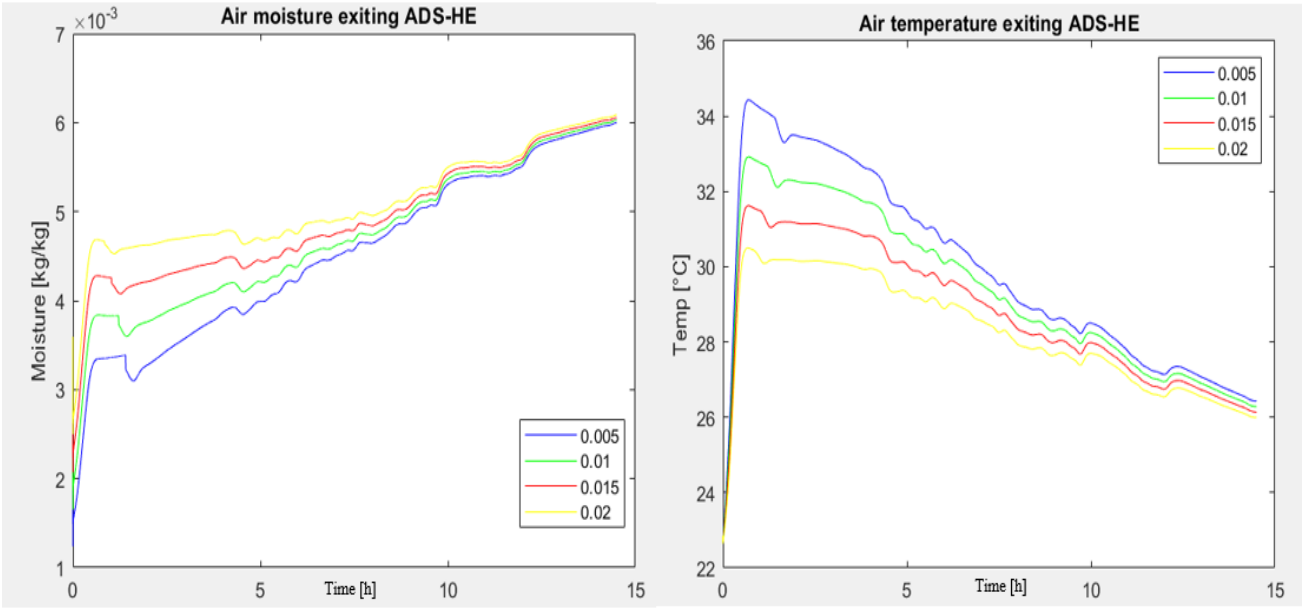

Figure 40. Test n° 36 –Initial water uptake influence

A higher initial content of water in the sorption bed causes less tendency to adsorb moisture, because many sites of adsorption have been already occupied by water molecule. This conclusion is confirmed by the experimental activity, indeed increasing the initial water uptake produces an air stream in outlet colder and wetter independently on air initial condition. As shown by previous figures, air moisture and temperature present same trends for all test. These trends are confirmed by the theory, indeed lower water adsorbed produces lower adsorption heat. Concerning the aim of adsorption phase, the optimal scenario is that characterized by the lowest initial water uptake, so 0.005 is the design value.

5.2 Results of regeneration test

The same procedure of paragraph 6.1 is applied to regeneration test with the addition of one project variable. This is the temperature of the battery inside the condenser, which has to be considered during regeneration only since it does not affect adsorption process. The controlled variables are the amount of water harvested in the condenser, air temperature exiting HRU and directed toward ADS-HE and the water uptake, whose initial value is set 0.1.

5.2.1 Influence of air flow rate

The influence of air flow rate has been evaluated also in regeneration using the same methodology adopted for adsorption test. Therefore, assuming he same regulation percentages, air and bed properties have been estimated as follows.

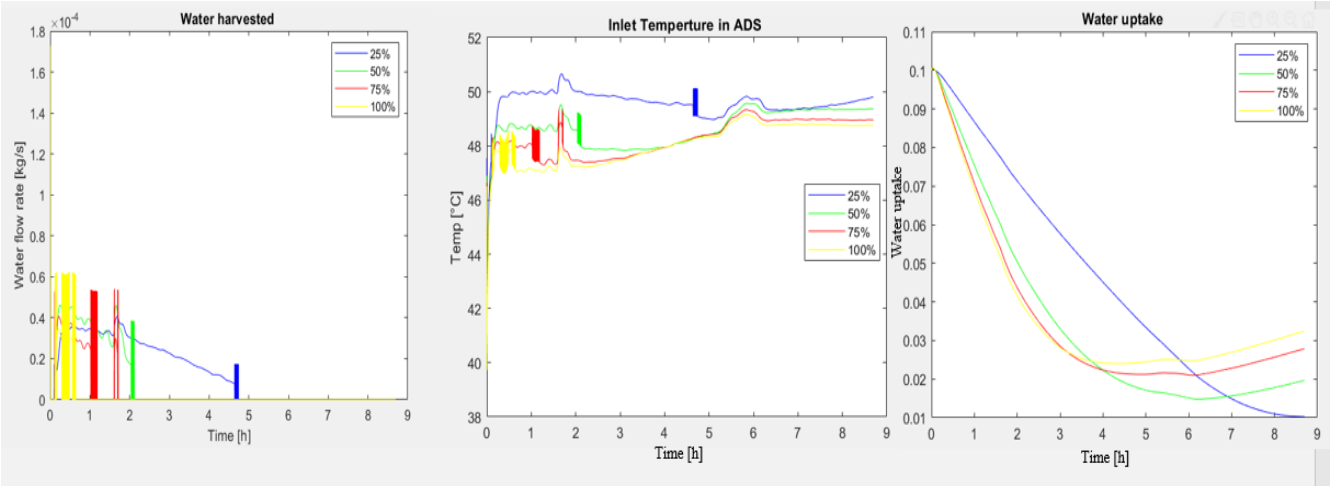

Figure 41. Test n° 1 – Air flow rate influence

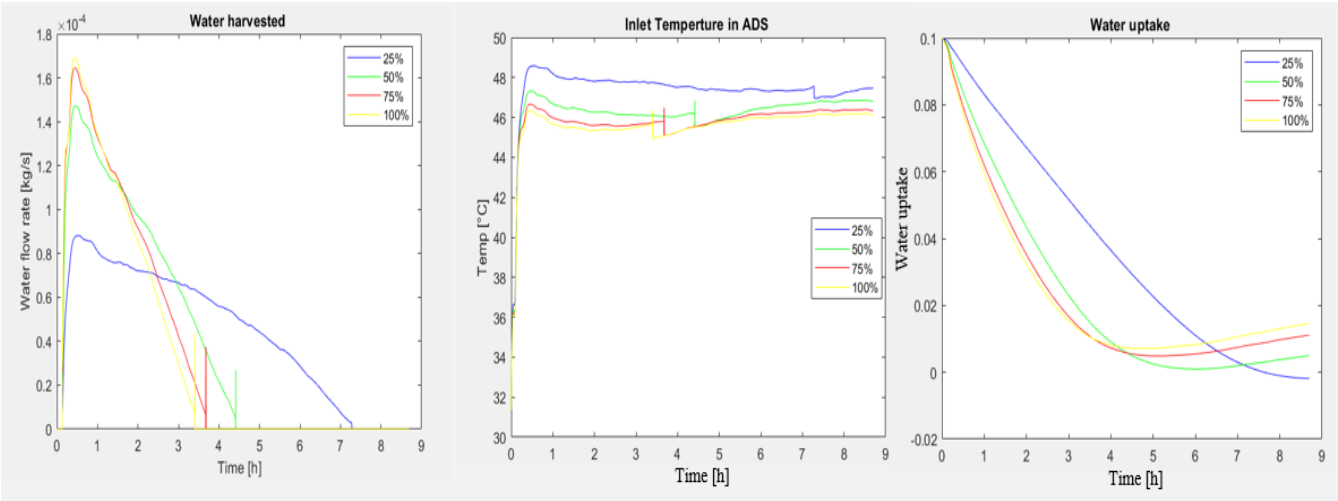

Figure 42. Test n° 3 – Air flow rate influence

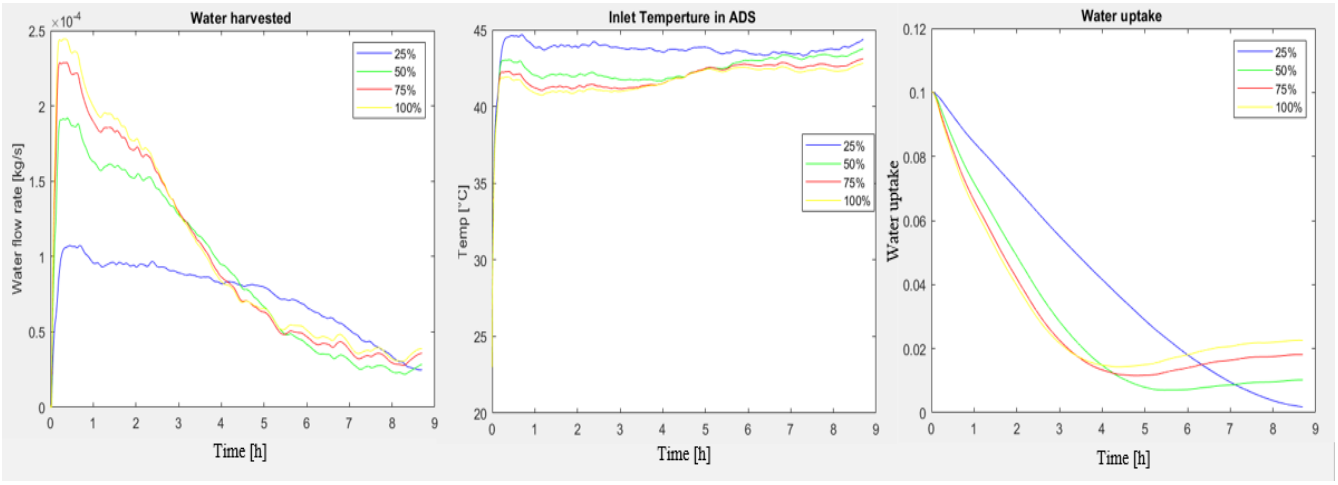

Figure 43. Test n° 9 – Air flow rate influence

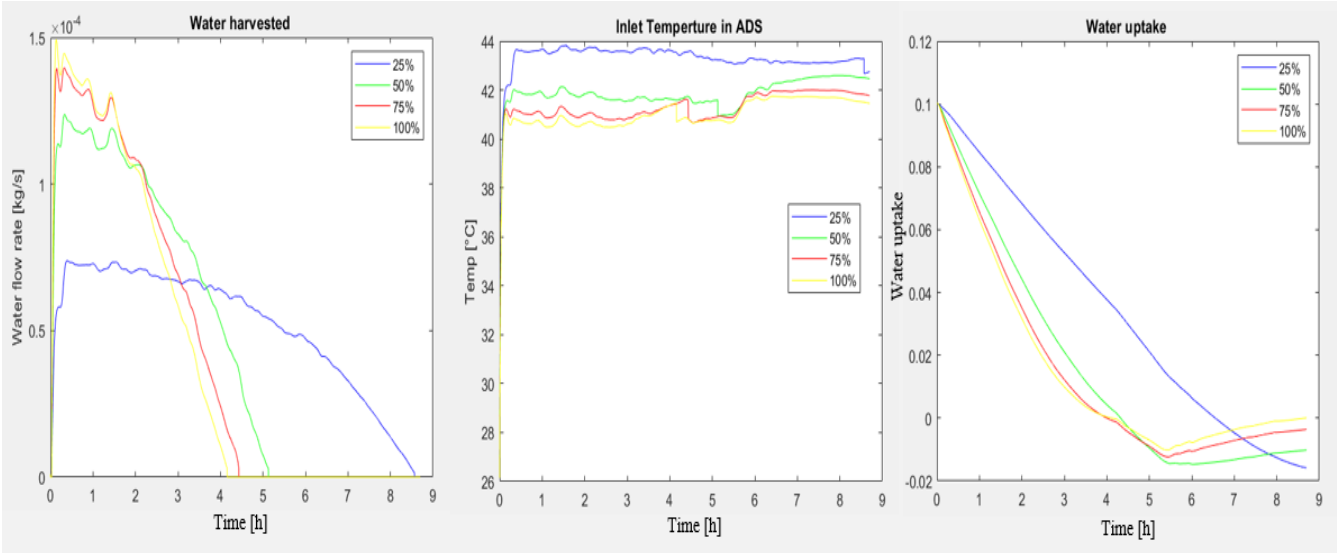

Figure 44. Test n° 23 – Air flow rate influence

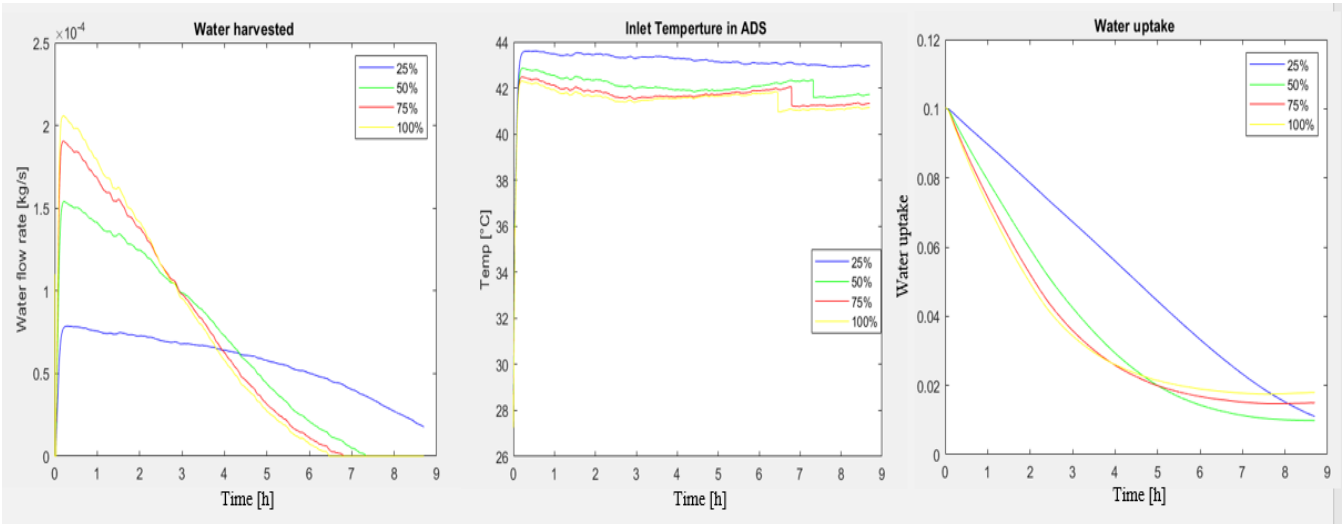

Figure 45. Test n° 29 – Air flow rate influence

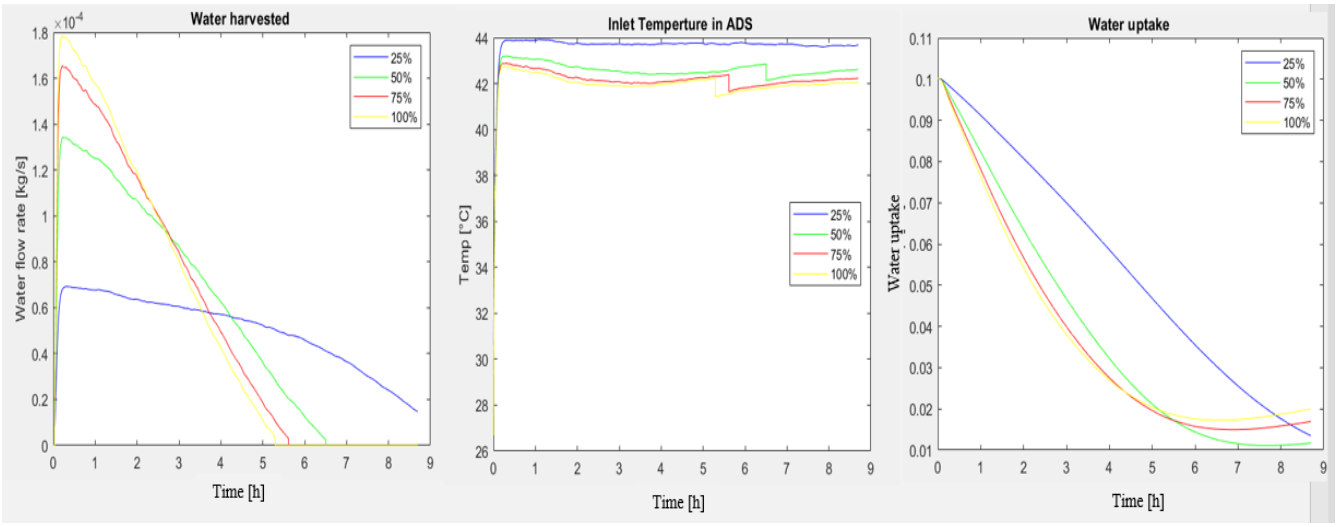

Figure 46. Test n° 33 – Air flow rate influence

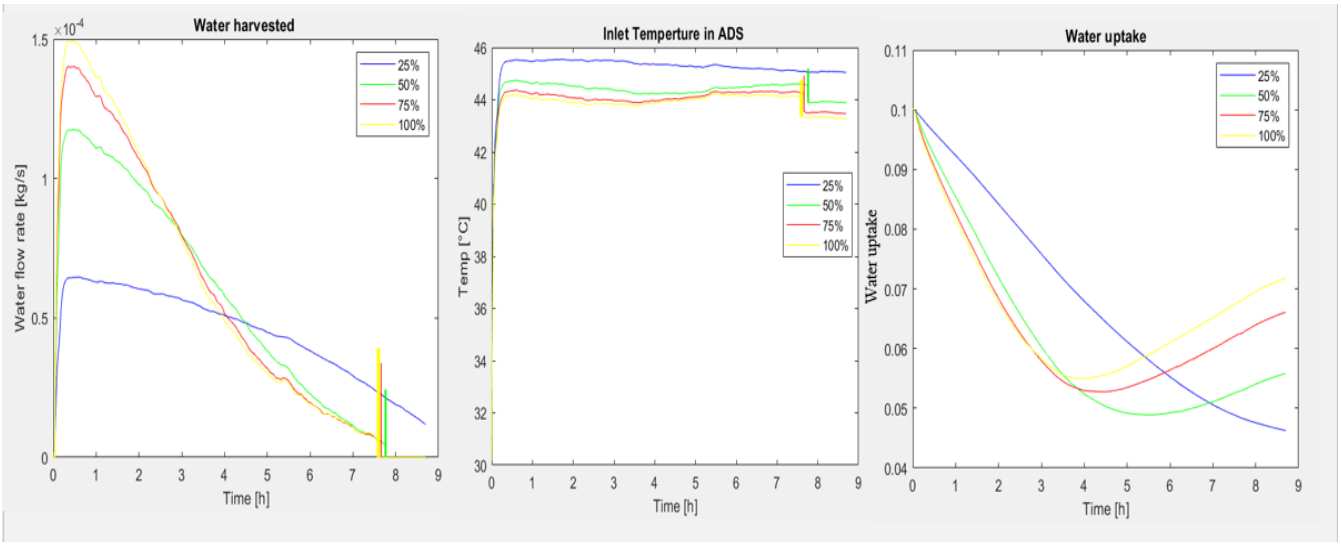

Figure 47. Test n° 37 – Air flow rate influence

Analysing experimental results, it is possible to observe how air flow rate influences variables of interest. In particular, water collected in the condenser increases with "$\dot{m}_a$" because the convective heat transfer between air and battery is enhanced by higher air velocity. Considering the constant air inlet surface at the condenser, the equation of continuity explains that air velocity growths if mass flow rate increases assuming constant thermodynamic conditions across the control volume. The growth in air speed provides higher convective coefficients, therefore more energy is exchanged and as result higher amount of water can be harvested. Concerning the trend of air temperature exiting HRU, the same physical principle can be considered. In fact, higher air velocity improves the heat exchange within HRU, so air in outlet (point 1 on Figure 27) results colder and the efficiency of HRU increases. On the other side the trend of water uptake is accelerated by air flow rate, as result the bed dries faster.

In some charts it is possible to notice instantaneous changes of water harvested or air temperature. This is causes by the cooling capacity of the battery according to external ambient conditions. In fact, may happen that in a fixed time step "t" the external cooling circuit is not

able to cool down the battery below air dew point, so condensation cannot take place and water harvested for that "t" is zero. In the next time step "t+dt" the battery could have reached a temperature lower than the actual dew point of air, therefore water collected is for sure non-zero. This situation may arise several times in the simulation, especially in those tests where ambient air is characterized by high temperature. It is important to recall that the external environment acts as cold sink, but it has thermodynamic limits.

5.2.2 Influence of initial water uptake

The sensitive analysis regarding the initial water uptake has been done also for regeneration phase. The values chosen are: 0.1, 0.15, 0.2, 0.25. Variables controlled are the same analysed previously.

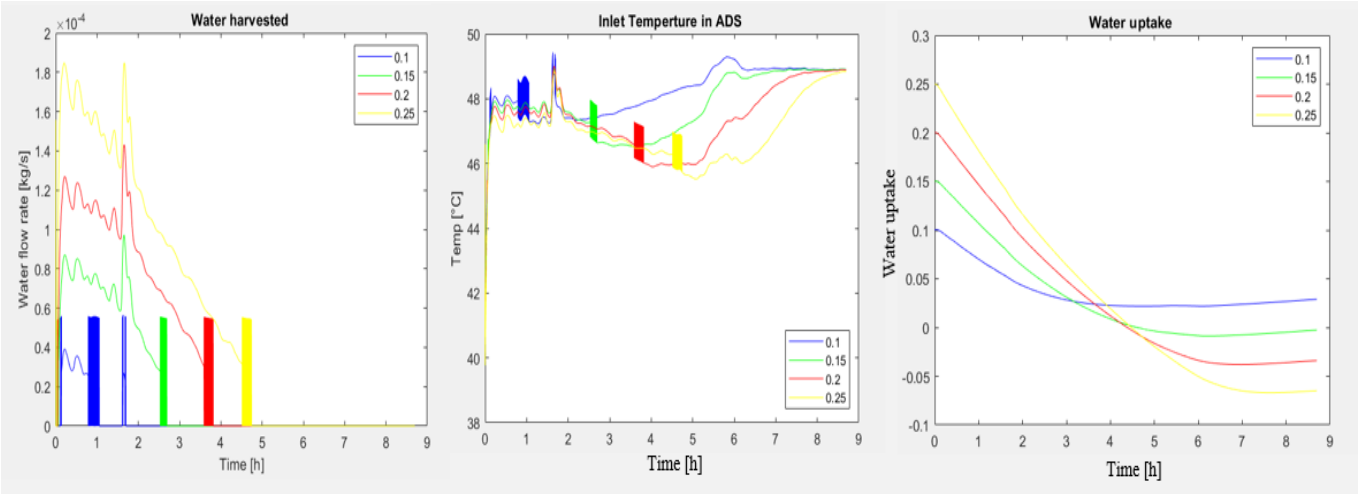

Figure 48. Test n° 1 – Initial moisture content influence

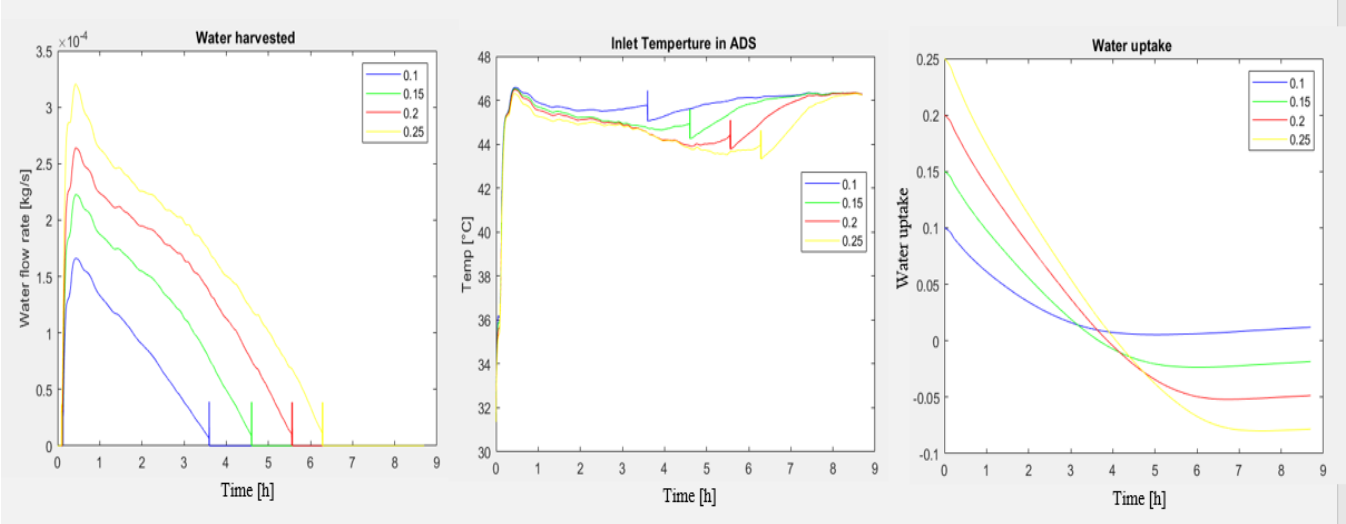

Figure 49. Test n° 3 – Initial moisture content influence

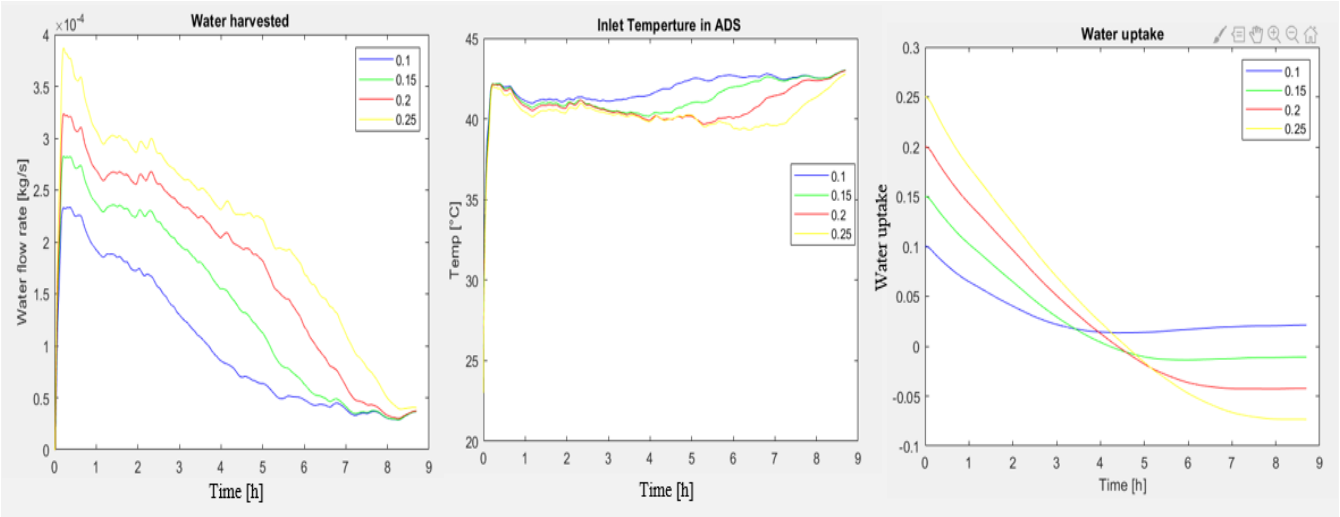

Figure 50. Test n° 9 – Initial moisture content influence

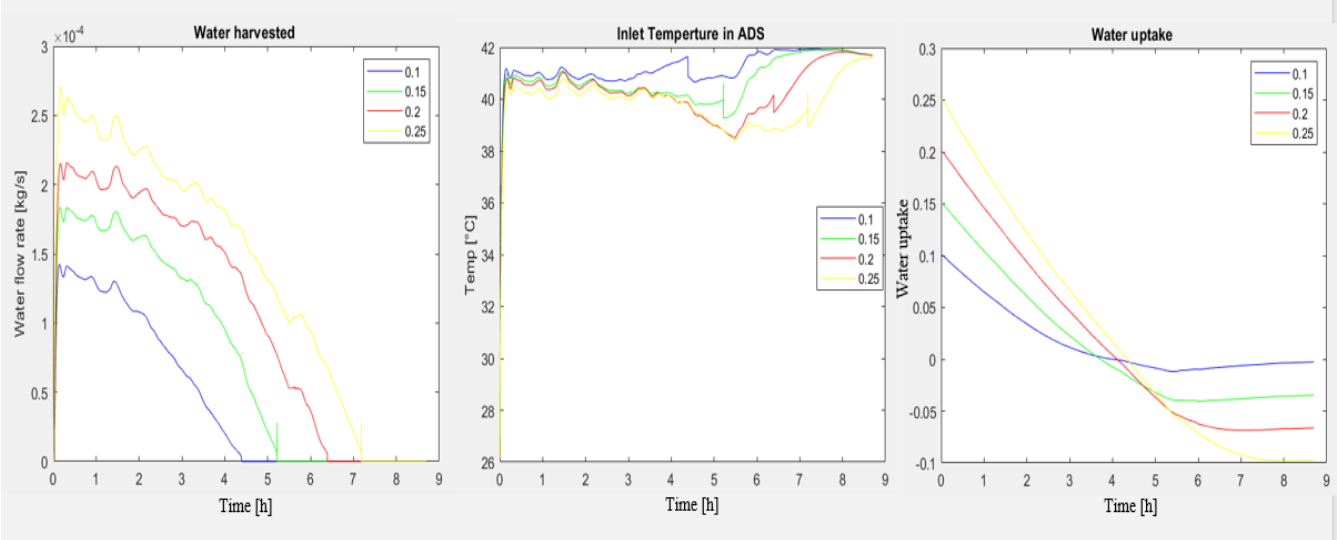

Figure 51. Test n° 23 – Initial moisture content influence

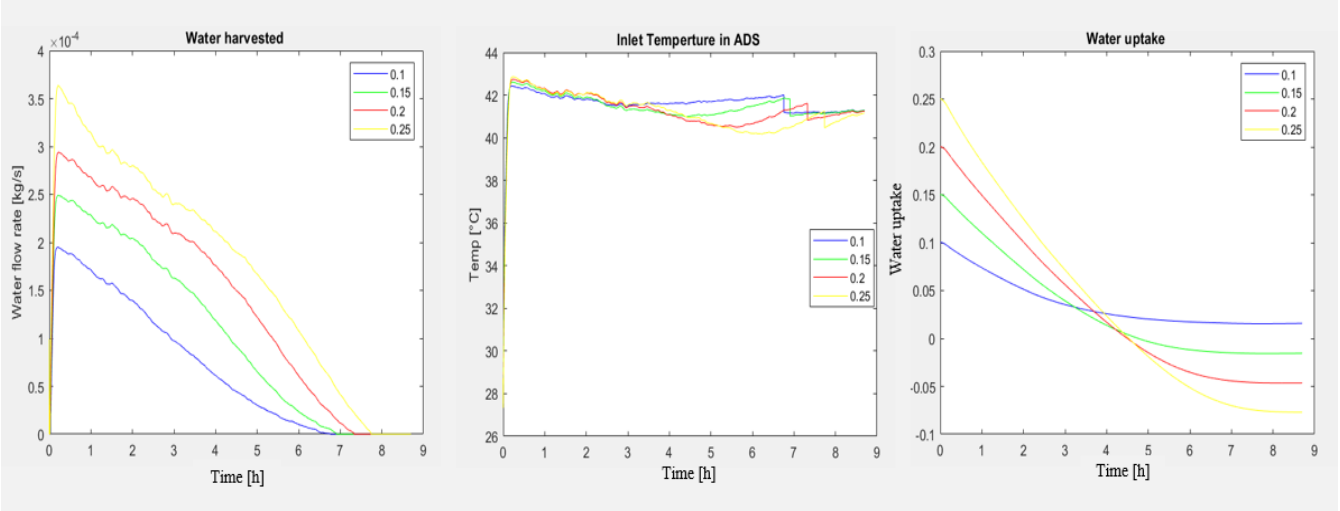

Figure 52. Test n° 29 – Initial moisture content influence

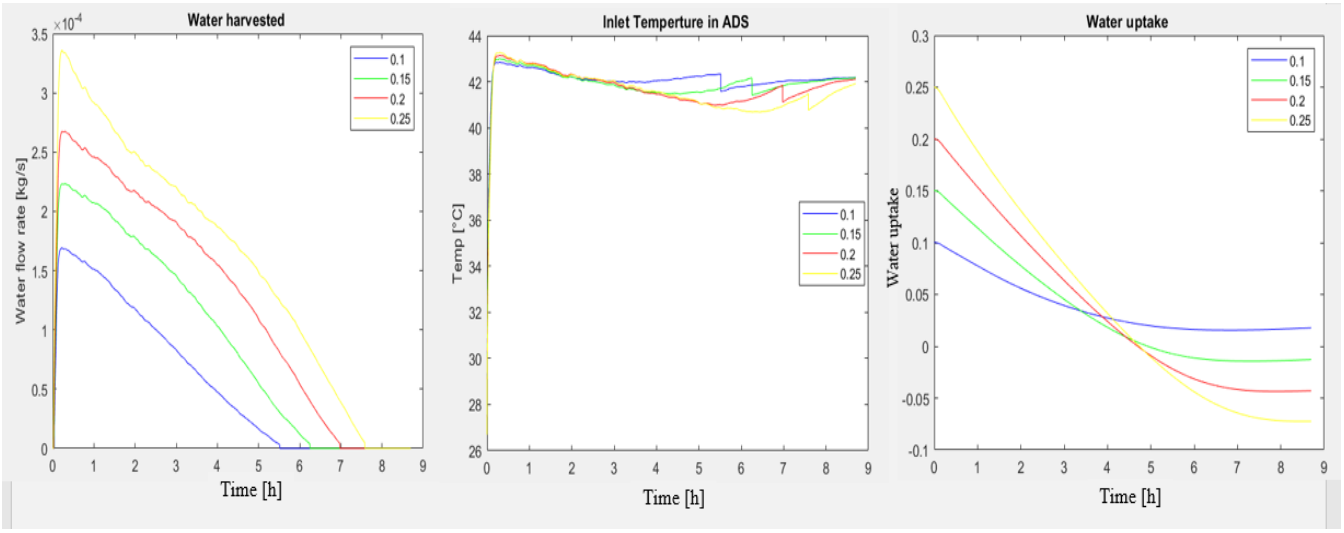

Figure 53. Test n° 33 – Initial moisture content influence

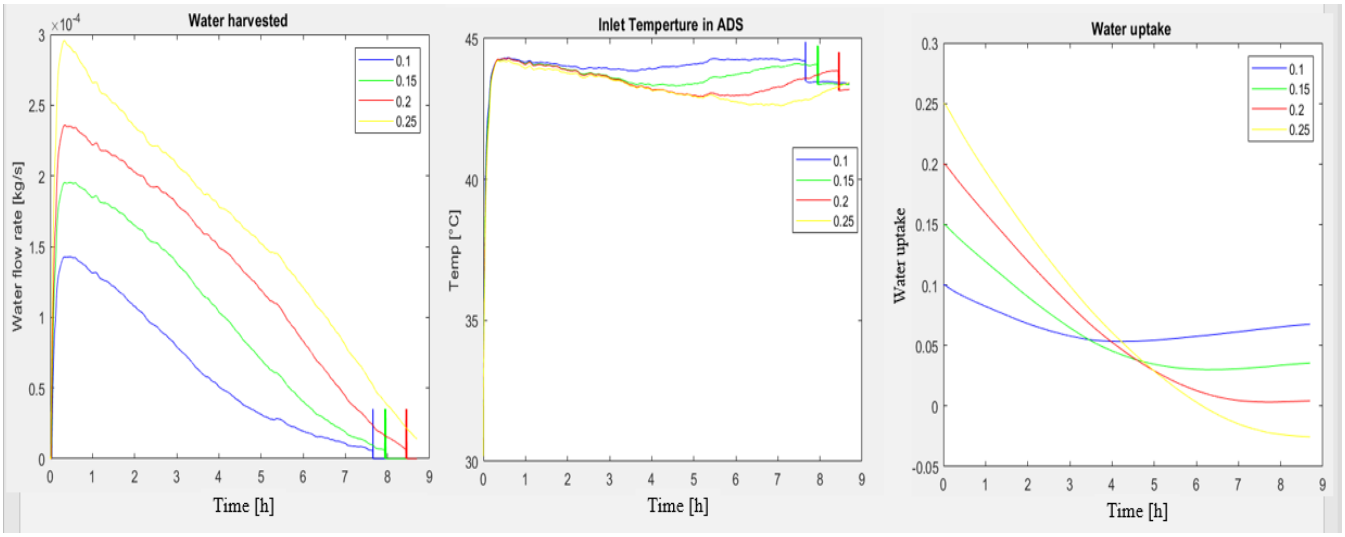

Figure 54. Test n° 37 – Initial moisture content influence

In agreement with results in adsorption phase, water harvested increases if the initial water uptake is higher because air entering the cooling system is colder and wetter. On the same physical principle we can state that, air temperature at the end of the process has a slightly inverse trend with the initial value of water uptake. On the other side water uptake trend in time is accelerated by high initial value, describing the tendency of the bed to desorb water if it is available in high amount.

5.2.3 Influence of temperature of cooling battery

The sensitive analysis related to the variable "T_{batt}" has been performed assuming that the external cooling system is always able to maintain a fixed temperature of the battery inside the condenser. The temperature of the battery has been fixed equal to : 15 °C, 20°C, 25°C and 30°C.

The variables controlled are water harvested and air temperature at the end of the cooling process. Results are summarized in the next charts:

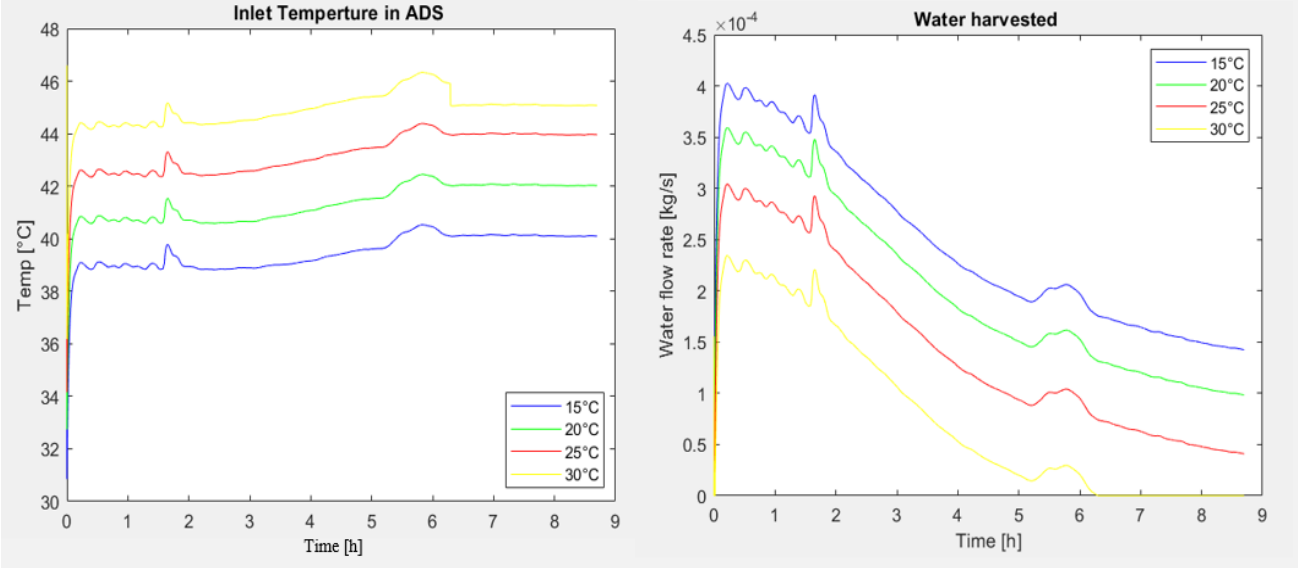

Figure 55. Test n° 1 – Battery temperature influence

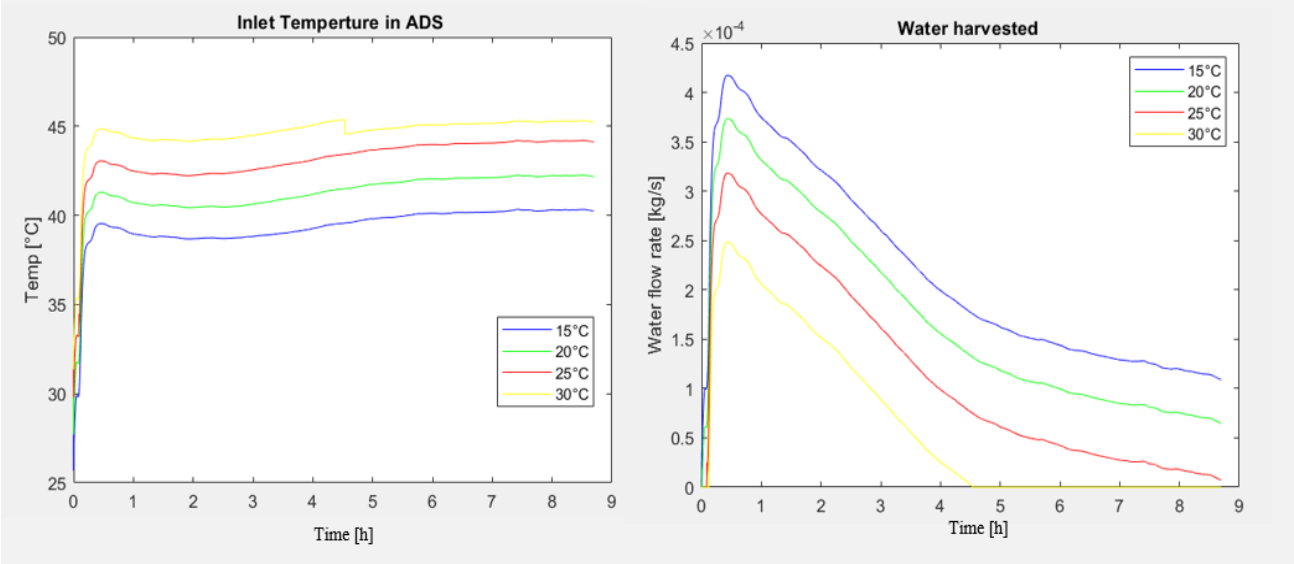

Figure 56. Test n° 3 – Battery temperature influence

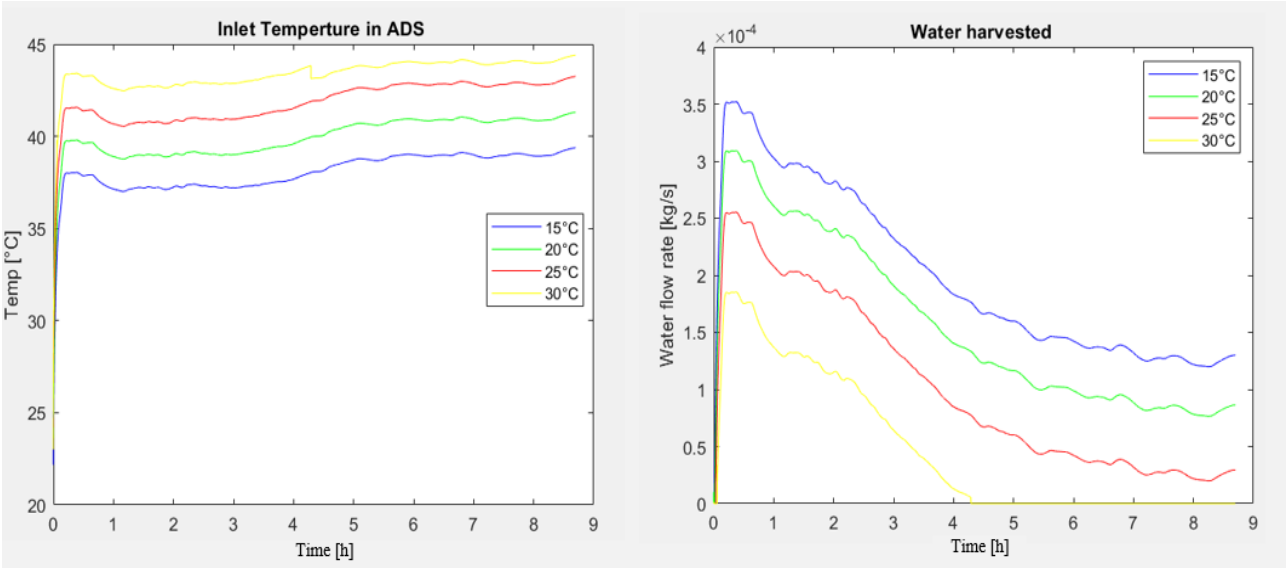

Figure 57. Test n° 9 – Battery temperature influence

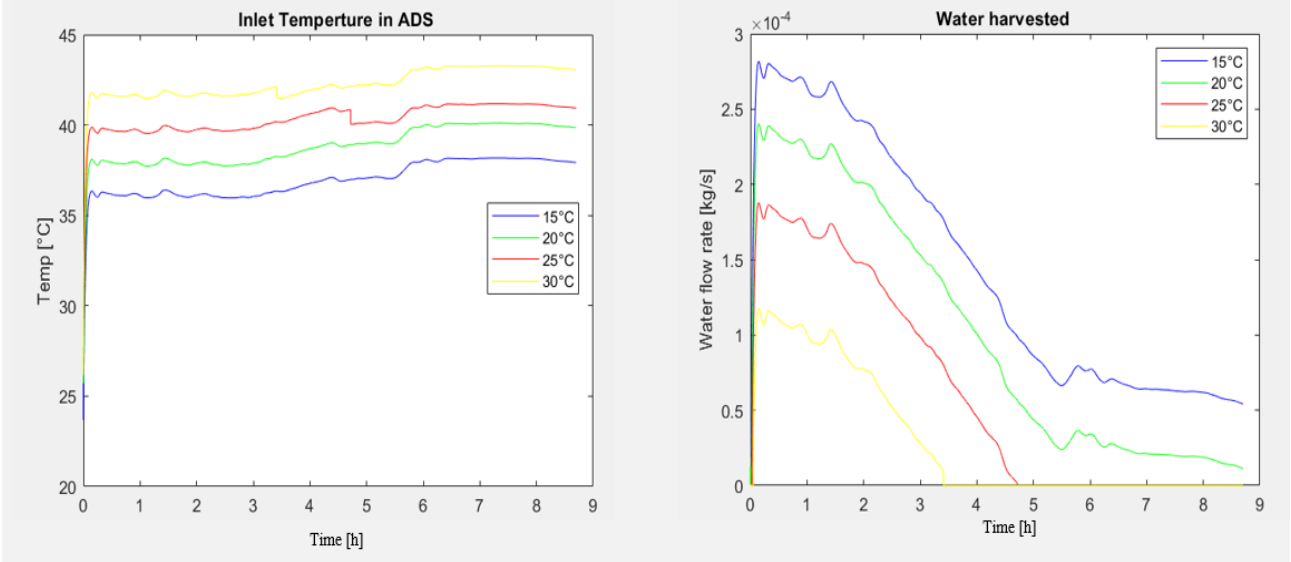

Figure 58. Test n° 23 – Battery temperature influence

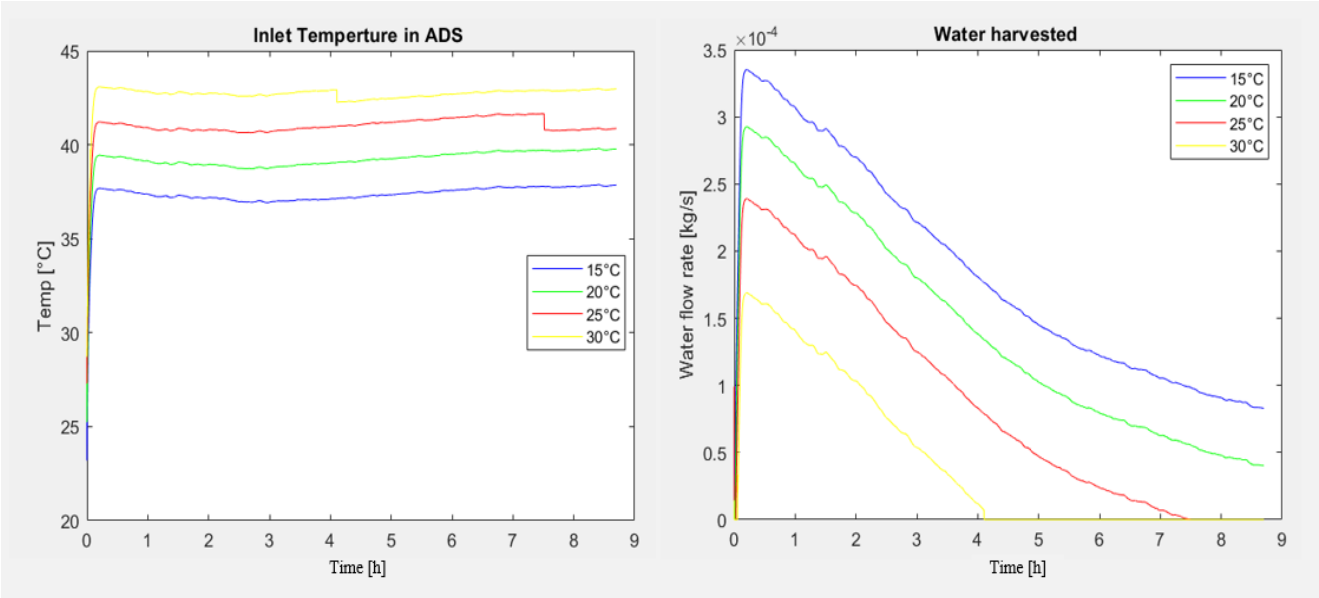

Figure 59. Test n° 29 – Battery temperature influence

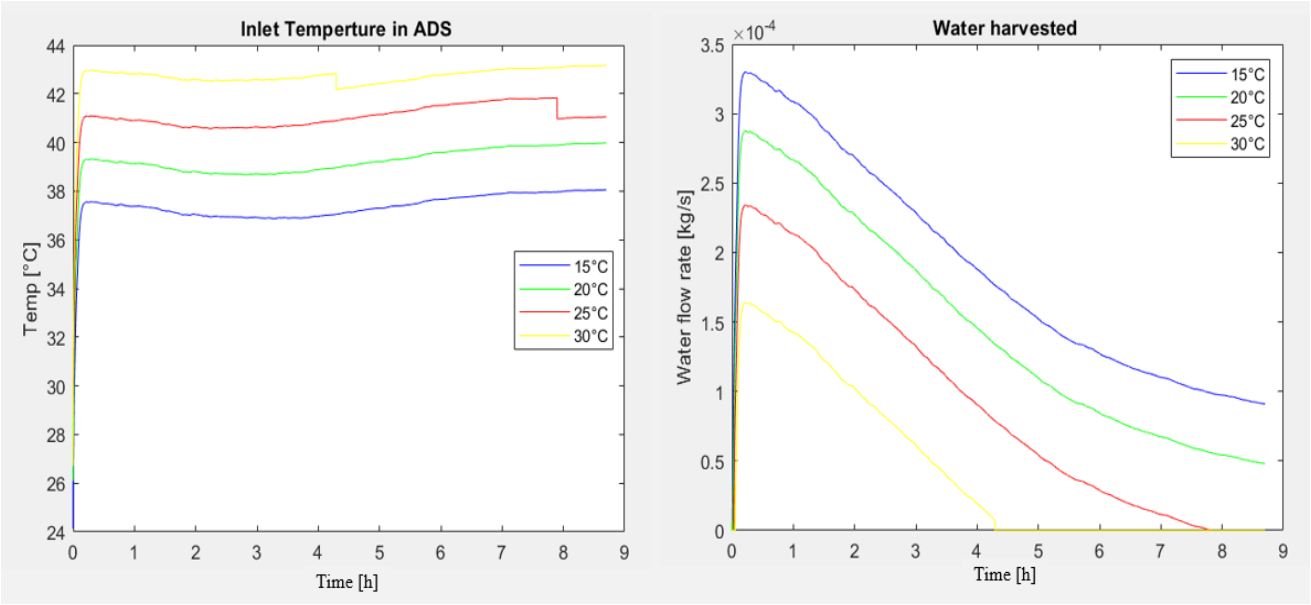

Figure 60. Test n° 33 – Battery temperature influence

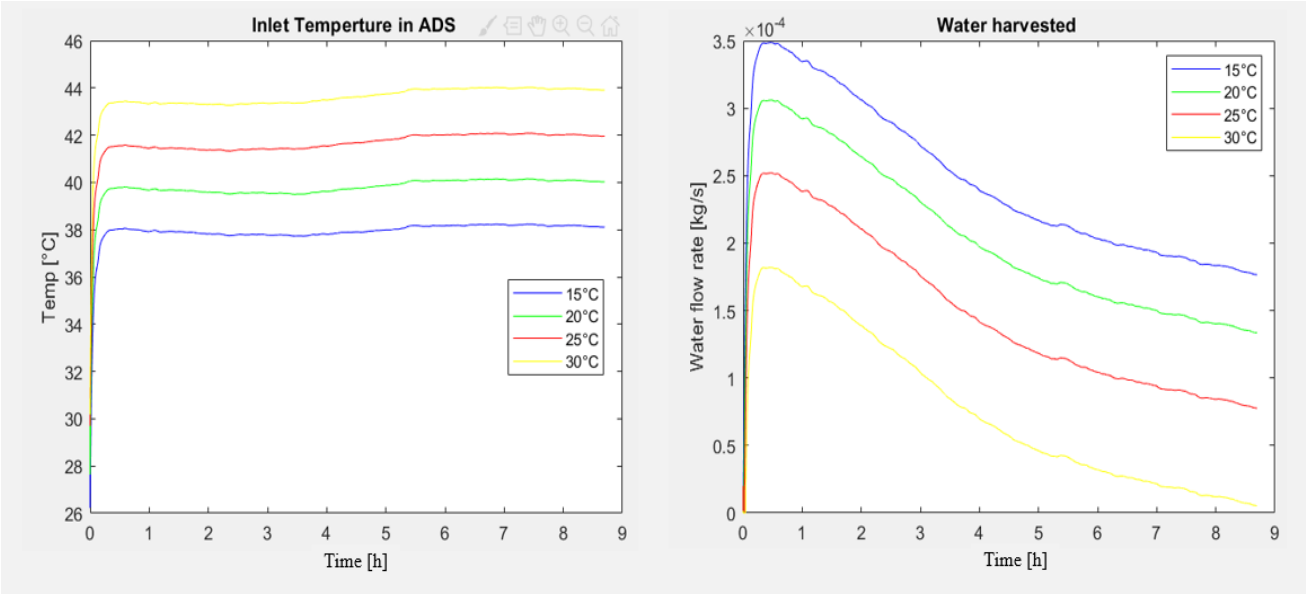

Figure 61. Test n° 37 – Battery temperature influence

As it was expected, lower the temperature of the cooling battery, higher the amount of water harvested because there is higher probability of being below the dew point. The direct consequence is the lower outlet temperature of exiting air stream. Moreover, it can be notice that at higher cooling temperature corresponds more instantaneous variations. This can be explained considering that in such cases the battery has more difficulty to reach a temperature that ensures condensation.

5.3 Model validation

The performance of regeneration model can be evaluated through the error analysis, in this way we can understand how far model results are from experimental outputs. The study of the error goes through the evaluation of three parameters:

- Relative error $\varepsilon = \frac{|X_{model} - X_{Exp}|}{X_{Exp}}$ (6.1)
- Variance $\sigma^2 = \sum_{i=1}^{n} \left(\frac{|X_{model} - X_{Exp}|}{X_{Exp}} \right)^2 * \frac{1}{n}$ (6.2)
- Root Mean Square value $RMS = \sqrt{\sigma^2}$ (6.3)

Regeneration tests are ordered in descending way as function of ambient temperature, they are simulated are the three parameters described are calculated. The variable subjected to error analysis are :

- Air inlet temperature at condenser
- Air outlet temperature at condenser

- Air inlet moisture at ADS-HE

These are the only variables for which experimental data are available in regeneration phase. Next figures provided relative errors of each variable analysed in histogram form, where results of tests are compared to show the influence of ambient conditions on the model. Histograms present nine timesteps, for each the error is calculated as the average in that interval.

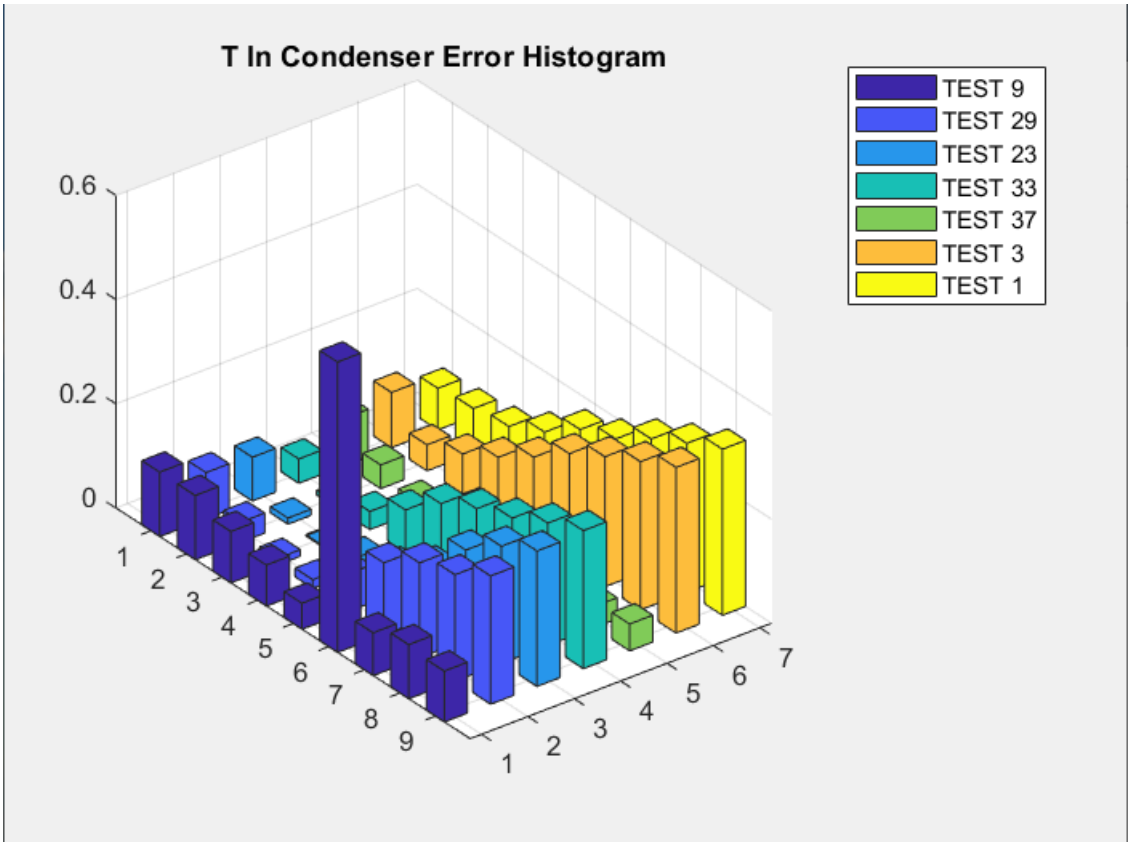

Figure 62. Relative error of air inlet temperature at condenser

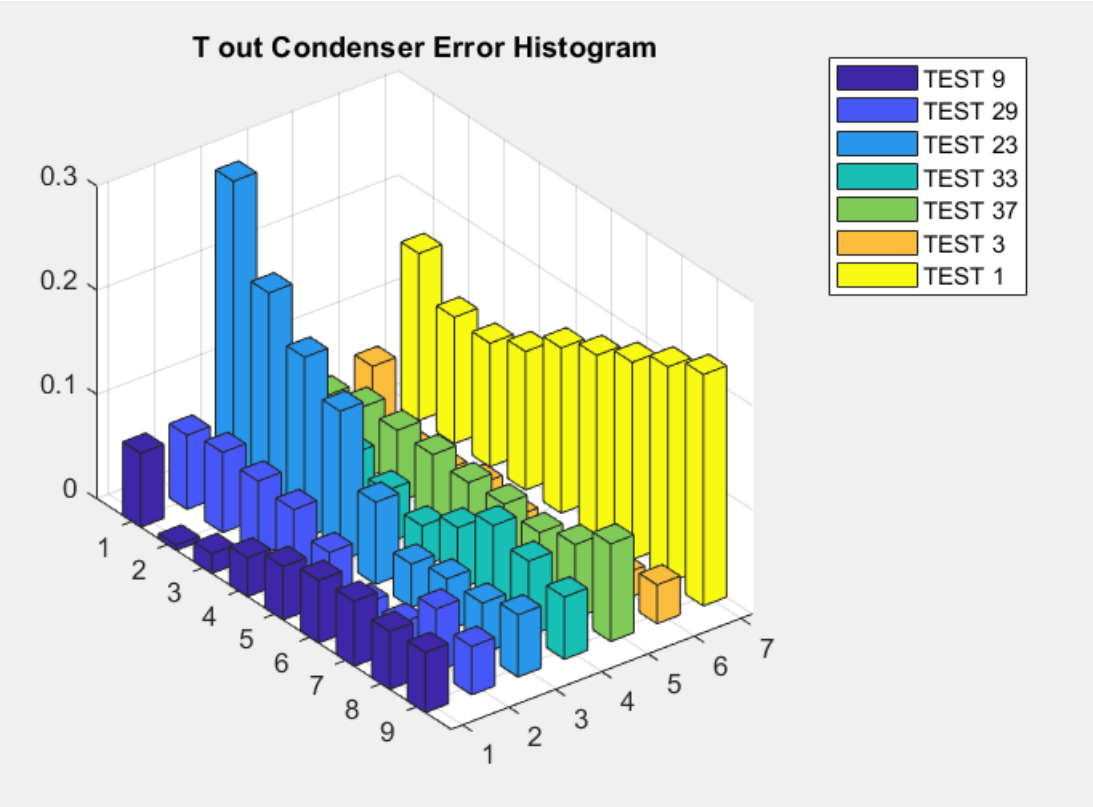

Figure 63. Relative error of air outlet temperature at condenser

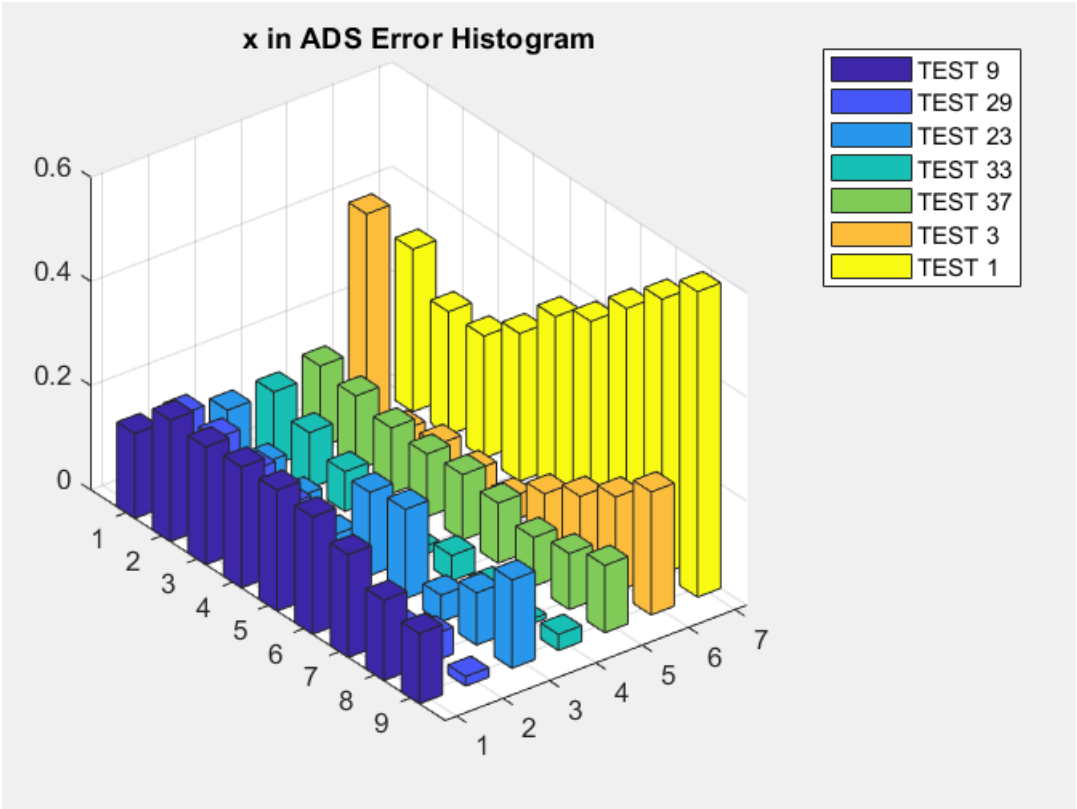

Figure 64. Relative error of air inlet moisture at ADS-HE

The next table provides results of variance and Root Mean Square value in addition to the average estimation of the relative error.

TEST	T AMB	Ambient moisture	VARIANCE			RMS			MEAN RELATIVE ERROR		
-	[°C]	[kg_w/kg]	T in cond	T out cond	X in ADS	T in cond	T out cond	X in ADS	T in cond	T out cond	X in ADS
9	22	0.0163	0.06	0.029	0.04	0.26	0.05	0.19	0.14	0.04	0.19
29	24	0.0174	0.0233	0.003	0.01	0.15	0.05	0.1	0.12	0.05	0.08
23	25	0.0207	0.027	0.022	0.019	0.16	0.15	0.13	0.11	0.12	0.11
33	26	0.0221	0.029	0.004	0.0048	0.17	0.06	0.07	0.14	0.06	0.05
37	29	0.026	0.003	0.005	0.016	0.05	0.07	0.12	0.038	0.07	0.12
3	30	0.0098	0.045	0.013	0.078	0.21	0.036	0.28	0.18	0.025	0.15
1	37.5	0.0363	0.045	0.03	0.17	0.21	0.17	0.41	0.19	0.16	0.39

Table 3 . Results of error analysis

Results of error analysis underline a difference between experiments and model. This can be explained considering that the model is degnied to work with an intial set of data provided by the expirience. Indeed, what should be done is to reorganize the model and let it able to work with a single intial value, that is updated with results carrried out from the regeneration process. In conclusion, these errors are attributed to the unconnection between the beginning and the end of the code, which still remains a possible upgrade of the model.

5.4 Breath performance

The analysis of the atmospheric water harvesting generator goes on with the evaluation of the energetic performance. All previous tests have been simulated again using the optimal value of each design variable, except for Test n°1 that lacks of a corresponding adsorption test. The purpose is to evaluate energy consumed in complete adsorption-regeneration cycles, this why Test n° 1 is excluded.

The specific consumption of primary energy "S_c" is used as reference for the performance of the system. This quantity is defined as the total primary energy required to produce 1 kg of pure water. As already mentioned, Breath makes use both of thermal and electrical energy to harvest water. Heat is supplied by solar panels installed in loco, therefore it is already considered primary energy. Electric energy requires a primary-conversion-factor that accounts for the average efficiency of electricity production from fossil fuels. The conversive factor used in the analysis is 0.38 . This value accounts for the overall conversion efficiency of the national power system.

The parameter S_c is calculated in two different scenarios, described as follows:

- Theoretical scenario: all water adsorbed is harvested in the condenser
- Real scenario: water produced is just that harvested in the condenser

Thermal energy used in regeneration is evaluated as sensible heat supplied by water during the process, using the well-known formula:

$$P_{th} = \dot{m}_w \, c_{p_w} \left(T_{w_{IN}} - T_{w_{OUT}} \right) \quad [W] \quad (6.4)$$

This quantity is estimated for each time step of the simulation and the corresponding thermal energy is given by the sum of all power contributes.
Electrical energy is the product between power of blowers and pumps discounted of regulation percentage, and the effective hours of operation. To do so, It is assumed a time of adsorption and regeneration respectively of 15 h and 9 h. In this way tests can be compared on the same base, and results in term of water produced are function of external condition only. Moreover, a single cycle has the timeframe of one day, therefore it is an useful value to estimate annual performance. Results in term of specific primary energy consumption are shown in the chart below:

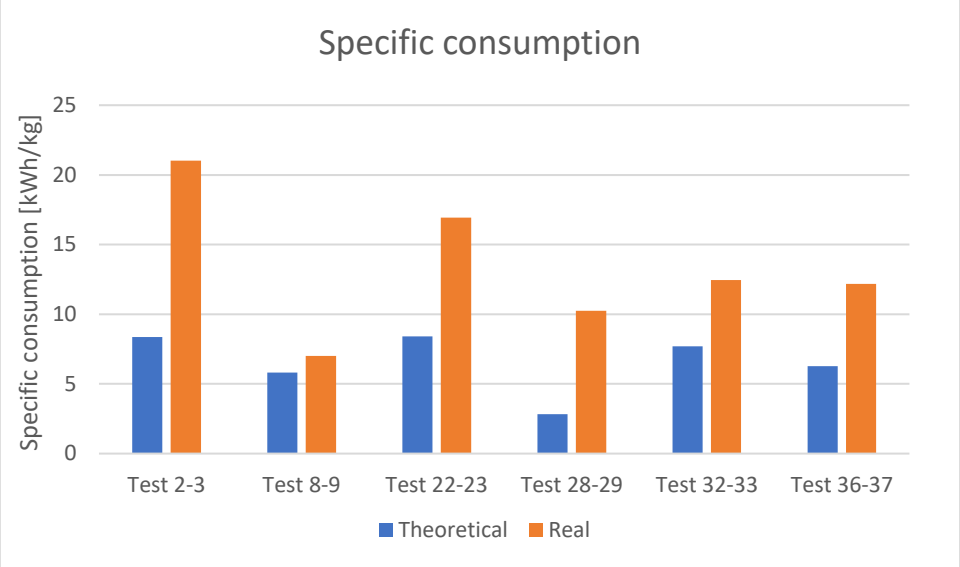

Figure 65. Comparison between theoretical and real specific energy consumption

TEST	Eel_{ADS} [kWh]	Eel_{RIG} [kWh]	Eth [kWh]	Water adsorbed [kg]	Water harvested [kg]	S_c ideal [kWh/kg]	S_c real [kWh/kg]
2-3	1.755	4.185	5.95	2.74	1.09	8.36	21.02
8-9	1.755	4.185	5.68	3.9	3.23	5.8	7.013
22-23	1.755	4.185	5.56	2.68	1.33	8.4	16.94
28-29	1.755	4.185	5.06	3.88	2.15	2.83	10.24
32-33	1.755	4.185	4.68	2.81	1.74	7.7	12.44
36-37	1.755	4.185	4.7	3.46	1.78	6.26	12.17

Table 4. Quantity used to estimate S_c

The simulation proved that thermal energy requirement is almost equal for each simulation, with an average value of 5.3 kWh/cycle, while electrical energy is always constant because fan regulation and time simulation have been assumed equal for all tests. This value is 5.94 kWh/cycle, and it is given by summing adsorption and regeneration contributes shown in Table .
Values estimated of energy consumption are used in the case study presented following.

5.5 Case study

The object of this paragraph is the development of a case study to evaluate the potential of Breath in real applications. For this purpose, three locations have been identified, these are: Mosul (Iraq), Casablanca (Morocco) and Bangkok (Thailand). Simulations have been performed considering the average monthly ambient data of each location, whose values have been taken from dataset available in Metonorm. Trends of ambient temperature and relative humidity are summarised for each location and shown in next figures:

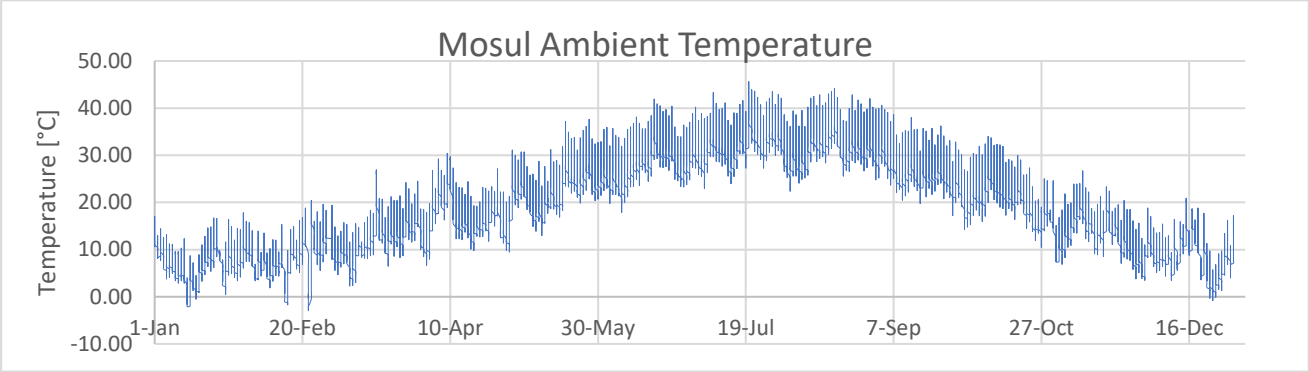

Figure 66. Mosul ambient temperature yearly trend

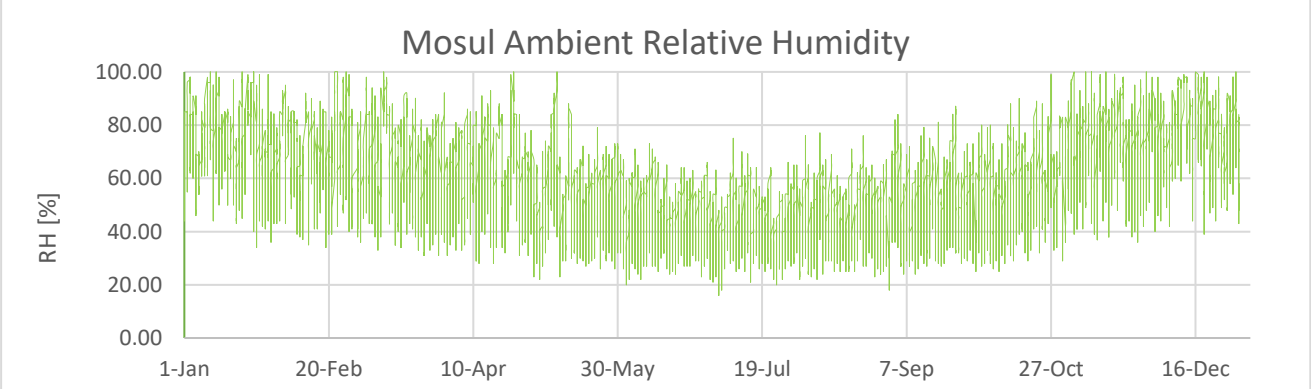

Figure 67. Mosul ambient RH yearly trend

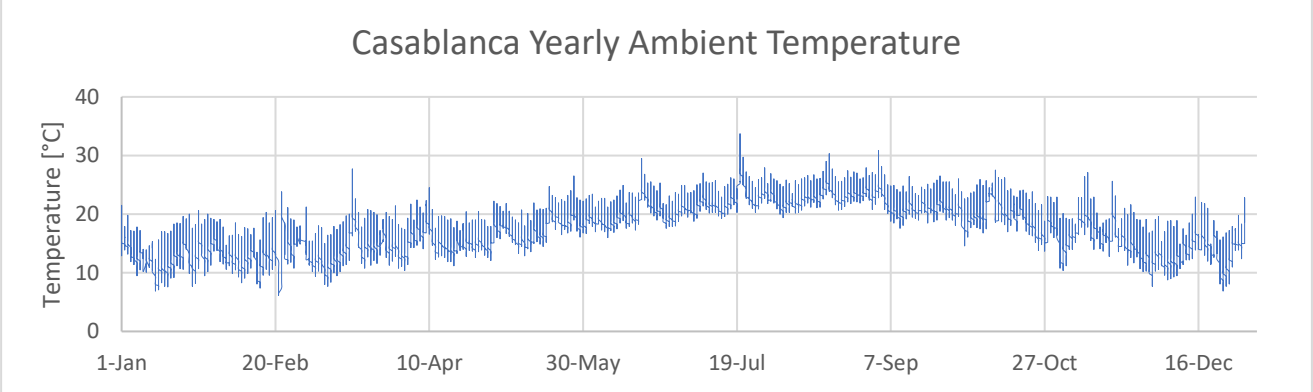

Figure 68. Casablanca ambient temperature yearly trend

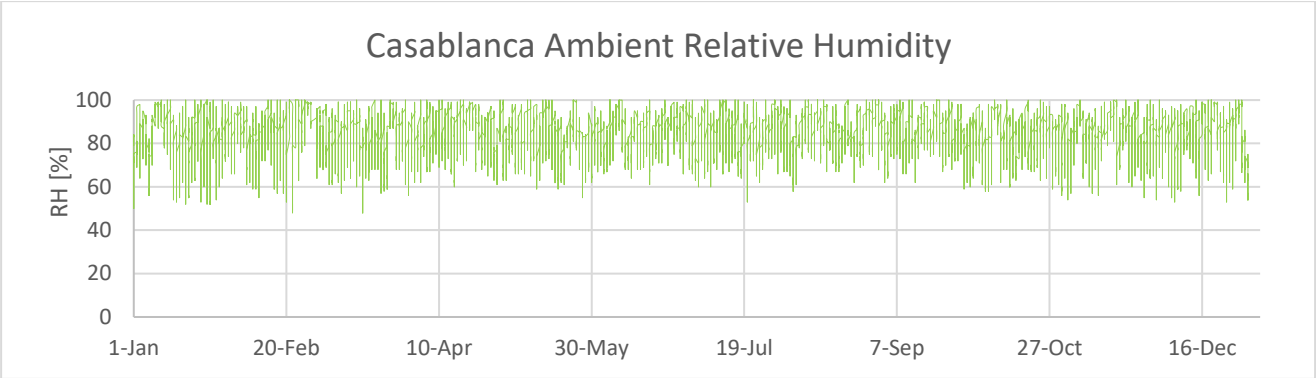

Figure 69. Casablanca ambient RH yearly trend

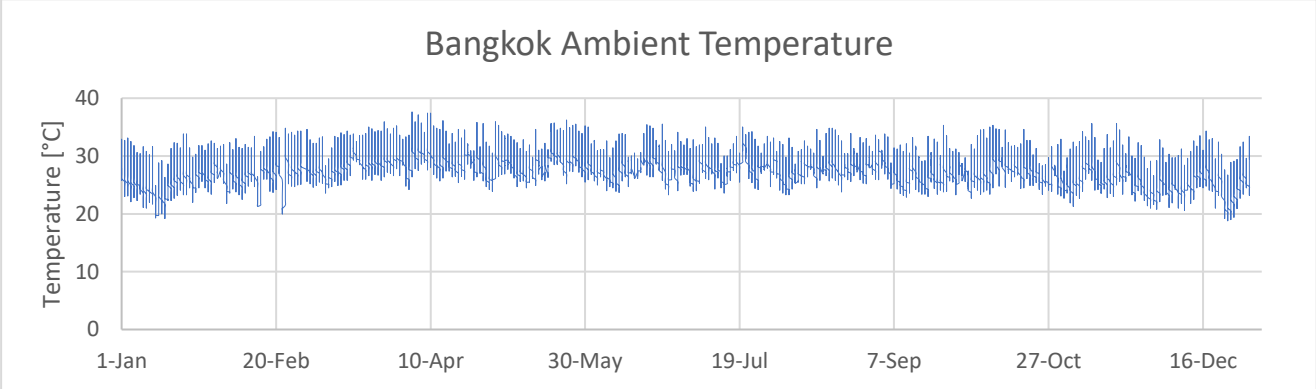

Figure 70. Bangkok ambient temperature yearly trend

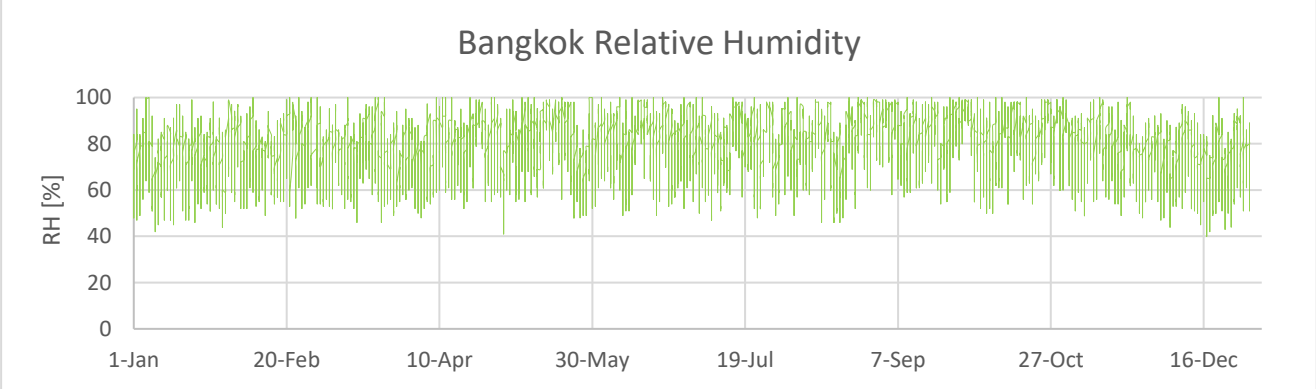

Figure 71. Bangkok ambient RH yearly trend

In the end, these data have been manipulated in order to get a 24 hour-representation of the average day for each month. Therefore, twelve days for each location are obtained, each characterized by 24 values, where a single value is the average hourly of the ambient condition for the reference month. These data are used to estimate water productivity of Breath in Mosul, Casablanca and Bangkok.

The first object of the analysis is to understand if it is more convenient to adsorb water during day or night. Indeed, ambient conditions changes between day and night, therefore we expect different rate of production. For this reason, productivity is estimated in two different timeframes: from 6 am to 9 pm is the reference timeframe for day-simulation, while 6 pm to 9

am is the one chosen for night-simulation. Moreover, it is assumed that water produced is equal to water adsorbed by Silica-gel and the adsorption phase lasts 15 hours.
Next figures provide values of average monthly water production for the three locations, respectively classified in day and night production:

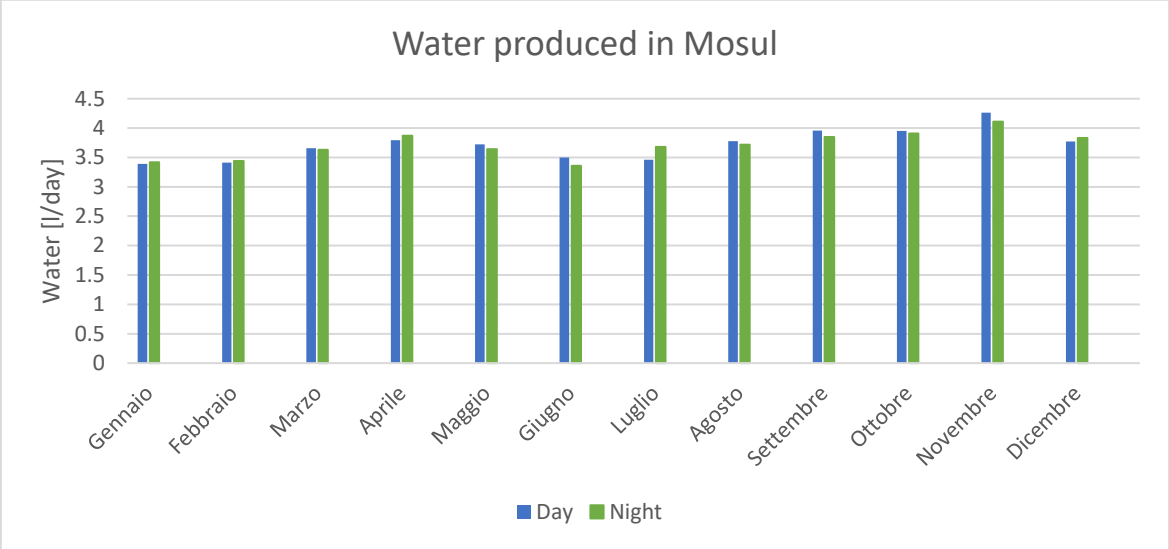

Figure 72. Rate of water production in Mosul

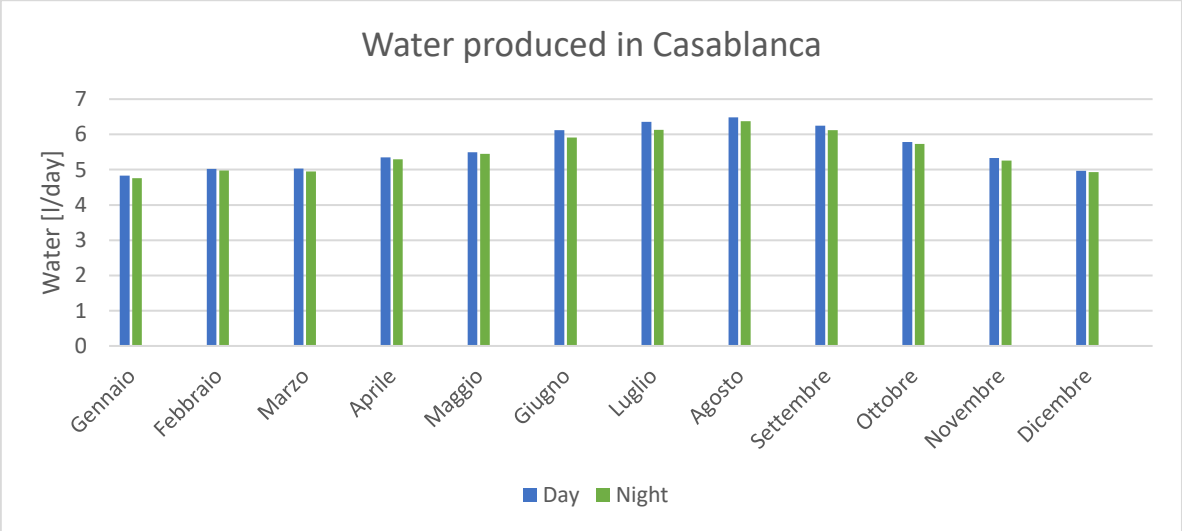

Figure 73. Rate of water production in Casablanca

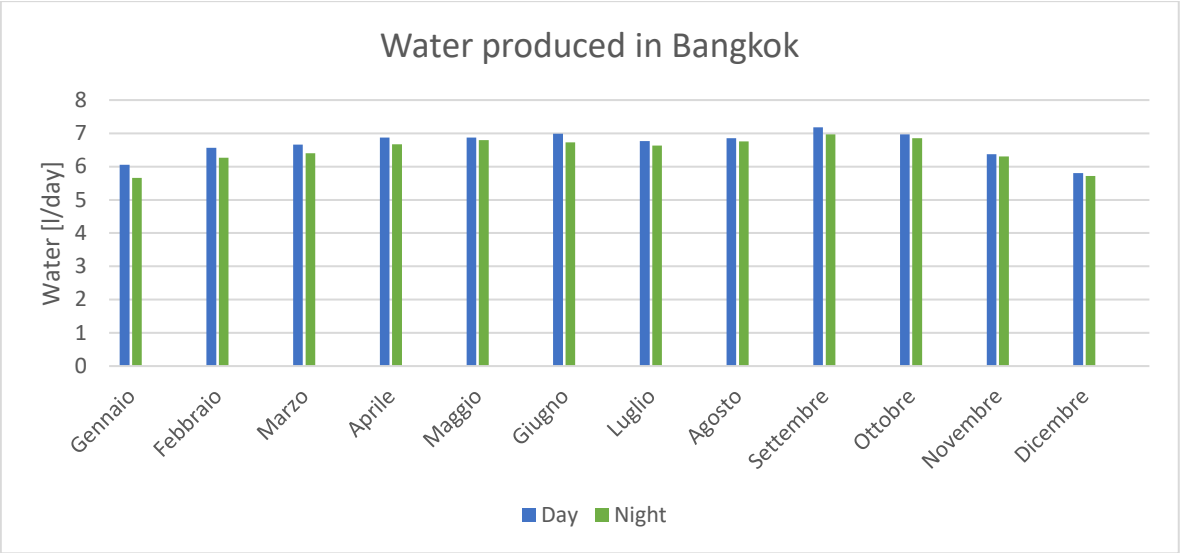

Figure 74. Rate of water production in Bangkok

As shown by the evidence, there is no difference in water production between day and night. This is a very important result if we just think at all possible applications of this innovative water generator. Indeed, the system is able to produce the same amount of freshwater almost in any moment of the day, so it can be activated according to the availability of energy that drives the process. For example, just think to integrate Breath in existing power plants. It could be used when low-grade heat is available obtaining a double useful effect: water production avoiding any kind of energy waste. In such application, the system could be installed almost in any water intensive industry.

The analysis continues with the economic study of Breath , using as reference parameter the average yearly water production "BWP". For each location, this parameter is calculated by taking the mean daily rate of production and multiplying it times 365 [day/year]. Considering that the Matlab model provides results in litre as unit of measure, this is then converted in cubic meter.

Final values are listed in the table below:

Mean rate of water production [m3/year]			
City	Mosul	Casablanca	Bangkok
Day	1.36	2.04	2.43
Night	1.35	2.004	2.37
Average	1.35	2	2.4

Table 5. Estimated rates of production

5.5.1 Integration with hydroponic greenhouse: Cash flow analysis

The cash flow analysis is performed considering the integration of Breath with the hydroponic greenhouse built at Energy Centre. Considering the total hosting capacity of the greenhouse equals to 180 plants and assuming to use salad as growing species, we are going to evaluate if this water generator is able to cover water requirement when installed in those locations already studied. Water requirement is estimated on the basis of the average water requested by a salad plant during the growing period. These data have been taken from literature, and they are equal

to 3 [l/plant] on average growing season of 40 days [water required by salad]. Assuming that after one culture is harvested an other is immediately planted so that continuity is ensured, the annual water requirement "WYR" of the greenhouse can be evaluated as follows:

$$WYR = n°_{plant}\ \ n°_{culture} * \frac{PWR}{1000} \quad \left[\frac{m^3}{year}\right] \quad (6.5)$$

where :

- $n°_{plant}$ is the number of plant hosted, equal to 180.
- PWR is the plant water requirement along the growing season, equal to 3 [l/plant]
- $n°_{culture}$ is the number of culture cultivable in the greenhouse for a given species along one year, evaluated as days in a year divided the value of growing season. In this analysis its value is 9, rounded in defect.

The WYR has been used as reference to evaluate the number of units of Breath required to satisfy the demand for water of the hydroponic greenhouse. This procedure is applied for all studied locations using the formula written below:

$$n°_{Breath,j} = \frac{WYR}{BWP_j} \quad [units] \quad (6.6)$$

where:

- BWP_j is the rate of production of Breath in the j-th location estimated previously

After having collected these data, the cash flow analysis is carried out considering four different scenarios, assuming that the cost of the technology will decrease from the starting value of 9000 [€/unit] down to 500 [€/unit], and a lifetime of the system equals to 15 years. Moreover, each scenario is provided in two different configurations, the base one and the improved. The improved configuration is characterized by the integration of photovoltaic panels to cover the electrical demand of Breath units. In any case, the estimation of the Net Present Value "NPV" of all scenarios is done starting from the evaluation of the following parameters:

- Evaluation of Capital Expenditures "CAPEX":
  -Base scenario: cost for purchasing Breath units
  -Improved scenario: cost of Breath units + cost of PV system

- Evaluation of Operative Expenditures "OPEX":
  -Base scenario: cost of electrical energy + Operation and Maintenance costs "O&M"
  -Improved scenario: O&M costs only

- Evaluation of Incomes:
  -Base scenario: savings of water and heat
  -Improved scenario: savings of water, heat and electrical energy

In the analysis, thermal and electrical energy consumptions are taken from experimental tests and they are respectively 5.3 [kWh_{th}/day/unit] and 5.94 [kWh_{el}/day/unit]. Unfortunately, unit

costs for these energy vectors are unavailable for the chosen locations, therefore they are assumed equal to energy costs in Italy: 0.069 [€/kWh$_{th}$] and 0.15 [€/kWh$_{el}$]. On the other side, water prices have been taken from the "Global water market review", that provides costs for water across the Word. O&M costs have been assumed equal to 1% of the initial investment, according to previous economic studies involving other innovative technology as Fuel cells.
The evaluation of NPV requires the discount rate "i", which is assumed equal to the Weighted Average Cost of Capital "WACC". This quantity is calculated assuming that the initial investment is equally divided in equity "E" and debt "D" capitals. The definition is given in the equation below:

$$WACC = k_e \frac{E}{D+E} + k_d \frac{D}{D+E} \quad (6.7)$$

where:
-k_e is the cost of equity assumed equal to 3% according to literature [40], [41], [41], [42]
-k_d is the cost of debt assumed equal to 5% according to literature [40], [41], [41], [42]

Eventually, the NPV is calculated as follows:

$$NPV = -I + \sum_{t=1}^{15} \frac{B_t}{(1+WACC)^t} \quad [€] \quad (6.8)$$

where:
-B_t is the cash flow rate of the t-th year, evaluated as difference between Incomes and OPEX costs
- I is the initial investment, or also called CAPEX costs.

Before showing results of the analysis, it is necessary to go deeper inside the methodology used to evaluate specifications of the photovoltaic system.

5.5.1.1 Photovoltaic system

Specifications of PV system are carried out from the energy balance between the load and the generator. In this application, the load is represented by the number of atmospheric water generators needed to cover the water demand, whose energy consumption derives from blowers and pumps within the system. Therefore, the energy of the load "E$_{load}$" is calculated for the three locations by multiplying the daily electrical requirement previously evaluated and the number of units. This quantity is then converted on yearly basis.

$$E_{load,j} = E_{el,Breath}\, n°_{Breath,j}\, 365 \quad \left[\frac{kWh_{el}}{year}\right] \quad (6.9)$$

PV characteristics in terms of nominal power "P$_n$" and total aperture area "S$_{PV}$" are evaluated using guidelines indicated in "IEC standard 61724" as follows:

$$E_{PV,j} = H_{g,j}\, S_{PV,j}\, \eta_{STC}\, PR = P_{n,j}\, h_{eq,j}\, PR \quad \left[\frac{kWh_{ele}}{year}\right] \quad (6.10)$$

where :

-$H_{g,j}$ is the global in-plane radiation of the j-th location in [kWh/m^2/year]
-η_{STC} is the efficiency of PV panel in standard test conditions
- PR is the performance ratio of the system, assumed 0.6.
-$h_{eq,j}$ is the number of equivalent hours given by $h_{eq,j} = \frac{H_{g,j}}{G_{STC}}$, where "G_{stc}" is equal to 1 [kW/m^2]

Considering the photovoltaic panel developed by LG with identification code "LG350Q1C-A5", results of the procedure are summarized in the next table:

LOCATION	$n°_{Breath}$	E_{load} [kWh/year]	H_g [kWh/(m^{2}year)]	P_n [kW$_p$]	S_{PV} [m^2]	$n°_{panel}$
Mosul	4	8672.4	1701.8	8.5	41.84	24
Casablanca	3	6504.3	1797.8	6	29.7	18
Bangkok	2	4336.2	1748.45	4.14	20.36	12

Table 6

The economic analysis is performed taking as reference cost for PV installations 1500 [€/kW$_p$]. This value has been calculated by Fraunhofer Institute for Solar Energy Systems, Germany, as average cost for PV installation worldwide.
Results of the economic analysis are provided in graphical form for all simulated scenarios, taking into account the following cost for purchasing a unit of Breath:

SCENARIO 1
The cost for the technology is taken equal to the actual investment for the laboratory system. This is equal to 9000 [€/unit].

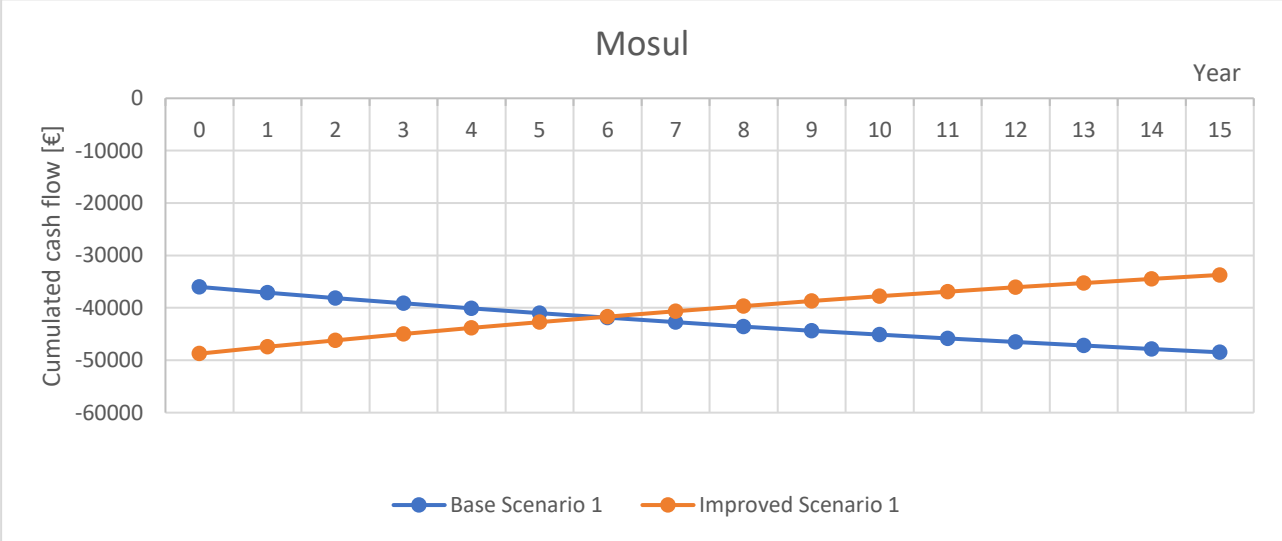

Figure 75. Mosul Scenario 1

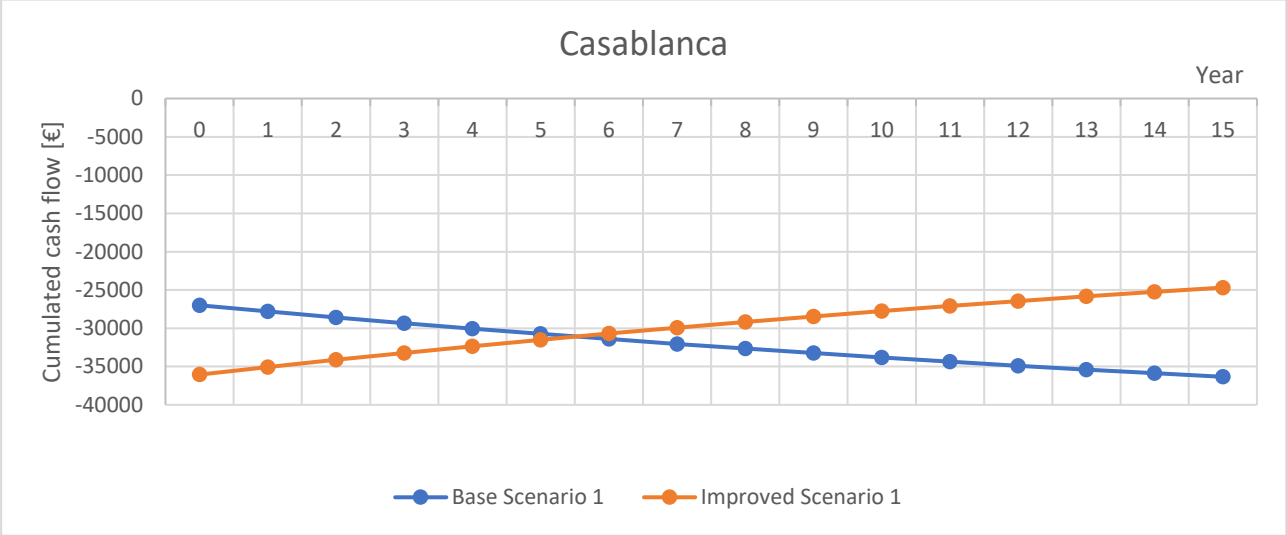

Figure 76. Casablanca Scenario 1

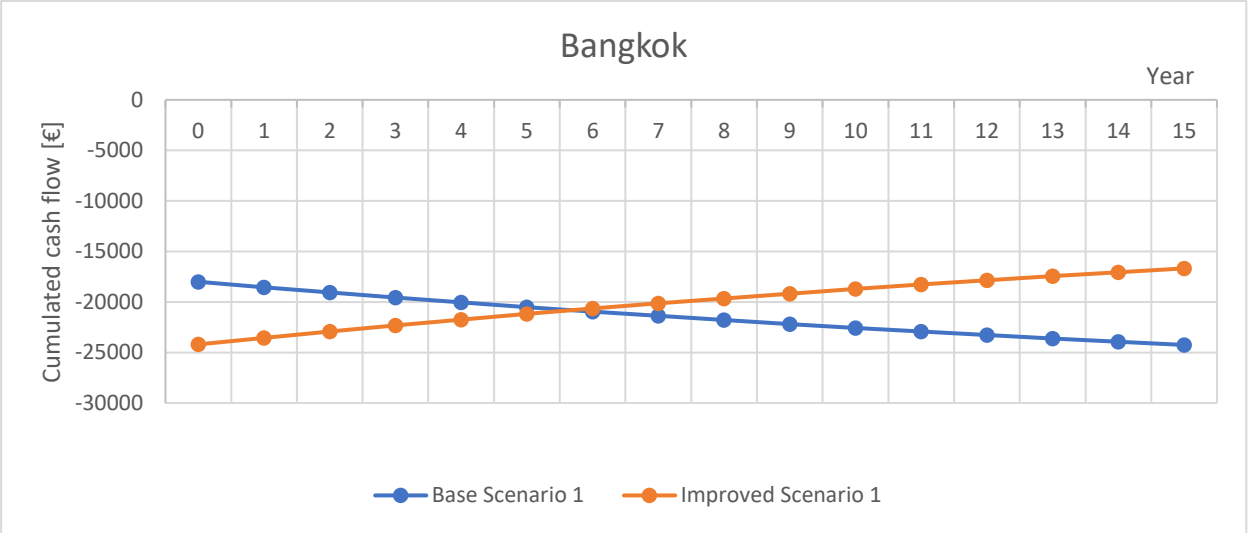

Figure 77. Bangkok Scenario 1

SCENARIO 2

The cost for the technology is taken equal to 5000 [€/unit] assuming to scale the cost of technology of 45% than the actual cost.

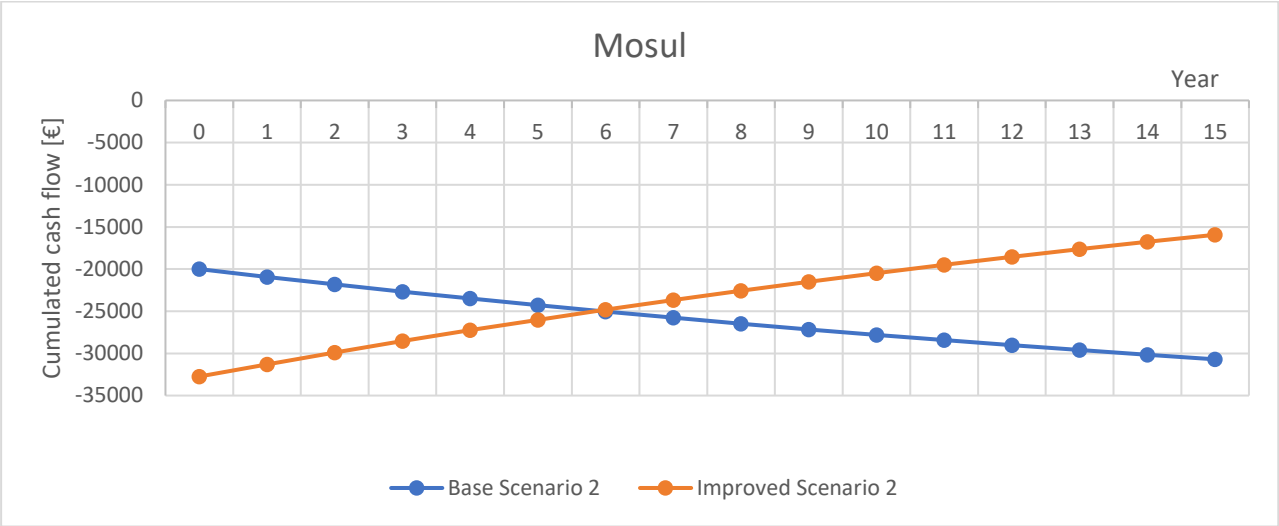

Figure 78. Mosul Scenario 2

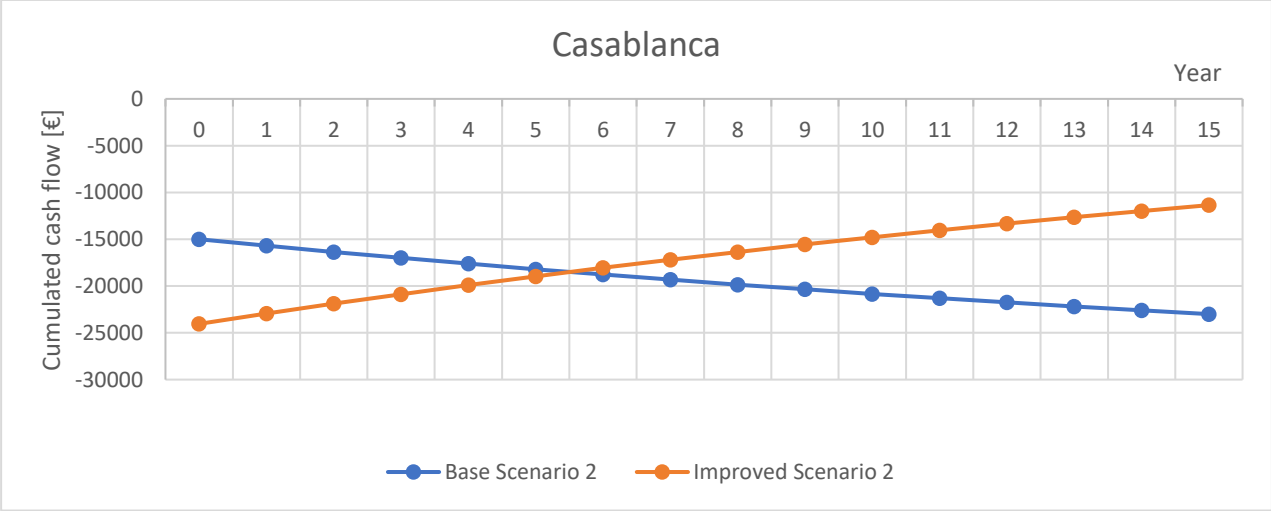

Figure 79. Casablanca Scenario 2

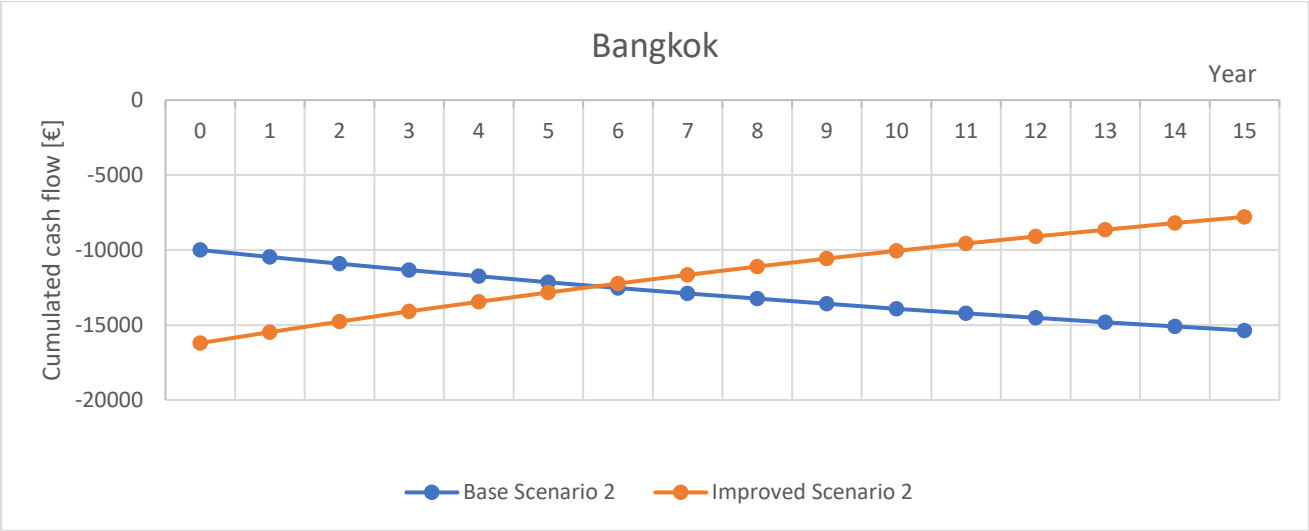

Figure 80. Bangkok Scenario 2

SCENARIO 3

The cost of technology is assumed equal to 1500 [€/unit]. This value should represent the market price for the early stage of commercialization.

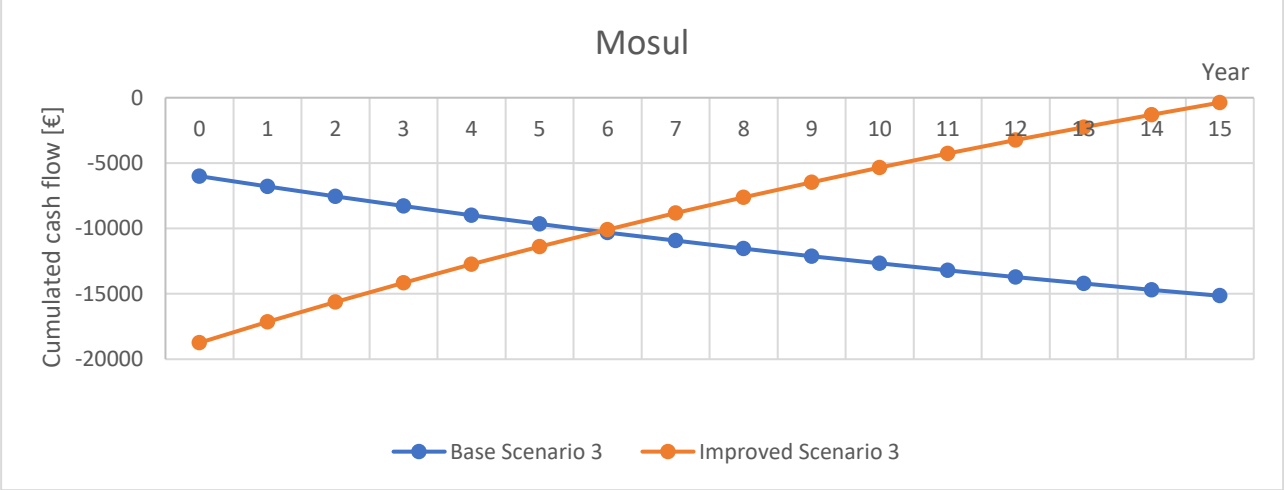

Figure 81. Mosul Scenario 3

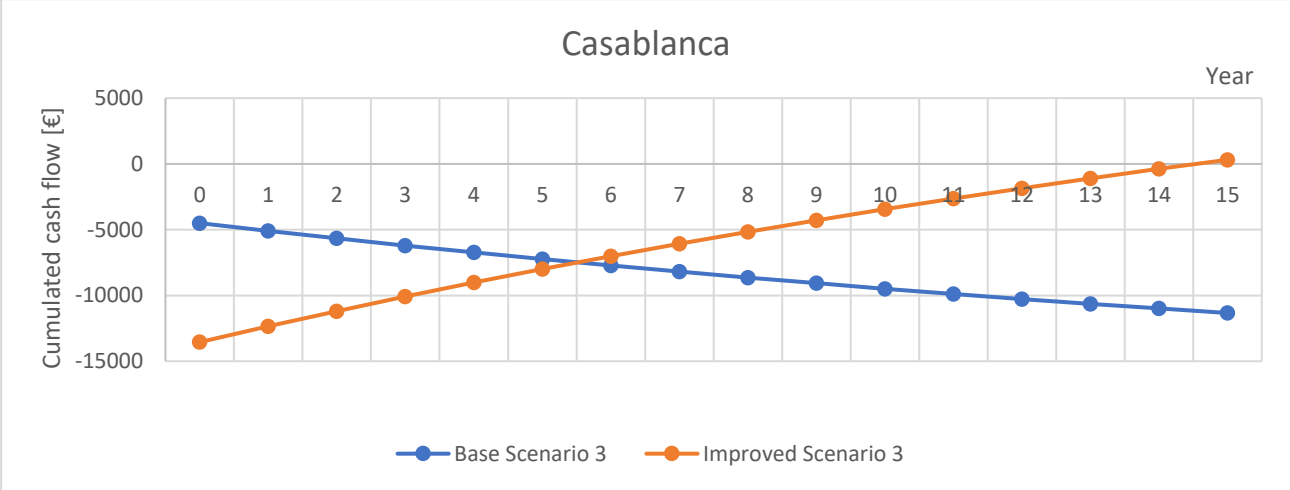

Figure 82. Casablanca Scenario 3

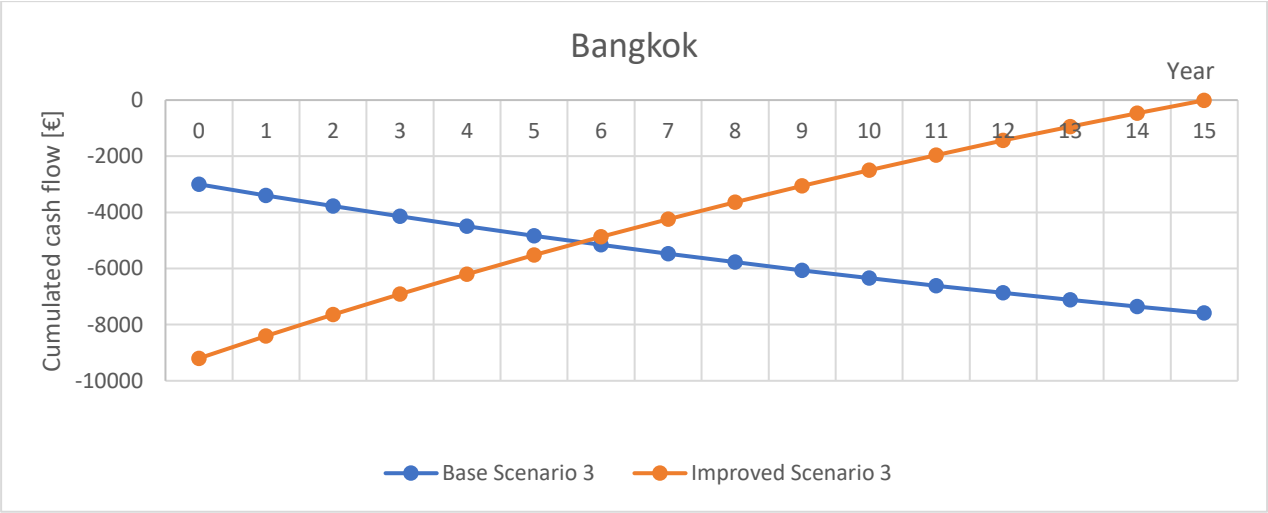

Figure 83. Bangkok Scenario 3

SCENARIO 4

The price of technology for this scenario is fixed equal to 500 [€/unit]. This price represents the optimal target for commercialization purposes.

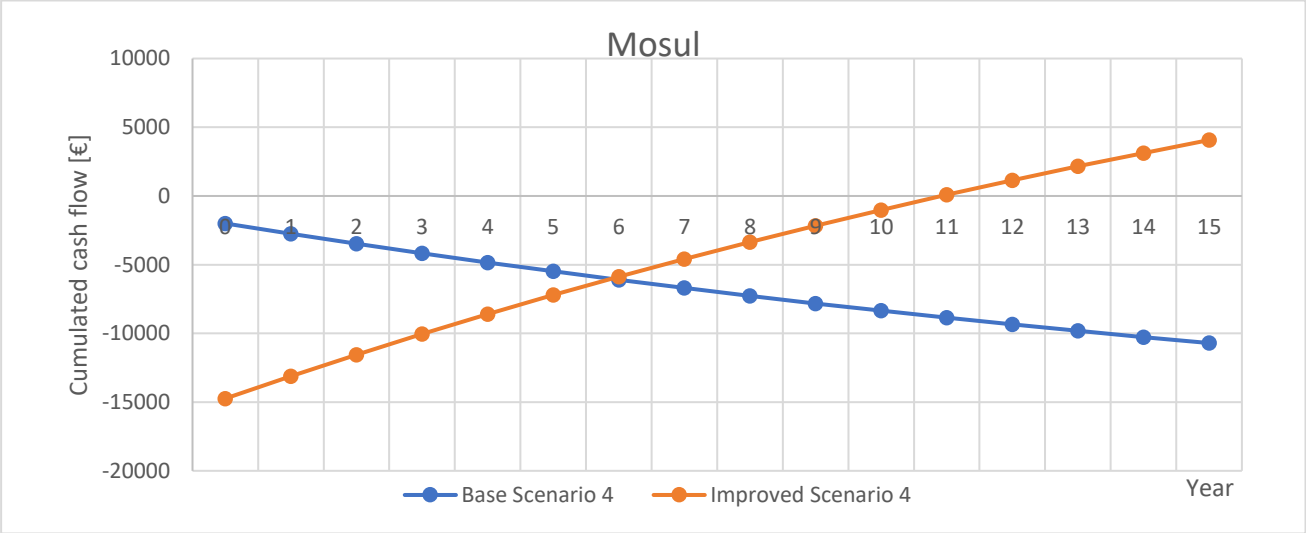

Figure 84. Mosul Scenario 4

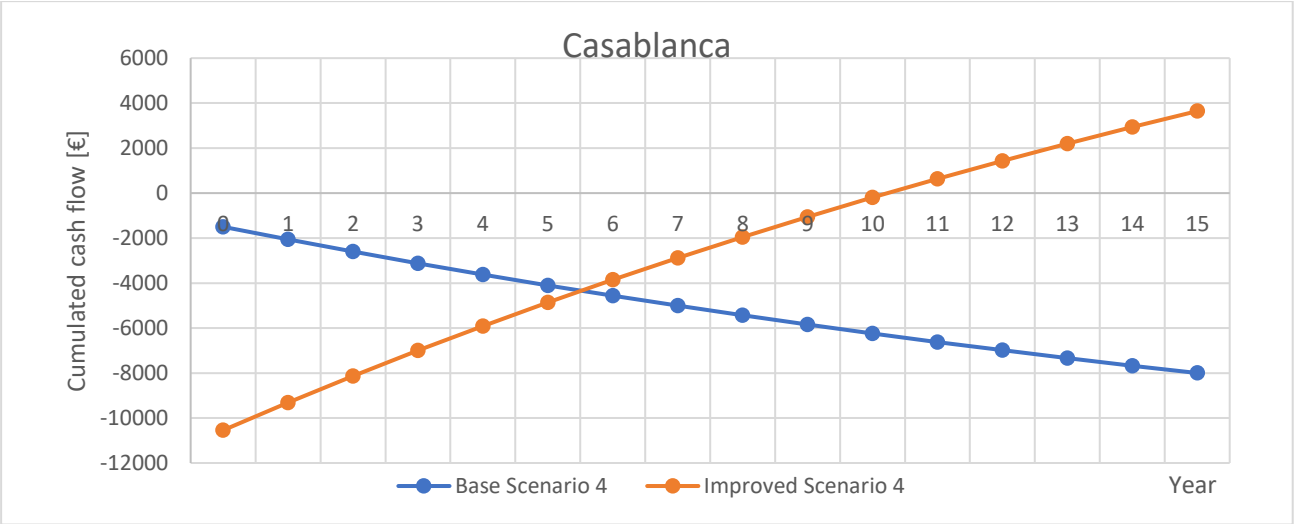

Figure 85. Casablanca Scenario 4

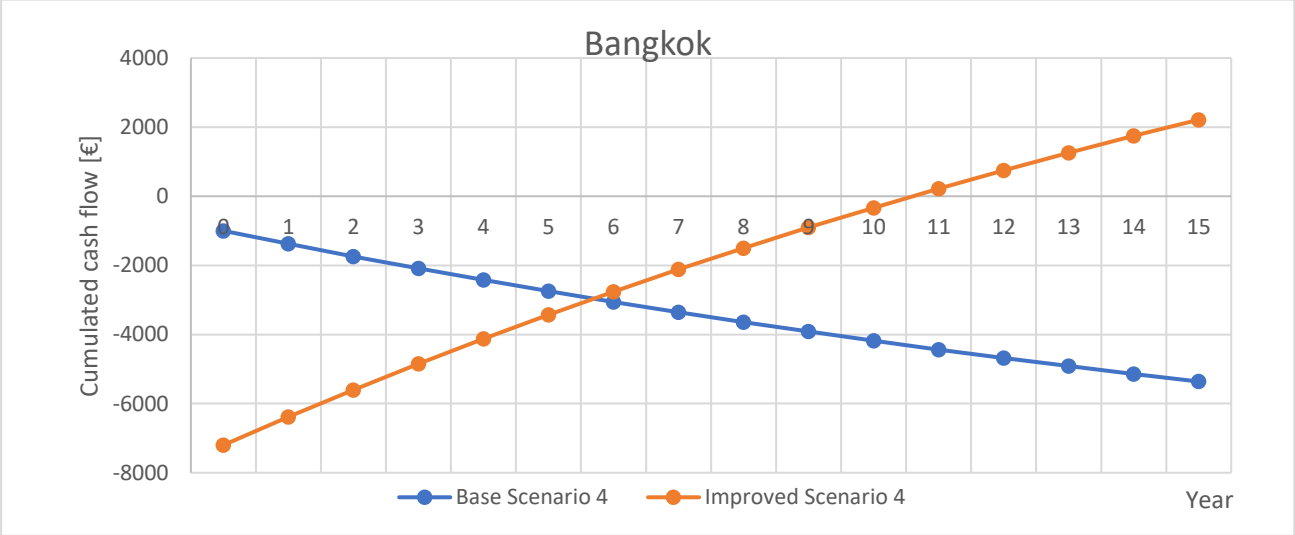

Figure 86. Bangkok Scenario 4

The graphical evaluation demonstrates a strong influence of Breath capital cost, indeed in both configurations of all scenarios the decrease of CAPEX costs causes a shift of the entire curve toward up. On the other side, the integration of PV system really improves the economy of the investment. It completely changes the trend of the curve which passes from a decreasing cumulated cash flow to an increasing one. As interesting result, the Pay Back Time "PBT" is almost reached in the improved configuration of scenario 4 for all locations and it is equal to system lifetime. Scenario 4 is the most promising with no doubts. Indeed both configurations get sensible improvements from the decreases of CAPEX costs. Base configuration results characterized by very low initial investment, while the improved trend recalls those commonly developed for PV installation. In fact Breath costs is almost negligible compared to that of PV system, so as water savings with electric ones.

An other key factor is the location used for the simulation. Indeed environmental conditions determine Breath productivity, and as consequence the number of water generator required. From this prospective, climates characterized by pseudo-constant trends of air temperature and relative humidity are the best for this water generator, as shown by the evidence. Therefore Bangkok results the best location among the others in all simulated scenarios.

6 Conclusion

The purpose of the work was to prove the potential of Breath as innovative system for atmospheric water harvesting able to cover water demand for food production. The first step involved the introduction of the energy-water-food problem along the World, considered as the research question of this work. In this context, many alternatives have already been exploited with important results, but the constant increase in water and food demands will require innovative solutions and alternative resources to those commonly used. Considering the water analysis performed in Chapter 1, the atmosphere is an interesting water resource not particularly investigated yet. Indeed, techniques used in this field involve mainly dehumidification for thermo-hygrometric comfort operated by common cooling systems. Currently the next frontier of atmospheric water harvesting is represented by adsorption process and Breath can be considered as one of the first device ever developed for the market.

The problem of food production has been partially solved with the development of hydroponic systems, innovative greenhouses that minimizes water consumption and improves quality of products.

The modelling of the system has been performed with the aim of testing the performance of Breath in different locations without the physical need of being in place. The Matlab model showed important improvements respect the previous made to simulate the adsorption process, but still it presents chances of upgrading. Anyway, the experimental procedure carried out design parameters that mostly influences the harvesting process. Air ambient conditions, initial water content in sorption material and the temperature of the cooling battery have been identified as drivers of the process. The temperature of cooling battery is one of the most important parameters in regeneration, so during water harvesting. Indeed, its value allows condensation of water vapour and the analysis demonstrated the need of having a value as lower as possible in order to maximize water production.

The energy analysis shows poor performance of Breath if compared to other technologies of the same field. Yet the specific energy consumption is too high, but the main advantage of this technology is that it can be powered integrally by renewable energy sources. Moreover, the heat needed to drive the process is characterized by very low exergy, therefore Breath is perfectly integrable in many industrial realities with availability of low-grade heat and the need of fresh water.

Considering the hydroponic greenhouse developed at Energy Centre, a case study has been developed to test the potential of the water generator.

Data of water productivity and energy consumption have been recorded from the experimental procedure in order to perform an economic analysis regarding the use of Breath to cover water demand of hydroponic greenhouse in three different locations: Mosul, Casablanca and Bangkok.

Results of the procedure have shown the strong impact both of the investment for the technology and the annual costs related to electric consumption. All analysed scenarios present a decreasing trend of the discounted cash flow, with a Net Present Value characterized by negative values for all locations. This result can be explained by making a comparison between savings and operating expenditures. Concerning volumes of energy and mass vectors involved, water and thermal energy are much cheaper that electricity, therefore the annual cash flow is always negative.

In order to invert this trend, a further analysis has been performed assuming to use photovoltaic system to cover demand for electrical energy of the system. This solution ensures an opposite trend of the NPV curve, conferring economic sustainability to the investment.
In conclusion, the innovative water generator is not ready for commercialization yet, due to high capital costs and poor production compared to other technologies, but it represents a very promising system for water production. Indeed, the applicative study has provided good results from the integration of Breath with hydroponic systems. At the actual state, the system would be able to sustain food production, yet this result is more interesting if we think at the degree of advancement of the technology which is still at laboratory stage.

7 Bibliography

[1] "900 @ population.un.org." [Online]. Available: https://population.un.org/wpp/Graphs/DemographicProfiles/Line/900.

[2] P. Andrews-Speed, S. Zhang, P. Andrews-Speed, and S. Zhang, "The Water-Energy-Food Nexus," *China as a Glob. Clean Energy Champion*, pp. 215–243, 2019, doi: 10.1007/978-981-13-3492-4_9.

[3] "pf0000226961 @ unesdoc.unesco.org." [Online]. Available: https://unesdoc.unesco.org/ark:/48223/pf0000226961.

[4] *Agricultural Outlook 2012-2021*. 2021.

[5] N. Unite, G. Mondiale, S. Uniti, and O. Mondiale, "L ' acqua in Italia," pp. 5–8, [Online]. Available: http://www.parks.it/acqua/finish/pdf/acqua.nel.mondo.e.in.italia.pdf.

[6] "44437ac88e08304db173bddee7659abf48e5fafe @ www.ifrc.org." [Online]. Available: https://www.ifrc.org/en/what-we-do/health/water-sanitation-and-hygiene-promotion/---infographics/.

[7] "258993278_The_Economic_Impacts_of_Climate_Change_Evidence_from_Agricultural_Output_and_Random_Fluctuations_in_Weather_Comment @ www.researchgate.net." [Online]. Available: https://www.researchgate.net/publication/258993278_The_Economic_Impacts_of_Climate_Change_Evidence_from_Agricultural_Output_and_Random_Fluctuations_in_Weather_Comment.

[8] R. Pujol, "Microorganisms in activated sludge and biofilm processes. Proceedings of a conference on microorganisms in activated sludge and biofilm processes, Paris, September 1993," *Water Sci. Technol.*, p. 29, 1994, [Online]. Available: https://www.nber.org/papers/w20352.pdf.

[9] A. Manzione, "Tesi completa." 2000.

[10] E. Jones, M. Qadir, M. T. H. van Vliet, V. Smakhtin, and S. Kang, "The state of desalination and brine production: A global outlook," *Sci. Total Environ.*, vol. 657, pp. 1343–1356, 2019, doi: https://doi.org/10.1016/j.scitotenv.2018.12.076.

[11] C. Ghenai, D. Kabakebji, I. Douba, and A. Yassin, "Performance analysis and optimization of hybrid multi-effect distillation adsorption desalination system powered with solar thermal energy for high salinity sea water," *Energy*, vol. 215, p. 119212, 2021, doi: 10.1016/j.energy.2020.119212.

[12] A. D. Khawaji, I. K. Kutubkhanah, and J.-M. Wie, "Advances in seawater desalination technologies," *Desalination*, vol. 221, no. 1, pp. 47–69, 2008, doi: https://doi.org/10.1016/j.desal.2007.01.067.

[13] "Multiple-effect_distillation @ en.wikipedia.org." [Online]. Available: http://en.wikipedia.org/wiki/Multiple-effect_distillation.

[14] A. M. K. El-Ghonemy, "Performance test of a sea water multi-stage flash distillation plant: Case study," *Alexandria Eng. J.*, vol. 57, no. 4, pp. 2401–2413, 2018, doi: 10.1016/j.aej.2017.08.019.

[15] "Multi-stage_flash_distillation @ en.wikipedia.org." [Online]. Available: https://en.wikipedia.org/wiki/Multi-stage_flash_distillation.

[16] S. Zhou, L. Gong, X. Liu, and S. Shen, "Mathematical modeling and performance analysis for multi-effect evaporation/multi-effect evaporation with thermal vapor compression desalination system," *Appl. Therm. Eng.*, vol. 159, no. May, p. 113759,

2019, doi: 10.1016/j.applthermaleng.2019.113759.
[17] S. W. Sharshir, N. Yang, G. Peng, and A. E. Kabeel, "Factors affecting solar stills productivity and improvement techniques: A detailed review," *Appl. Therm. Eng.*, vol. 100, pp. 267–284, 2016, doi: https://doi.org/10.1016/j.applthermaleng.2015.11.041.
[18] M. Rezaei, D. M. Warsinger, J. H. Lienhard V, M. C. Duke, T. Matsuura, and W. M. Samhaber, "Wetting phenomena in membrane distillation: Mechanisms, reversal, and prevention," *Water Res.*, vol. 139, pp. 329–352, 2018, doi: https://doi.org/10.1016/j.watres.2018.03.058.
[19] S. Al-Amshawee, M. Y. B. M. Yunus, A. A. M. Azoddein, D. G. Hassell, I. H. Dakhil, and H. A. Hasan, "Electrodialysis desalination for water and wastewater: A review," *Chem. Eng. J.*, vol. 380, p. 122231, 2020, doi: https://doi.org/10.1016/j.cej.2019.122231.
[20] J. N. Israelachvili, *Intermolecular and Surface Forces: Third Edition*. Elsevier Inc., 2011.
[21] A. H. Shourideh, W. Bou Ajram, J. Al Lami, S. Haggag, and A. Mansouri, "A comprehensive study of an atmospheric water generator using Peltier effect," *Therm. Sci. Eng. Prog.*, vol. 6, no. February, pp. 14–26, 2018, doi: 10.1016/j.tsep.2018.02.015.
[22] "Thermoelectric_cooling @ en.wikipedia.org." [Online]. Available: https://en.wikipedia.org/wiki/Thermoelectric_cooling.
[23] "Thermoelectric_effect @ en.wikipedia.org." [Online]. Available: https://en.wikipedia.org/wiki/Thermoelectric_effect#Peltier_effect.
[24] N. I. Ibrahim, F. A. Al-Sulaiman, and R. Saidur, "Performance assessment of water production from solar cooling system in humid climate," *Energy Convers. Manag.*, vol. 127, pp. 647–655, 2016, doi: https://doi.org/10.1016/j.enconman.2016.09.056.
[25] B. B. Saha, A. Akisawa, and T. Kashiwagi, "Solar/waste heat driven two-stage adsorption chiller: the prototype," *Renew. Energy*, vol. 23, no. 1, pp. 93–101, 2001, doi: https://doi.org/10.1016/S0960-1481(00)00107-5.
[26] *Muttakin M., Ito K., Saha B.B. (2020) Solar Thermal-Powered Adsorption Chiller. In: Tyagi H., Chakraborty P., Powar S., Agarwal A. (eds) Solar Energy. Energy, Environment, and Sustainability. Springer, Singapore. https://doi.org/10.1007/978-981-15-0675-8_. .*
[27] "groundwater-extraction @ www.sciencedirect.com." [Online]. Available: https://www.sciencedirect.com/topics/earth-and-planetary-sciences/groundwater-extraction.
[28] "concept-ground-water-extraction @ emis.vito.be." [Online]. Available: https://emis.vito.be/en/bat/tools-overview/sheets/concept-ground-water-extraction.
[29] "Gel_di_silice @ it.wikipedia.org." [Online]. Available: https://it.wikipedia.org/wiki/Gel_di_silice#Usi.
[30] "Idroponica @ it.wikipedia.org." [Online]. Available: https://it.wikipedia.org/wiki/Idroponica.
[31] Scielo, "Scielo @ Www.Scielo.Br." 2005, doi: http://dx.doi.org/10.1590/S0104-59702008000200011.
[32] G. Xu, W. Guan, S. Shi, and D. Blersch, "Adsorption model development for mass transport characteristics of MFEP structure by physisorption method," *Chem. Eng. J.*, vol. 354, no. May, pp. 922–931, 2018, doi: 10.1016/j.cej.2018.08.080.
[33] G. Klein, "Principles of adsorption and adsorption processes," *Reactive Polymers, Ion Exchangers, Sorbents*, vol. 4, no. 1. p. 62, 1985, doi: 10.1016/0167-6989(85)90037-6.
[34] "a-heat-transfer-correlation-for-transient-vapor-uptake-of-powdere @ kyushu-u.pure.elsevier.com." [Online]. Available: https://kyushu-u.pure.elsevier.com/en/publications/a-heat-transfer-correlation-for-transient-vapor-uptake-of-powdere.

[35] “books @ books.google.it.” [Online]. Available: https://books.google.it/books?hl=it&lr=&id=YBaNaLurTD4C&oi=fnd&pg=PR21&dq=Incropera+FP.+Introduction+to+heat+transfer.+Wiley%3B+2007&ots=tQMCakoK6E&sig=_i7W5LlT35zUsDoz55iLHEFmWuk#v=onepage&q&f=false.
[36] C. O. Popiel and J. Wojtkowiak, “Simple formulas for thermophysical properties of liquid water for heat transfer calculations (from 0°c to 150°c),” *Heat Transf. Eng.*, vol. 19, no. 3, pp. 87–101, 1998, doi: 10.1080/01457639808939929.
[37] “NTU_method @ it.qaz.wiki.” [Online]. Available: https://it.qaz.wiki/wiki/NTU_method.
[38] C. Nozioni, “Appunti ed Esercizi di Fisica Tecnica e Macchine Termiche,” pp. 1–38, 2010, [Online]. Available: http://www.dimnp.unipi.it/forgione-n/hx.pdf.
[39] R. Tu and Y. Hwang, “Reviews of atmospheric water harvesting technologies,” *Energy*, vol. 201, p. 117630, 2020, doi: https://doi.org/10.1016/j.energy.2020.117630.
[40] T. Design, “Exergo-economic analysis and design improvement of energy systems Thermal Design and Optimization Outline of the lecture • Exergo-economic cost analysis,” pp. 1–20.
[41] T. Design, “Exergy Cost Analysis.”
[42] T. Design, “Exergy Cost Analysis: application to a CHP system,” pp. 1–21.

8 Attachments

8.1 Breath Matlab code

```
clc

clear all
close all
%%Names of air states differs from those considered in the paper. In
%%particular we have the following assignments:
%%On the LEFT: air states on the thesis
%%On the RIGHT: respective air states on the code
%%Point 1 == Point 4
%%Point 2 == Point 1
%%Point 3 == Point 2
%%Point 4 == Point 3
%Quando il grafico schizza instantaneamente vuol dire che in un breve
%intervallo di tempo la batteria condenza e non in maniera alternata. Ciò
%comporta che un instante prima la produzione di acqua è zero, mentre
%l'instante dopo è un valore più elevato.



RIG=0;
perc=90;
test_time=15; %[h]
wws=0.005;
table_txt=importdata('C:\Users\Cristiano\Desktop\Polito\Tesi_Tirocinio\Tesi\Txt\ADS
\TEST28.txt');


%ADSORPTION HEAT EXCHANGER
[RH_out
,Ta_out,Xa_out,Ts_out,Tw_out,M_wAds,m_wAds,Tai,rhi,W_bed,Qfan,Ti,Xi,Text]=Adsorber(
RIG,table_txt,perc,test_time,wws);
%END ADS-HE
n=length(Ta_out);
%Starting air condition in POINT 3
if RIG==1;
    Tamb=Tai(1)-1;
    rh_amb=rhi(1);
    Ps_amb=Psat(Tamb);  %[Pa]
    xa_amb=xa(rh_amb,Ps_amb); %[kg_w/kg]
    %Initial conditions POINT 3
    Ta_3=Tamb;  %[°C]
    RH_3=rhi(1);
    P_3=Psat(Ta_3); %[Pa]
    xa_3=xa(RH_3,P_3); %[kg_w/kg]
    xa_3sat=xa(1,P_3); %[kg_w/kg]
    ha_3=hentalpy(Ta_3,xa_3);
    h3_sat=hentalpy(Ta_3,xa_3sat);
    cp_a3=Ca(xa_3)*1000;
    rho_a3=rho_air(Ta_3);
    %Condesation water initial conditions
    r_w=2490e3; %[J/kg] latent heat of condensation
    P_w=42;
    Ht=6;
    Tw_1=Tamb; %Initial temperature of consensation water
```

```
    Tw_2=Tw_1;
    m_w=P_w/Ht/9.8;
    cp_w=Cpw(Tw_1)*1000;
    T_batt=Tamb;
    for i=1:n
        %Air from rigeneration:POINT 1
        Ta_1=Ta_out(i);
        xa_1=Xa_out(i);
        cp_a1=Ca(Xa_out(i))*1000; %[kg/s]
        rho_a1=rho_air(Ta_out(i)); %[kg/m3]
        %%HRU

[Ta_4,xa_4,Ta_2,xa_2,m_a1,m_a2,m_a3]=HRU(Ta_1,xa_1,cp_a1,rho_a1,Qfan,Ta_3,xa_3sat,c
p_a3,rho_a3);
        %%END HRU
        ha_2=hentalpy(Ta_2,xa_2);
        cp_a2=Ca(xa_2)*1000; %[J/kg/K]
        %%CONDENSER

[T_batt,Ta_3,xa_3sat,h3_sat,cp_a3,rho_a3,xa_3,Tw_1]=CONDENSER(m_a2,xa_2,cp_a2,Ta_2,
ha_2,xa_3sat,T_batt,Tw_1,h3_sat,Tamb,xa_amb);
        %%END CONDENSER
        if (xa_1-xa_3)>=0
            m_water(i)=m_a1*(xa_1-xa_3);
        else
            m_water(i)=0;
        end
        Ta1(i)=Ta_1;
        Ta2(i)=Ta_2;
        Ta3(i)=Ta_3;
        Tbatt(i)=T_batt;
        Ta4(i)=Ta_4;
        xa1(i)=xa_1;
        xa2(i)=xa_2;
        xa3(i)=xa_3sat;
        xa4(i)=xa_4;
    end
    M_wHarv(ww)=sum(m_water); %[kg]
end
Time=[0:1:n-1];
% %%ERROR
% %Outlet temperature HRU/ Inlet to condenser
% r_T2=abs(Ta2-T2')./T2'*100;
% S_T2=sum((r_T2/100).^2)/length(r_T2);
% s_T2=sqrt(S_T2);
% r2=mean(r_T2)/100;
% %Outlet temperature Condenser/ Inlet to HRU
% r_T3=abs(Ta3-T3')./T3'*100;
% S_T3=sum((r_T3/100).^2)/length(r_T3); %Variance
% s_T3=sqrt(S_T3); %RMS
% r3=mean(r_T3)/100;
% %Inlet mioisture at ADS
% r_x4=abs(xa4-Xi')./Xi'*100;
% S_x4=sum((r_x4/100).^2)/length(r_x4); %Variance
% s_x4=sqrt(S_x4); %RMS
```

```
% r4=mean(r_x4)/100;
% %Matrix for 3D bar plot
% ll=length(r_T2);
% t_bar=1:1:Time(end)/3600;
% col_T2=zeros(length(t_bar),1);
% col_T3=zeros(length(t_bar),1);
% col_x4=zeros(length(t_bar),1);
% jj=1;
% hh=1;
% while i<=ll & jj<=t_bar(end)
%     st2=0;
%     st3=0;
%     sx4=0;
%     nn=0;
%     while Time(hh)<=t_bar(jj)*3600
%         st2=st2+r_T2(hh);
%         st3=st3+r_T3(hh);
%         sx4=sx4+r_x4(hh);
%         nn=nn+1;
%         hh=hh+1;
%     end
%     col_T2(jj)=st2/nn;
%     col_T3(jj)=st3/nn;
%     col_x4(jj)=sx4/nn;
%     jj=jj+1;
% end
% %Matrix for bar graph
% M_b=zeros(length(col_T2),3);
%
% M_b(:,1)=col_T2/100;
% M_b(:,2)=col_T3/100;
% M_b(:,3)=col_x4/100;
%
% %
% % figure(8)
% % plot(Time/3600,r_T2/100)
% % hold on
% % plot(Time/3600,r_T3/100)
% % plot(Time/3600,r_x4/100)
% % legend('T in cond','T out cond','x in ADS')
% % title('Relative error')
% % xlabel('Time [h]')
% % ylabel('Error')
%
%
% figure(9)
% bar3(M_b,0.5)
% grid on
% legend('T in cond','T out cond','x in ADS')




% bb=length(m_water);
% te=[0:1:bb-1]'/3600;
```

```
% figure(1)
% plot(te,Tbatt)
% hold on
% %legend('15°C','20°C','25°C','30°C')
% xlabel('Time [s]')
% ylabel('Temperature [°C]')
% title('Battery temperature ')

% color=['b','g','r','y'];
% te=[0:1:length(W_bed)-1]'/3600;
%
% figure(2)
% plot(te,m_water,color(ww))
% hold on
% legend('0.1','0.15','0.2','0.25')
% title('Water harvested ')
% xlabel('Time [h]')
% ylabel('Water flow rate [kg/s]')
%
%
% figure(5)
% plot(te,Ta4,color(ww))
% hold on
% legend('0.1','0.15','0.2','0.25')
% title('Inlet Temperture in ADS ')
% xlabel('Time [h]')
% ylabel('Temp [°C]')
%
% figure(6)
% plot(te,W_bed,color(ww))
% hold on
% legend('0.1','0.15','0.2','0.25')
% title('Water uptake')
% xlabel('Time [h]')

% figure(5)
% plot(te,Ta_out,color(KK))
% hold on
% legend('0.005','0.01','0.015','0.02')
% title('Air temperature exiting ADS-HE')
% xlabel('Time [s]')
% ylabel('Temp [°C]')
%
% figure(7)
% plot(te,Xa_out,color(KK))
% hold on
% legend('0.005','0.01','0.015','0.02')
% title('Air moisture exiting ADS-HE  ')
% xlabel('Time [s]')
% ylabel('Moisture [kg/kg]')




if RIG==1
```

```
    M_wHarv
    Eth

else
    M_wAds

end
```

Published with MATLAB® R2018b

8.2 Adsorber Matlab code

```
function [RH_out
,Ta_out,Xa_out,Ts_out,Tw_out,M_wAds,m_wAds,Tai,rhi,W_bed,Qfan,Ti,Xi,Text]=Adsorber(
RIG,table_txt,perc,test_time,wws)

load('Bankok.mat')
AAA=BangkokBangkokhourS1;


t_Gen=AAA(:,1);
t_Feb=AAA(:,3);
t_Mar=AAA(:,5);
t_Apr=AAA(:,7);
t_Mag=AAA(:,9);
t_Giu=AAA(:,11);
t_Lug=AAA(:,13);
t_Ago=AAA(:,15);
t_Set=AAA(:,17);
t_Ott=AAA(:,19);
t_Nov=AAA(:,21);
t_Dic=AAA(:,23);

rh_Gen=AAA(:,2);
rh_Feb=AAA(:,4);
rh_Mar=AAA(:,6);
rh_Apr=AAA(:,8);
rh_Mag=AAA(:,10);
rh_Giu=AAA(:,12);
rh_Lug=AAA(:,14);
rh_Ago=AAA(:,16);
rh_Set=AAA(:,18);
rh_Ott=AAA(:,20);
rh_Nov=AAA(:,22);
rh_Dic=AAA(:,24);

t_Gen=[t_Gen;t_Gen];
t_Feb=[t_Feb;t_Feb];
t_Mar=[t_Mar;t_Mar];
t_Apr=[t_Apr;t_Apr];
t_Mag=[t_Mag;t_Mag];
t_Giu=[t_Giu;t_Giu];
```

```
t_Lug=[t_Lug;t_Lug];
t_Ago=[t_Ago;t_Ago];
t_Set=[t_Set;t_Set];
t_Ott=[t_Ott;t_Ott];
t_Nov=[t_Nov;t_Nov];
t_Dic=[t_Dic;t_Dic];

rh_Gen=[rh_Gen;rh_Gen];
rh_Feb=[rh_Feb;rh_Feb];
rh_Mar=[rh_Mar;rh_Mar];
rh_Apr=[rh_Apr;rh_Apr];
rh_Mag=[rh_Mag;rh_Mag];
rh_Giu=[rh_Giu;rh_Giu];
rh_Lug=[rh_Lug;rh_Lug];
rh_Ago=[rh_Ago;rh_Ago];
rh_Set=[rh_Set;rh_Set];
rh_Ott=[rh_Ott;rh_Ott];
rh_Nov=[rh_Nov;rh_Nov];
rh_Dic=[rh_Dic;rh_Dic];

%Empty vector
T_gen=[];
T_feb=[];
T_mar=[];
T_apr=[];
T_mag=[];
T_giu=[];
T_lug=[];
T_ago=[];
T_set=[];
T_ott=[];
T_nov=[];
T_dic=[];

Rh_gen=[];
Rh_feb=[];
Rh_mar=[];
Rh_apr=[];
Rh_mag=[];
Rh_giu=[];
Rh_lug=[];
Rh_ago=[];
Rh_set=[];
Rh_ott=[];
Rh_nov=[];
Rh_dic=[];

for i=18:32 %Prendo le ore che mi servono
   c=ones(11085/15,1);
   t1=t_Gen(i)*c;
   t2=t_Feb(i)*c;
   t3=t_Mar(i)*c;
   t4=t_Apr(i)*c;
   t5=t_Mag(i)*c;
   t6=t_Giu(i)*c;
```

```
    t7=t_Lug(i)*c;
    t8=t_Ago(i)*c;
    t9=t_Set(i)*c;
    t10=t_Ott(i)*c;
    t11=t_Nov(i)*c;
    t12=t_Dic(i)*c;

    r1=rh_Gen(i)*c;
    r2=rh_Feb(i)*c;
    r3=rh_Mar(i)*c;
    r4=rh_Apr(i)*c;
    r5=rh_Mag(i)*c;
    r6=rh_Giu(i)*c;
    r7=rh_Lug(i)*c;
    r8=rh_Ago(i)*c;
    r9=rh_Set(i)*c;
    r10=rh_Ott(i)*c;
    r11=rh_Nov(i)*c;
    r12=rh_Dic(i)*c;

    T_gen=[T_gen; t1];
    T_feb=[T_feb; t2];
    T_mar=[T_mar; t3];
    T_apr=[T_apr; t4];
    T_mag=[T_mag; t5];
    T_giu=[T_giu; t6];
    T_lug=[T_lug; t7];
    T_ago=[T_ago; t8];
    T_set=[T_set; t9];
    T_ott=[T_ott; t10];
    T_nov=[T_nov; t11];
    T_dic=[T_dic; t12];

    Rh_gen=[Rh_gen; r1];
    Rh_feb=[Rh_feb; r2];
    Rh_mar=[Rh_mar; r3];
    Rh_apr=[Rh_apr; r4];
    Rh_mag=[Rh_mag; r5];
    Rh_giu=[Rh_giu; r6];
    Rh_lug=[Rh_lug; r7];
    Rh_ago=[Rh_ago; r8];
    Rh_set=[Rh_set; r9];
    Rh_ott=[Rh_ott; r10];
    Rh_nov=[Rh_nov; r11];
    Rh_dic=[Rh_dic; r12];
end
Tai=T_dic;
RHi=Rh_dic/100;
RH_can=RHi;
Tai_can=Tai-1;
%COLUMNS:
%1 - date
%2 - RH inlet SAWG
%3 - RH outlet SAWG
%4 - T air inlet SAWG
```

```
%5 - T air outlet SAWG
%9 - T air UTA
%10 - RH air UTA
%11 - X intlet SAWG
%12 - X outlet SAWG
%13 - T mandata primario
%14 - T ritorno primario
%15 - T mandata secondario
%16 - T ritorno secondario
%17 - Portata primario
%18 - Portata condensazione
%23 - Cella di carico

time=table_txt.data(:,1);
RHi=table_txt.data(:,2);
RHo=table_txt.data(:,3);
Tai=table_txt.data(:,4);
Ta_out_exp=table_txt.data(:,5);
Tai_can=table_txt.data(:,9);
RH_can=table_txt.data(:,10);
Xa_out_exp=table_txt.data(:,12);
Tm_p=table_txt.data(:,13);
Tr_p=table_txt.data(:,14);
Tm_sec=table_txt.data(:,15);
Tr_sec=table_txt.data(:,16);
G_w=table_txt.data(:,17)/60; %in kg/s
G_2=G_w.*abs(Tm_p-Tr_p)./abs(Tm_sec-Tr_sec);
V2=G_2/1000/(pi*(16e-3)^2/4);
loadcell=table_txt.data(:,23);
t2=table_txt.data(:,6); %Experimental inlet temperature at condenser
t3=table_txt.data(:,7); %Experimental outlet temperature at condenser



%UTA T sensor crashed in test 26.
%average temp. difference between UTA and inlet
DT_avg=1;
%In regeneration test xa must be catched by exp data and not corrected
if RIG==0
    Tai=Tai_can+DT_avg;
    Xa_i=xa(RHi,Psat(Tai));

    else RIG~=0
                Xa_i=table_txt.data(:,11);
end


%--- FILE CLOSING ---
fclose('all');
%even nr. = Ads.Test - odd nr. = Reg.Test
%Interparticle Diffusion Including
DIFF=1;
% %Simulation time
% test_time=9;
Qfan=airVflowrate(RIG,perc);
```

```
%Simulated phase and relative air flowrate
if RIG==0
    Ts0=Tai(1);

    s_t=' Adsorption '
    Wi=0.005;
else
    Ts0=Tai(1);
    %index to select air flowrate in case of reg.

    s_t=' Rigeneration ';
    Wi=wws;
end


%---------- PACKED BED PARAMETERS ----------
Dp=3e-3;
C_vap=1885;
Rp=Dp/2;
teta_angle=75; %packing angle in degrees
e_b=g_v(teta_angle*pi/180);
a_s=6*(1-e_b)/Dp;
L1_bed=65e-2;
L2_bed=65e-2;
H=10e-2;
Hp=1e-2; %height of upper/lower empty space
H_bed=10e-2+2*Hp;
Vbed=L1_bed*L2_bed*H; %total volume of finned HEX
V_net=Vbed*0.863; % 13% of finned HEX volume represented by fins and tubes
Hp=1e-2; %height of upper/lower empty space
V_add=2*(L1_bed*L2_bed*Hp); %volume represented by upper and lower additive space
V_total=V_net+V_add;
Ns=6*(1-e_b)*V_total/pi/Dp^3; %number of spheres
rho_s=1129;
Vs=(1-e_b)*V_total; %silica gel volume in m3
%KNOWN DATA
Msg=20.5; %mass of silica gel in old prototype
Ms=20.5+V_add*(1-e_b)*750; %estimated silica gel mass in kg - bulk density is used
M_batt=loadcell(1)-(1+Wi)*Ms;
% rho_bed=rho_s*(1-void)+1.225*void;
rho_bed=750; %bulk density of the silica gel bed
Ab=L1_bed*H_bed;
%GRID DEFINITION
dx=3e-3;
xx=[0:dx:L1_bed]';
%B.C. - Boundary conditions
%Superficial water content
Ws_old=Wi*ones(length(xx),1);
Ws_new=Ws_old;

Tair=zeros(length(time),length(xx)); %Matrix for time evolution of air temperature
Xair=zeros(length(time),length(xx)); %Matrix for time evolution of air moisture
content
Ts=zeros(length(time),length(xx)); %Matrix for time evolution of bed temperature
Ts(1,:)=Ts0; %initial bed T distribution
```

```
Ts_old=Ts0*ones(length(xx),1);
Ts_out=zeros(length(time),1);
Ts_out(1)=Ts0;
%Initial axial condition
Xair(1,:)=Xa_i(1);
Tair(1,:)=Tai(1);
Ta_out=[];
Ta_out(1)=Ta_out_exp(1);
Xa_out=[];
Xa_out(1)=Xa_out_exp(1);
Q_xa=zeros(length(xx),1);
Q_Ta=zeros(length(xx),1);

%FINS/WATER AND TUBE DATA
S_tot=16.13;
S_f=15.2;
Ae=2*0.65*0.1;
a_f=S_tot/(0.12*0.65*0.65); %surface of fins + tube per volume
Tw_old=Tm_sec(1)*ones(length(xx),1);
Tw_new=Tw_old;
if RIG==0
    U=0.58; %heat transfer coefficient with fins+tubes in W/m2K
    U_l=0;
else
    U=21.05;
    %     U_l=6.89; %heat transfer coefficient with ambient air in W/m2K
    U_l=0;
end
a_c=Ae/Vbed; %surface of lateral walls per volume

%SIMULATION TIME and PARAMETERS
%air initial conditions - Ta(x,t=ti); Xa(x,t=ti); Wbed(x,t=ti);
%RH(x=65cm,t=ti)
Xa_old=Xair(1,:)';
Ta_old=Tair(1,:)';
W_bed(1)=Wi;
%Relative humidity of outlet air
RH_out(1)=RHa(Xa_out_exp(1),Psat(Ta_out_exp(1)));
%experimental data
j=1;
t=0;
Xi=[];
Ti=[];
Xo=[];
To=[];
Te=[];
Tm_s=[];
Tr_s=[];
rho=[];
rhi=[];
l_c=[];
v_w=[];
g2=[];
gw=[];
% T2=[];
```

```
% T3=[];
%time configurations
dt=1;
 while t<=test_time*3600
   delta=(time(j+1)-time(j))*3600;
    t=t+delta;
    K=floor(delta/dt);
    X_in=Xa_i(j)*ones(K,1);
    T_in=Tai(j)*ones(K,1);
%     T_2=t2(j)*ones(K,1);
%     T_3=t3(j)*ones(K,1);
    T_out=Ta_out_exp(j)*ones(K,1);
    X_out=Xa_out_exp(j)*ones(K,1);
    v_water=V2(j)*ones(K,1);
    Text=Tai_can(j)*ones(K,1);
    TS2=Tm_sec(j)*ones(K,1);
    TR2=Tr_sec(j)*ones(K,1);
    RHO=RHo(j)*ones(K,1);
    RHI=RHi(j)*ones(K,1);
    g_w=G_w(j)*ones(K,1);
    g_2=G_2(j)*ones(K,1);
    w=loadcell(j)*ones(K,1);
%     T2=[T2 ; T_2];
%     T3=[T3; T_3];
    Xi=[Xi; X_in];
    Ti=[Ti; T_in];
    Xo=[Xo; X_out];
    To=[To; T_out];
    Te=[Te; Text];
    rho=[rho; RHO];
    rhi=[rhi; RHI];
    Tm_s=[Tm_s; TS2];
    Tr_s=[Tr_s; TR2];
    l_c=[l_c; w];
    v_w=[v_w; v_water];
    gw=[gw; g_w];
    g2=[g2; g_2];
     j=j+1;
end
L=length(Ti);
te(1)=0;
tx=strcat('Simulated time: ',num2str(test_time),' hours - grid dx:',num2str(dx),' m
- time dt:',num2str(dt),' s');
disp(tx);
%Pressure drop
PD=zeros(length(xx),1);
p_drop=[];
P_a=zeros(length(xx),1);
P_a(1)=101325;
%inlet air speed
V_in=[];
V_in(1)=Qfan/3600/Ab;
%outlet water temperature
Tw_out=[];
Tw_out(1)=Tm_sec(1);
```

```
for ii=1:L-1
    te(ii+1)=te(ii)+dt;
    %external ambient temperature
    T_ext=Te(ii);
    %Air density and viscosity
    rho_a_T=rho_air(Ta_old);
    visc_air=mu_air(Ta_old+273.15);
    %Air mass flux/ air velocity
    %Correction factor for desorption diffusion and flowrate
    if RIG==1
        FP=1;
        Am=1;
        Ak=1;
        As=1;
        A_KG=1;
        %tortuosity factor
        t_f=1;
    else
        FP=1;
        Am=1;
        Ak=1;
        As=1;
        A_KG=1;
        %tortuosity factor
        t_f=1;
    end
    Ga=Qfan/3600*rho_a_T;
    v_air=Ga./rho_a_T/Ab;
    %     v_air=Qfan/3600/Ab;
    ga=Ga/Ab;
    %Reynolds number
    Re=rho_a_T.*v_air*Dp./visc_air;
    %Pressure drop - Ergun
    PD=(150*(1-e_b)./Re+1.75).*(dx*(1-
e_b)./rho_a_T/e_b^3/Dp).*(v_air.*rho_a_T/Ab/3600).^2;
    for j=1:length(xx)-1
        P_a(j+1)=P_a(j)-PD(j);
    end
    p_drop(ii)=P_a(end)-P_a(1);
    V_in(ii)=sqrt((Qfan/3600/Ab)^2+2/1.225*p_drop(ii));
    V=linspace(V_in(ii),Qfan/3600/Ab,length(xx));
    v_air=V'*FP;

    %Heat of adsorption
    HA=Hads(Ws_old)*1000;
    %Diffusivity (molecular) of water vapor in air
    Dm=D_wa(Ta_old)*Am;
    %Knudsen diffusivity
    Dke=D_ke(Ts_old)*Ak;
    %Surface diffusivity
    Ds=D_coeff(HA/1000,Ts_old)*As;
    %Schmidt number;
    N_Sc=visc_air./rho_a_T./(Dm);
    %Air thermal capacity
```

```
    Cpa=Ca(Xa_old)*1000;
    %silica gel thermal capacity
    Cps=Cs(Ws_old)*1000;
    %S=SSR model - P=PGC model - JW=John Wiley
    %     h_m=hmS(ga,Re); %mass transfer coefficient - SSR model or PGC model
    %     h_t=hhS(ga,Cpa,Re); %heat transfer coefficient - SSR model of PCG model
    h_m=hm_jw(Dm,Re,N_Sc).*rho_a_T;
    h_t=hh_jw(Re);
    %Adsorption isotherm
    RHs=RH_s_new(Ws_old,Ts_old);
    %Equilibrium conditions near silica gel particles
    Xs=xa(RHs,Psat(Ts_old));
    %OVERALL MASS TRANSFER COEFFICIENT [1/s] - In case of diffusion
    K0=Ws_old(1)*rho_s/Xa_old(1)/rho_a_T(1);
    %empty-degree of the particle
    %     e_p=0.496;
    e_p=0.35;
    %effective diffusion coefficient
    D_eff=1./(t_f./Dm+t_f./Dke)+(1-e_p)./e_p*K0*Ds/t_f;
    Kp=60*e_p*D_eff/Dp^2./K0;
    %overall hm calculation
    K_AS=1./(1./(h_m./rho_a_T*a_s)+1./((1-e_b)*Kp.*K0));
    K_G=K_AS.*rho_a_T/a_s;
    if DIFF==1
        h_m=K_G*A_KG;
    else
    end

    %MATRICES COEFFICIENTS
    %1-xair
    k_x1=v_air/e_b/dx;
    k_x2=h_m*a_s/e_b./rho_a_T;
    %2-T silica gel
    k_Ts1=HA.*h_m*a_s/rho_s/(1-e_b)./Cps;
    k_Ts2=h_t*a_s/rho_s/(1-e_b)./Cps;
    %3-Tair
    k_a1=v_air/e_b/dx;
    k_a2=C_vap*h_m*a_s.*(Xa_old-Xs)/e_b./rho_a_T./Cpa;
    k_a3=h_t*a_s/e_b./rho_a_T./Cpa;
    k_a4=U*a_f/e_b./rho_a_T./Cpa;
    k_a5=a_c*U_l/e_b./rho_a_T./Cpa;
    %Heat by friction effect

Q_f=1./Cpa/e_b./rho_a_T.*(Ga/2).*(ga./rho_a_T/e_b).^2.*(a_s*friction(Re)/e_b/Ab);
%friction heat
    %Fins
    %alluminium properties
    Cp_al=900;
    k_al=250;
    rho_al=2700;
    %avg properties with tubes in Cu
    k_avg=365;
    cp_avg=675;
    rho_avg=3910;
    alfa_m=k_avg/rho_avg/cp_avg;
```

```
k_f=a_f*U/rho_avg/cp_avg;
%water
rho_w=1000;
cpw=4186;
kw=0.6;
%     k_w2=v_w(ii)/dx;
k_w2=g2(ii)/dx/rho_w/Ab;
k_w3=U*a_f/rho_w/cpw;

%BACKWARD EULER
%water temperature matrix
main_w=(1+dt*k_w2+dt*k_w3)*ones(length(xx),1);
sub_w=-(dt*k_w2)*ones(length(xx),1);
M_w=spdiags([sub_w main_w],[-1 0],length(xx),length(xx));
M_w(1,1)=1;
M_w(1,2)=0;
%Air temperature matrix
main_Ta=(1+dt*(k_a1+k_a3+k_a4+k_a5));
sub_Ta=-dt*k_a1;
M_Ta=spdiags([sub_Ta main_Ta],[-1 0],length(xx),length(xx));
M_Ta(1,1)=1;
M_Ta(1,2)=0;
%Air moisture matrix
main_xa=(1+dt*(k_x1+k_x2));
sub_xa=-dt*(k_x1);
M_xa=spdiags([sub_xa main_xa],[-1 0],length(xx),length(xx));
M_xa(1,1)=1;
M_xa(1,2)=0;

%----- SOLUTION -----
%AIR MOISTURE CONTENT
Q_xa=Xa_old+dt*k_x2.*Xs;
Q_xa(1)=Xi(ii);
Xa_new=M_xa\Q_xa;
%BED UPTAKE and DIFFUSION
Ws_new=Ws_old+dt*h_m*a_s/rho_bed.*(Xa_old-Xs);
W_bed(ii+1)=W_bed(ii)+dt*Ga(1)*(Xa_new(1)-Xa_new(end))/Ms;
%AIR TEMPERATURE
Q_Ta=Ta_old+dt*(k_a3).*Ts_old+dt*k_a4.*Tw_old+dt*k_a5*T_ext+Q_f*dt;
Q_Ta(1)=Ti(ii);
Ta_new=M_Ta\Q_Ta;
%BED TEMPERATURE
Ts_new=(Ts_old+dt*k_Ts1.*(Xa_old-Xs)+dt*k_Ts2.*Ta_old)./(1+dt*k_Ts2);
%WATER TEMPERATURE
if RIG==0
    Tw_new=(Tw_old+dt*k_w3*Ta_old)/(1+dt*k_w3);
else
    Q_w=Tw_old+dt*k_w3*Ta_old;
    Q_w(1)=Tm_s(ii);
    Tw_new=M_w\Q_w;
end

%---SOLUTION UPDATE---
RH_out(ii+1)=RHa(Xa_new(end),Psat(Ta_new(end)));
Ta_out(ii+1)=Ta_new(end);
```

```
    Xa_out(ii+1)=Xa_new(end);
    Ts_out(ii+1)=Ts_new(end);
    Tw_out(ii+1)=Tw_new(end);
    Ts_old=Ts_new;
    Ta_old=Ta_new;
    Xa_old=Xa_new;
    Ws_old=Ws_new;
    Tw_old=Tw_new;
    %Thermal power supplied in regeneration
    if RIG==1
        pth(ii)=g2(ii)*Cpw(Tm_s(ii))*1000*(Tm_s(ii)-Tw_new(end)); %[kW]

    end
end

M_system=(1+W_bed)*Ms+M_batt;
if RIG==1
    M_wAds=M_system(1)-M_system(end); %[kg]
    m_wAds=M_wAds/test_time; %[l/h] %Average water production rate
    Pth=mean(pth)/1000; %[kW]
    Eth=Pth*test_time; %[kWh]
else
    M_wAds=M_system(end)-M_system(1); %[kg]
    m_wAds=M_wAds/test_time; %[l/h] %Average water production rate
end

end
```

Published with MATLAB® R2018b

8.3 Heat recovery unit Matlab code

```
function
[Ta_4,xa_4,Ta_2,xa_2,m_a1,m_a2,m_a3]=HRU(Ta_1,xa_1,cp_a1,rho_a1,Qfan,Ta_3,xa_3sat,c
p_a3,rho_a3)
%%HRU
AA=0.0004677;
BB=0.02444;
CC=1.359;
DD=45.98;
EE=604.6;
FF=0.622;
GG=101325;
r_w=2500e3; %[J/kg] Latent condensation heat of water
%Geometry of cooling systems
%%heat recovery unit-HRU
k=0.05; %[W/m/K] thermal conductivity
s=0.5e-3; %fin tichness
l=40e-2; %Characteristic length
A=l*19e-2*150*2; %Contact surface
h=50e-2; %[m]
p=19e-2; %[m]
Ain=h*p-p*s*500; %Inlet surface
Pr=0.7055;
k_air=0.027; %in W/mK
```

```
        m_a1=Qfan/3600/rho_a1;  %[kg/s]
        m_a3=m_a1;
        m_a2=m_a1;
        %Saturation pressure at a given T with RH=100%
        ps=101325*xa_1/(0.622+xa_1);
        C=[0.0004677 0.02444  1.359 45.98  604.6-ps];
        solutions=roots(C);
        real=find(imag(solutions)==0 & solutions>=0);
        T_dew1=solutions(real);
        dH_dew1=cp_a1*(Ta_1-T_dew1); %[J/kg]

        %%heat recovery unit-HRU
        %e-NTU METHOD
        v_a1=Qfan/3600/Ain; %[m/s] air velocity
        v_a3=m_a3/rho_a3/Ain; %[m/s];
        %hi ed he
        Re1=Rey(rho_a1,v_a1,l,mu_air(Ta_1+273.15));
        Re3=Rey(rho_a3,v_a3,l,mu_air(Ta_3+273.15));
        Nu_1=Nu(Re1,Pr);
        Nu_3=Nu(Re3,Pr);
        h1=Nu_1*k_air/l; %[W/m2/K]
        h3=Nu_3*k_air/l; %[W/m2/K]
        %Overall thermal resistance
        R=1/h1/A+s/k/A+1/h3/A;  %[K/W]
        U=1/R; %[W/K]
        %implementation of e-NTU method
        C_a1=cp_a1*m_a1; %[W/K]
        C_a3=cp_a3*m_a3; %[W/K]
        C_min=min(C_a1,C_a3); %[W/K]
        C_max=max(C_a1,C_a3); %[W/K]
        Q_max1=C_min*(Ta_1-Ta_3); %[W] %Ideal power exchanged
        NTU=U/C_min;
        r=C_min/C_max;
        ep1=(1-exp(-NTU*(1-r)))/(1-r*exp(-NTU*(1-r))); %Efficieny of heat exchanger
        Q1=ep1*Q_max1; %[W] %Real power exchanged
        Ta_4=Ta_3+Q1/C_a3; %[°C]
        xa_4=xa_3sat; %[kg_w/kg]
        dH3=Q1/m_a3;  %[J/kg]
        if dH3>dH_dew1
            %The transformation involves both sensible and latent heat transfer
            C=[cp_a1*AA (-r_w*FF*AA-r_w*xa_1*AA+cp_a1*BB-cp_a1*Ta_1*AA+dH3*AA)...
                (-r_w*FF*BB-r_w*xa_1*BB+cp_a1*CC-cp_a1*Ta_1*BB+dH3*BB) (-r_w*FF*CC-
r_w*xa_1*CC+cp_a1*DD-cp_a1*Ta_1*CC+dH3*CC) ...
                (-r_w*FF*DD-r_w*xa_1*DD-cp_a1*GG+cp_a1*EE-cp_a1*Ta_1*DD+dH3*DD) ...
                (-r_w*FF*EE+r_w*xa_1*GG-r_w*xa_1*EE+cp_a1*GG*Ta_1-
cp_a1*Ta_1*EE+dH3*(EE-GG))];
             solutions=roots(C);
             real=find(imag(solutions)==0 & solutions>=0);
             ta_2=solutions(real);
             Ta_2=min(ta_2); %[°C]
             xa_2=0.622*Psat(Ta_2)/(101325-Psat(Ta_2)); %[kg_w/kg]
            %disp('condensation in the HRU')
        else
            %Outlet air temperature
```

```
            Ta_2=Ta_1-Q1/C_a1; %[°C]
            xa_2=xa_1; %[kg_w/kg]
        end
         %%END e-NTU METHOD
end
```

Published with MATLAB® R2018b

8.4 Condenser Matlab code

```
% function
[T_batt,Ta_3,xa_3sat,h3_sat,cp_a3,rho_a3,xa_3,Tw_1]=CONDENSER(m_a2,xa_2,cp_a2,Ta_2,
ha_2,xa_3sat,T_batt,Tw_1,h3_sat,Tamb,xa_amb)
function
[T_batt,Ta_3,xa_3sat,h3_sat,cp_a3,rho_a3,xa_3,Tw_1,Tw_2,Tw_3,Tw_4]=CONDENSER(m_a2,x
a_2,cp_a2,Ta_2,ha_2,xa_3sat,T_batt,Tw_1,h3_sat,Tamb,xa_amb)
%Geometry
%Condenser
n_tube=13;
l=46e-2; %[m]
P=3e-2; %[m]
H=18e-2; %[m]
L=10e-2; %[m]
r_tube=0.4e-2; %[m]
Ai=2*pi*r_tube*l*n_tube; %[m2]
Afin=200*P*L*2; %[m2]
Ae=Ai+Afin; %[m2]
A_w=pi*r_tube^2; %[m2]
Bf=0.15; %bypass factor;
r_w=2490e3; %[J/kg] latent heat of condensation
P_w=42; %[W]
Ht=6; %[m]
m_w=P_w/Ht/9.8; %Water flow rate [kg/s]
cp_w=Cpw(Tw_1)*1000;
%%CONDENSER
        %Saturation pressure at a given T with RH=100%
        ps=101325*xa_2/(0.622+xa_2);
        C=[0.0004677 0.02444  1.359 45.98  604.6-ps];
        solutions=roots(C);
        real=find(imag(solutions)==0 & solutions>=0);
        T_dew2=solutions(real); %[°C]
        m_a2t=(1-Bf)*m_a2; %Air flow in contact with the battery
%         dH_23=m_a2t*(cp_a2*(Ta_2-T_batt)+r_w*(xa_2-xa_3sat)); %[W] Calore ceduto
alla batteria
        if T_dew2>(T_batt+2);
            dH_23=m_a2t*(cp_a2*(Ta_2-T_batt)+r_w*(xa_2-xa_3sat)); %[W] Calore
ceduto alla batteria
            xa_3=(m_a2t*xa_3sat+m_a2*Bf*xa_2)/m_a2; %Moisture POINT 3 assuming the
adiabatic mix with bypass air flow
            rho_w=Rho_w(Tw_1);
            %Outlet physical state of point 3
            ha_3=(m_a2t*h3_sat+m_a2*Bf*ha_2)/m_a2;%[J/kg]
            cp_a3=Ca(xa_3)*1000;   %[J/kg/K]
            %Condeser external circuit
```

```
            Tw_2=Tw_1+dH_23/m_w/cp_w; %[°C]
            m_w1=m_w/2; %[kg/s]
            v_w=m_w1/n_tube/Rho_w(Tw_1)/A_w; %[m/s]
            m_tube=m_w1/n_tube; %[kg/s]
            Tw_3=Tw_2; %[°C]
            Pr=0.7055; %Prandlt number for air
            Pr_w=pr_w(Tw_2); %Prandlt number for cooling water
            rho_w=Rho_w(Tw_2); %[kg/m3]
            cp_w=Cpw(Tw_3)*1000; %[J/kg/K]
            cp_a=Ca(xa_amb)*1000; %[J/kg/K]
            rho_a=rho_air(Tamb); %[kg/m3]
            Pa=170; %[W] Electric power of external fans
            Av=pi*(13e-2)^2/4; %[m2]
            v_a=(Pa*2/Av/rho_a)^(1/3); %[m/s] Velocity of cooling air
            m_a=v_a*rho_a*Av; %[kg/s]
            %e-NTU METHOD
            Re_a=rho_a*v_a*P/mu_air(Tamb+273.15);
            Re_w=rho_w*v_w*2*r_tube/(8.9e-4);
            Nu_a=0.023*Re_a^(0.8)*Pr^(0.4);
            Nu_w=0.023*Re_w^(0.8)*Pr_w^(0.4);
            k_a=0.027; %[W/m/K]
            k_w=0.63; %[W/m/K]
            ha=Nu_a*k_a/P;  %[W/m2/K]
            hw=Nu_w*k_w/2/r_tube; %[W/m2/K]
            R=1/hw/Ai+1/ha/Ae; %[K/W]
            U=1/R; %[W/K]
            Cmin=min(cp_a*m_a,cp_w*m_w1); %[W/K]
            Cmax=max(cp_a*m_a,cp_w*m_w1); %[W/K]
            Qmax=Cmin*(Tw_3-Tamb); %[W/K]
            NTU=U/Cmin;
            w=Cmin/Cmax;
            e=1-exp(1/w*NTU^(0.22)*(exp(-w*NTU^(0.78))-1));
            Q=e*Qmax; %[W]
            Tw_4=Tw_3-Q/cp_w/m_w1; %[°C]
            Ta_o=Tamb+Q/cp_a/m_a; %[°C]
            %END e-NTU METHOD
            Tw_1=Tw_4;
            %POINT 3 outlet condition
            T_batt=(Tw_1+Tw_2)/2+1;  %[°C]
            Ta_3sat=T_batt;
            Ta_3=(ha_3-2501.2*xa_3)/(1.005+1.82*xa_3);
            P_3=Psat(Ta_3); %[Pa]
            xa_3sat=xa(1,P_3); %[kg_w/kg]
            h3_sat=hentalpy(Ta_3sat,xa_3sat);
            %xa_3sat=Xi(i+1);
            cp_a3=Ca(xa_3sat)*1000; %[J/kg/K]
            rho_a3=rho_air(Ta_3); %[kg/m3]
        else
            %Condensation cannot take place since ambient temperature i
            %higher than dew point at condenser, therefore I would use an
            %colder cooling source than air
            %m_a2t=(1-Bf)*m_a2; %Air flow in contact with the battery
            xa_3=xa_2; %Moisture POINT 3 assuming the adiabatic mix with bypass air
flow
            dH_23=m_a2*cp_a2*(Ta_2-T_batt);
```

```
            %Outlet physical state of point 3
            ha_3=(m_a2t*h3_sat+m_a2*Bf*ha_2)/m_a2;%[J/kg]
            cp_a3=Ca(xa_3)*1000;    %[J/kg/K]
            %Condeser external circuit
            Tw_2=Tw_1+dH_23/m_w/cp_w; %[°C]
            m_w1=m_w/2; %[kg/s]
            %e-NTU METHOD
            v_w=m_w1/n_tube/Rho_w(Tw_1)/A_w; %[m/s]
            m_tube=m_w1/n_tube; %[kg/s]
            Tw_3=Tw_2; %[°C]
            Pr=0.7055; %Prandlt number for air
            Pr_w=pr_w(Tw_2); %Prandlt number for cooling water
            rho_w=Rho_w(Tw_2); %[kg/m3]
            cp_w=Cpw(Tw_3)*1000; %[J/kg/K]
            cp_a=Ca(xa_amb)*1000; %[J/kg/K]
            rho_a=rho_air(Tamb); %[kg/m3]
            Pa=170; %[W] Electric power of external fans
            Av=pi*(13e-2)^2/4; %[m2]
            v_a=(Pa*2/Av/rho_a)^(1/3); %[m/s] Velocity of cooling air
            m_a=v_a*rho_a*Av; %[kg/s]
            Re_a=rho_a*v_a*P/mu_air(Tamb+273.15);
            Re_w=rho_w*v_w*2*r_tube/(8.9e-4);
            Nu_a=0.023*Re_a^(0.8)*Pr^(0.4);
            Nu_w=0.023*Re_w^(0.8)*Pr_w^(0.4);
            k_a=0.027; %[W/m/K]
            k_w=0.63; %[W/m/K]
            ha=Nu_a*k_a/P;  %[W/m2/K]
            hw=Nu_w*k_w/2/r_tube; %[W/m2/K]
            R=1/hw/Ai+1/ha/Ae; %[K/W]
            U=1/R; %[W/K]
            Cmin=min(cp_a*m_a,cp_w*m_w1); %[W/K]
            Cmax=max(cp_a*m_a,cp_w*m_w1); %[W/K]
            Qmax=Cmin*(Tw_3-Tamb); %[W/K]
            NTU=U/Cmin;
            w=Cmin/Cmax;
            e=1-exp(1/w*NTU^(0.22)*(exp(-w*NTU^(0.78))-1));
            Q=e*Qmax; %[W]
            Tw_4=Tw_3-Q/cp_w/m_w1; %[°C]
            Ta_o=Tamb+Q/cp_a/m_a; %[°C]
            %END e-NTU METHOD
            Tw_1=Tw_4;
            T_batt=(Tw_1+Tw_2)/2+1;  %[°C]
            Ta_3sat=T_dew2;
            Ta_3=Ta_2-dH_23/m_a2/cp_a2;
            P_3=Psat(Ta_3); %[Pa]
            xa_3sat=xa(1,P_3); %[kg_w/kg]
            h3_sat=hentalpy(Ta_3sat,xa_3sat);
            cp_a3=Ca(xa_3sat)*1000; %[J/kg/K]
            rho_a3=rho_air(Ta_3); %[kg/m3]

        end
        T_batt=T_batt;
        Tw_1=Tw_1;
```

```
end
```

Published with MATLAB® R2018b

8.5 Matlab functions for air, water and Silica-gel properties

```
function Cpa=Ca(xa)

%Air thermal capacity
Cpa= (1.884*xa+1.005*(1-xa)); %in kj/kgK
end
```

```
function Cpw=Cpw(T)
%Water specific heat
Cpw=((4.2174356-0.0056181625*T+0.0012992528*T.^(1.5)-
0.00011535353*T.^(2)+4.14964*10^(-6)*T.^(2.5)));
end
```

```
function Cs=Cs(q)

%Silica gel thermal capacity
C_s=0.921;
Cs= (4.178*q+C_s); %in kj/kgK
end
```

```
function D_coeff=D_coeff(Hads,Ts)
%MASS TRANSFER IN POROUS MEDIA
%Effective surface diffusion coefficient (T in °C)
D0=1.6e-6;
D_coeff= D0*exp(-0.947*Hads./(Ts+273.15)); %Hads is in kJ/kg
end
```

```
function D_ke=D_ke(T)
%MASS TRANSFER IN POROUS MEDIA
%Knudsen diffusivity (T in °C)
p_r=11*10^(-10); %average pore radius
D_ke= 22.86*p_r*(T+273.15).^0.5;
end
```

```
function D_s=D_s(T)
%MASS TRANSFER IN POROUS MEDIA
%Surface diffusion coefficient - Arrhenius (T in °C)
Ds0=2.9*10^(-4);
Ea=41500;
R=8.314;
D_s= Ds0*exp(-Ea/R./(T+273.15));
```

```
end
```

```
function D_wa=D_wa(T)
%MASS TRANSFER IN POROUS MEDIA
%Diffusivity of water vapour in air (T in °C)

D_wa= 1.735*10^(-9)*1/1.01325*(T+273.15).^1.685;
end
```

```
function friction=friction(Re)

%Friction thermal dispersion
if (0<=Re<200)
    friction= 19.336*Re.^(-0.616);
elseif (200<=Re<500)
    friction= 4.064*Re.^(-0.313);
elseif (500<=Re<5000)
    friction= 1.478*Re.^(-0.15);
else
   friction=0.35;
end


end
```

```
function g_v=g_v(teta)
%Packed bed empty degree
g_v=1-pi./(6*(1-cos(teta)).*sqrt(1+2*cos(teta)));
end
```

```
function Hads= Hads(W)

%Adsorption heat
if W<=0.05
    Hads=(3500-12400.*W);
else
    Hads=(2950-1400.*W); %in kj/kg
end
end
```

```
function h=hentalpy(T,x)
h=1.005*T+2501.2*x+1.82*T*x; %Air hentalpy
end
```

```
function hh_jw=hh_jw(Re)
%HEAT AND MASS TRANSFER
```

```
% - John Wiley empirical correlations
k_air=0.027; %in W/mK
radius=1.5e-3;
Pr=0.7055;
hh_jw= k_air/(2*radius)*(2.0+0.6*Re.^0.5*Pr^(1/3));
end
```

```
function hhP=hhP(G,Ca,Re)
%HEAT AND MASS TRANSFER
% - Pesaran-Mills empirical correlations - SSR model (Solid Side Resistance)
hhP= 0.683*G.*Ca.*Re.^(-0.51);
end
```

```
function hhS=hhS(G,Ca,Re)
%HEAT AND MASS TRANSFER
% - Pesaran-Mills empirical correlations - SSR model (Solid Side Resistance)
hhS= 1.60*G.*Ca.*Re.^(-0.42); %in W/m^2s
end
```

```
function hm_jw=hm_jw(D_i,Re,Sc)
%HEAT AND MASS TRANSFER
% - John Wiley empirical correlations
k_air=0.027; %in W/mK
radius=1.5e-3;
Pr=0.7055;
hm_jw= D_i/(2*radius).*(2.0+0.6*Re.^0.5.*Sc.^(1/3)); %in m/s
end
```

```
function hmP=hmP(G,Re)
%HEAT AND MASS TRANSFER
% - Pesaran-Mills empirical correlations - PGC model (Pseudo Gas
% Controlled)
hmP= 0.704*G.*Re.^(-0.51);
end
```

```
function hmS=hmS(G,Re)
%HEAT AND MASS TRANSFER
% - Pesaran-Mills empirical correlations - SSR model (Solid Side Resistance)
hmS= 1.70*G.*Re.^(-0.42); %in kg/m^2s
end
```

```
function k_w=k_w(T)
%Water thermal conductivity
k_w=(0.5650285+0.0026363895*T-0.00012516934*T.^(1.5)-1.5154918*10^(-6)*T.^(2)-
0.0009412945*T.^(0.5));
```

```
end
```

```
function mu_air= mu_air(T)

%dry air dynamic viscosity
mu_air= (T-300)./50*23.6*10^(-7)+184.6*10^(-7); %T in Kelvin
end
```

```
function mu_w=mu_w(T)
%Water dynamic viscosity
mu_w=1/(557.82468+19.408782*T+0.1360459*T.^2-3.1160832*10^(-4)*T.^3);
end
```

```
function Nu=Nu(Re,Pr)
%Nusselts number
Nu=(0.023*Re^(0.8)*Pr^(0.4));
end
```

```
function pr_w=pr_w(T)
%Prandlt number for water
pr_w=(1/(0.074763403+0.0029020983*T+2.8606181*10^(-5)*T.^2-8.1395537*10^(-
8)*T.^3));
end
```

```
function Psat= Psat(T)

% AIR Saturation pressure at a given T
Psat= 0.0004677*T.^4 + 0.02444*T.^3 + 1.359*T.^2 + 45.98*T + 604.6;
end
```

```
function Re=Rey(rho,v,l,mu)
%Reynolds number
Re=(rho*v*l/mu);
end
```

```
function RH_s_new= RH_s_new(q,Ts)
%Lab tested adsortion isotherm
S1=-2.26e-3;
S2=1.28e-4;
S3=7.96e0;
S4=-1.15e-2;
S5=-2.07e-5;
S6=-3.87e1;
S7=8.63e-3;
```

```
S8=8.15e1;
S9=-8.56e-7;
RH_s_new= S1*Ts + S2*Ts.^2 + S3*q + S4*q.*Ts + S5*q.*Ts.^2 + S6*q.^2 + S7*q.^2.*Ts
+ S8*q.^3 + S9*Ts.^3;
end
```

```
function RHa=RHa(xa,Psat)
%air relative humidity
RHa=xa./(0.622+xa)*101325./Psat;
end
```

```
function Rho_w=Rho_w(T)
%Water density as function of temperature
Rho_w=(999.79684+0.068317355*T-0.010740248*T.^2+0.00082140905*T.^(2.5)-
2.3030988*10^(-5)*T.^(3));
end
```

```
function xa= xa(RH,Psat)

%humid air moisture content
xa= 0.622*RH.*Psat./(101325-RH.*Psat);
end
```

8.6 Technical sheet of photovoltaic panel used in the analysis

LG NeON® R is new powerful product with global top level performance. Applied new cell structure without electrodes ***60 cell*** *and enhanced its reliability. LG NeON® R demonstrates LG's on the front, LG NeON® R maximized the utilization of light* efforts to increase customer's values beyond efficiency. It *features enhanced warranty, durability, performance under real environment, and aesthetic design suitable for roofs.*

Enhanced Warranty

LG now offer 25 years product warranty to accommodate performance warranty as well. LG NeON® R has an enhanced performance warranty. After 25 years, LG NeON® R is guaranteed at least 87.0% of initial performance.

Aesthetic Roof

LG NeON® R has been designed with aesthetics in mind: no electrode on the front that makes new product more aesthetic. LG NeON® R can increase the value of a property with its modern design.

Better Performance on a Sunny Day

LG
Life's Good

Innovation for a Better Life

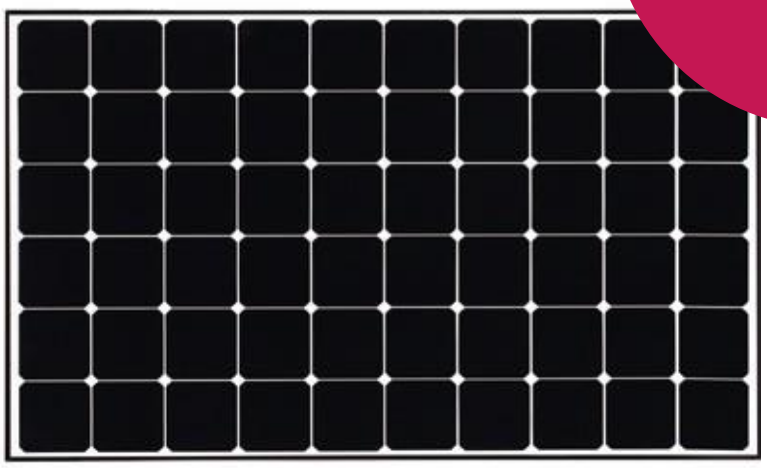

LG NeON® R

LG350Q1C-A5

LG NeON® R now performs better on a sunny days thanks to its improved temperature coefficient.

About LG Electronics

High Power Output

The LG NeON® R has been designed to significantly enhance its output making it efficient *even in limited space.*

Outstanding Durability

With its newly reinforced frame design, LG NeON® R can endure a front load up to 6000 Pa, and a rear load up to 5400 Pa.

Near Zero LID (Light Induced Degradation)

The n-type cells used in LG NeON® R have almost no boron, which may cause the initial performance degradation, leading to less LID.

LG NeON® R **LG350Q1C-A5**

Mechanical Properties

LG Electronics is a global player who has been committed to expanding its capacity, based on solar energy business as its future growth engine. We embarked on a solar energy source research program in 1985, supported by LG Group's rich experience in semi-conductor, LCD, chemistry, and materials industry. We successfully released first *Mono X® series to the marke 2010, which were exported to 32 countries in the following 2 years, thereafter. In 2013, NeON™ (previously known as Mono X® NeON) & 2015 NeON2 with CELLO technology won "Inters Award", which proved LG is the leader of innovation in the industry.*

Cells	*6 x 10*
Cell Vendor	*LG*
Cell Type	*Monocrystalline / N-type*
Cell Dimensions	*161.7 x 161.7 mm / 6 inches*
Dimensions (L x W x H)	*1700 x 1016 x 40 mm* *66.93 x 40.0 x 1.57 inch*
Front Load	*6,000Pa / 125 psf*
Rear Load	*5,400Pa / 113 psf*
Weight	*18.5 kg / 40.79 lb*
Connector Type	*MC4*
Junction Box	*IP68 with 3 Bypass Diodes*
Length of Cables	*1000 mm x 2 ea*
Glass	*High Transmission Tempered Glass*
Frame	*Anodized Aluminium*

Certifications and Warranty

Certifications	*IEC 61215, IEC 61730-1/-2* *UL 1703* *IEC 61701 (Salt mist corrosion t est)* *IEC 62716 (Ammonia corrosion test)* *ISO 9001*
Module Fire Performance (USA)	*Type 1*
Fire Resistance Class (CANADA)	*Class C (ULC / ORD C1703)*
Product Warranty	*25 years*
Output Warranty of Pmax	*Linear warranty***

***1) First 5 years : 95%, 2) After 5th year : 0.4% annual degradation, 3) 25 years : 87.0%*

Electrical Properties (STC *)

Module	***350***
Maximum Power (Pmax)	*350*
MPP Voltage (Vmpp)	*36.1*
MPP Current (Impp)	*9.70*
Open Circuit Voltage (Voc)	*42.7*
Short Circuit Current (Isc)	*10.77*
Module Efficiency	*20.3*
Operating Temperature	*-40 ~ +90*
Maximum System Voltage	*1000*
Maxim um Series Fuse Rating	*20*

Power Tolerance (%)	*0 ~ +3*

** STC (Standard Test Condition): Irradiance 1,000 W/m², Ambient Temperature 25 °C, AM 1.5*
** The nameplate power output is measured and determined by LG Electronics at its sole and absolute discretion.*
** The typical change in module efficiency at 200 W/m² in relation to 1000 W/m² is -2.0%.*

Electrical Properties (NOCT*)

Module	***350***
Maximum Power (Pmax)	*264*
MPP Voltage (Vmpp)	*36.0*
MPP Current (Impp)	*7.32*
Open Circuit Voltage (Voc)	*40.1*
Short Circuit Current (Isc)	*8.67*

** NOCT (Nominal Operating Cell Temperature): Irradiance 800 W/m², ambient temperature 20 °C, wind speed 1 m/s*

Temperature Characteristics

NOCT	44 ± 3 °C
Pmpp	-0.30 %/°C
Voc	-0.24 %/°C
Isc	0.04 %/°C

Characteristic Curves

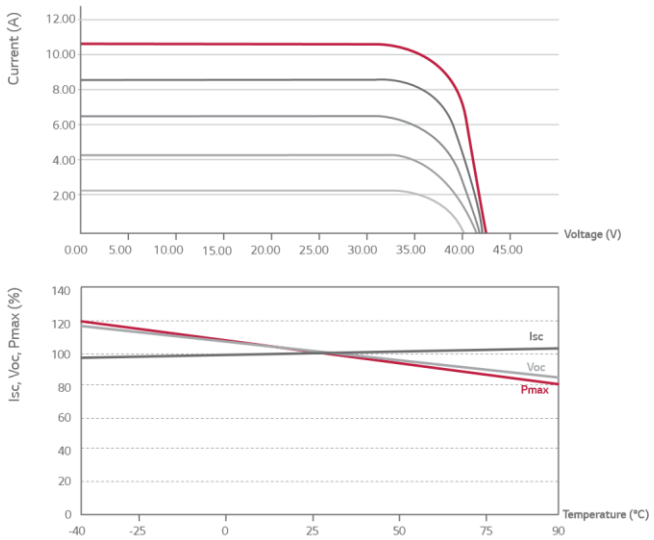

Dimensions (mm/in)

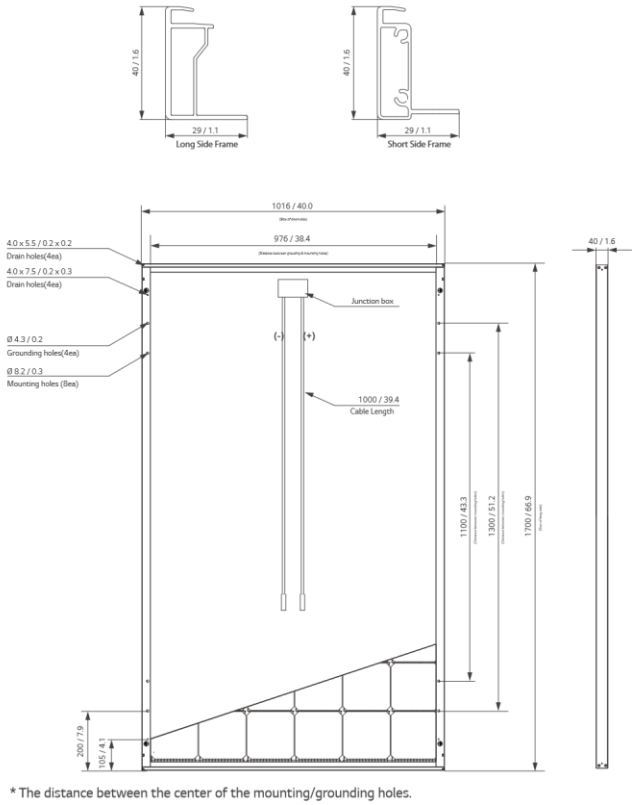

* The distance between the center of the mounting/grounding holes.

LG Life's Good

North America Solar Business Team
LG Electronics U.S.A. Inc
1000 Sylvan Ave, Englewood Cliffs, NJ 07632

Contact: lg.solar@lge.com
www.lgsolarusa.com

Product specifications are subject to change without notice.
DS-T1-72-W-G-P-EN-60630

Innovation for a Better Life